UNIVERSIDAD DE CONCEPCIÓN

Centro de Investigación en Ingeniería Matemática (CI^{2}MA)

A Banach space mixed formulation for the unsteady Brinkman problem with spatially varying porosity

Alonso J. Bustos, Sergio Caucao

PREPRINT 2025-26

SERIE DE PRE-PUBLICACIONES

A Banach space mixed formulation for the unsteady Brinkman problem with spatially varying porosity*

Alonso J. Bustos† Sergio Caucao‡

Abstract

We propose and analyze a new mixed formulation for the Brinkman equations with spatially varying porosity, modeling the time-dependent flow of an incompressible fluid through heterogeneous porous media. The formulation is developed within a Banach space framework and introduces the stress and vorticity tensors as additional unknowns. This approach eliminates the pressure, which can be recovered via post-processing, yielding a stress-velocity-vorticity system. The well-posedness of the continuous problem is proved under an appropriate small-porosity assumption, by employing monotone operator techniques together with recent advances on the solvability of perturbed saddle-point problems in Banach spaces. At the discrete level, we first introduce a semidiscrete continuous-in-time scheme employing finite element spaces stable for elasticity, such as the PEERS and Arnold–Falk–Winther elements. We prove the well-posedness of this scheme and derive the corresponding *a priori* error estimates. Subsequently, a fully discrete method is obtained by applying the backward Euler scheme for the time discretization, for which we also establish well-posedness and derive optimal convergence rates with respect to the spatial and temporal discretization parameters. Under this setting, momentum is conserved provided that the porosity, the permeability tensor, and the external forces are piecewise constant. Finally, several two- and three-dimensional numerical experiments, involving both manufactured and non-manufactured solutions, are presented, which confirm the theoretical convergence rates and highlight the capability of the proposed method to handle challenging geometries featuring strong contrasts in physical parameters such as permeability and porosity.

Key words: unsteady Brinkman equations, mixed finite element methods, stress-velocity-vorticity formulation, Banach spaces

Mathematics subject classifications (2000): 65N30, 65N12, 65N15, 35Q79, 80A20, 76R05, 76D07

1 Introduction

Flows in porous media play a central role in many branches of applied sciences, ranging from geophysical and biological systems to diverse engineering processes. Examples include subsurface flow problems, heat and mass transfer in pipes, liquid composite molding, the behavior and influence of

*This research was partially supported by ANID-Chile through Centro de Modelamiento Matemático (FB210005) and Fondecyt project 1250937; by Grupo de Investigación en Análisis Numérico y Cálculo Científico (GIANuC^2), Universidad Católica de la Santísima Concepción; and by Centro de Investigación en Ingeniería Matemática (CI^{2}MA), Universidad de Concepción.

†CI^{2}MA and Departamento de Ingeniería Matemática, Universidad de Concepción, Casilla 160-C, Concepción, Chile, email: `albustos2020@udec.cl`.

‡GIANuC^2 and Departamento de Matemática y Física Aplicadas, Universidad Católica de la Santísima Concepción, Casilla 297, Concepción, Chile, email: `scaucao@ucsc.cl`.

osteonal structures, and computational fuel cell dynamics. The mathematical modeling of such flows requires a careful balance between macroscopic effective laws and microscopic fluid dynamics, depending on the characteristics of the medium and the regime of the flow. While simplified descriptions are often sufficient in the limiting cases of very low velocities, characteristic of Darcy-type flows, or in highly permeable media, where the behavior approaches that of Stokes flows, more refined models become necessary when viscous effects within the pore structure or interactions with adjacent free-flow regions cannot be neglected. In this regard, the Brinkman equations [10] offer a consistent framework for modeling fluid motion in porous media, overcoming the main limitations of Darcy's law. Brinkman's model arises as an extension that incorporates a viscous term analogous to that of the Stokes equations, while retaining the resistance exerted by the solid skeleton of the porous medium. This combination endows the model with a hybrid character: in the limit of very low permeability it recovers Darcy's behavior, whereas in highly permeable regimes it approaches the Stokes system. For this reason, the Brinkman model is particularly useful in coupling problems involving fluid-porous interfaces and, more generally, in flows through heterogeneous porous structures where the fully homogenized Darcy description is insufficient but a detailed pore-scale Stokes model remains impractical.

The mathematical analysis and numerical discretization of the Brinkman problem inherit the well-known difficulties associated with both the Darcy and the Stokes equations. A key distinction between these two models lies in the functional setting of the velocity. Namely, in the Stokes problem, velocities belong to $\mathbf{H}^1$, whereas in the Darcy case they are only in $\mathbf{H}(\mathrm{div})$. In the classical velocity-pressure formulation, this difference in regularity requires either the use of Stokes elements enriched with stabilization or penalty terms to enforce normal continuity, or the use of $\mathbf{H}(\mathrm{div})$-conforming elements with additional degrees of freedom to impose tangential continuity. These strategies allow, on the one hand, Stokes elements to capture the Darcy regime [11], and on the other hand, $\mathbf{H}(\mathrm{div})$-conforming finite elements to be extended consistently to the Stokes regime [31]. Another approach, also explored in the literature, is to employ divergence-preserving velocity reconstruction operators that map Stokes elements into an $\mathbf{H}(\mathrm{div})$-conforming space, leading naturally to weak Galerkin finite element formulations [34]. Beyond velocity-pressure formulations, alternative mixed strategies introduce additional unknowns, giving rise to pseudostress-based methods [28, 32] and vorticity-velocity-pressure schemes in both augmented and non-augmented forms [2, 5]. Some of the aforementioned approaches have also been investigated in the time-dependent setting. In particular, the companion model given by the unsteady Brinkman–Forchheimer equations has received considerable attention. This model extends the Brinkman formulation by including a nonlinear term in the velocity, which accounts for inertial effects that become relevant when the flow through the porous medium attains intermediate velocities. In [23], the authors analyze a pseudostress-velocity formulation of this problem and establish existence and uniqueness of solutions for the continuous, semidiscrete continuous-in-time, and fully discrete settings. Similar results are obtained in a velocity-vorticity-pressure formulation [4], as well as in a three-field method involving the velocity, its gradient, and the pseudostress tensor [22].

The aim of this work is to analyze the time-dependent Brinkman model under the assumption that the porosity may vary in space. Spatially varying porosity allows the Brinkman equations to capture local differences in fluid storage and resistance, variations in permeability, and a modified mass conservation law reflecting the pore volume, thereby representing the heterogeneous structure of real porous media. From a mathematical perspective, this variability introduces challenges similar to those encountered in the Stokes problem with variable density [21] or in the convective Brinkman–Forchheimer problem with variable porosity [19]. In turn, the analysis to be developed employs techniques similar to those used for the unsteady Brinkman–Forchheimer equations and related models [22,23,39]. To derive a mixed formulation, the stress and vorticity tensors are introduced, allowing the elimination of the pressure, which can be recovered by post-processing, and leading to a stress-velocity-vorticity formulation. This formulation is based on a Banach-space framework, providing natural flexibility to adapt the scheme to multiphysics problems. Such adaptability is particularly important and has motivated several studies on coupled problems where the Banach-space setting is essential [12, 13, 15, 18, 22, 23]. Under this framework, the techniques employed in [4, 22, 23] to establish well-posedness are no longer applicable. Indeed, while those approaches crucially rely on the monotonicity properties of the underlying operators, such monotonicity is lost in our formulation due to the introduction of the stress and vorticity variables with spatially varying porosity. To overcome this difficulty, we introduce an auxiliary problem, equivalent to the original one, but endowed with a monotone operator. This reformulation allows us, under a smallness assumption on the porosity, to prove existence and uniqueness of the continuous solution by combining classical results on monotone operators, recent advances on perturbed saddle-point problems [25], and a fixed-point strategy. To the best of the authors' knowledge, the strategy of recovering monotonicity through an auxiliary problem and establishing well-posedness via a fixed-point argument in Bochner spaces is novel, and appears to be applicable to other problems as well. Once the solvability of the continuous problem has been established, similar arguments can be employed to derive the semidiscrete continuous-in-time and fully discrete schemes. For the spatial discretization, classical PEERS and Arnold–Falk–Winther elements are considered, while the backward Euler method is used for time stepping. Possible generalizations to other schemes are also feasible. In this setting, well-posedness of the discrete problem is established in a manner analogous to the continuous case, and an error analysis is carried out. Combined with the approximation properties of the finite element subspaces, this provides the theoretical rates of convergence in both space and time. With these choices of spatial and temporal discretizations, the fully discrete scheme inherits momentum conservation, a key feature for developing reliable numerical methods since it reflects the physical balance encoded in the continuous model.

The rest of the paper is organized as follows. In the remainder of this section, we introduce the standard notation and functional spaces. In Section 2, we describe the model problem of interest and we focus on the derivation of the stress-velocity-vorticity mixed formulation. In Section 3, we establish the well-posedness of the weak mixed formulation through an auxiliary problem that is equivalent to the original one. In Section 4, we present a semidiscrete continuous-in-time scheme, provide particular families of stable finite element spaces, and derive error estimates for the proposed methods. Section 5 is devoted to the analysis of the fully discrete approximation. In Section 6, we present numerical examples in 2D and 3D that illustrate the theoretical results and highlight potential applications in challenging physical settings. Finally, in Section 7 we conclude the paper by summarizing the strategies employed in the analysis and outlining possible directions for future work.

Preliminary notations. Let $\Omega \subset \mathrm{R}^d$, $d \in \{2,3\}$, denote a bounded domain with Lipschitz boundary Γ and let $\mathbf{n}$ be the outward unit normal vector on Γ. For $\mathrm{s} \geq 0$ and $\mathrm{p} \in [1,+\infty]$, we denote by $\mathrm{L}^\mathrm{p}(\Omega)$ and $\mathrm{W}^{\mathrm{s},\mathrm{p}}(\Omega)$ the usual Lebesgue and Sobolev spaces endowed with the norms $\|\cdot\|_{\mathrm{L}^\mathrm{p}(\Omega)}$ and $\|\cdot\|_{\mathrm{W}^{\mathrm{s},\mathrm{p}}(\Omega)}$, respectively. Note that $\mathrm{W}^{0,\mathrm{p}}(\Omega) = \mathrm{L}^\mathrm{p}(\Omega)$. If $\mathrm{p} = 2$, we write $\mathrm{H}^\mathrm{s}(\Omega)$ in place of $\mathrm{W}^{\mathrm{s},2}(\Omega)$, and denote the corresponding norm by $\|\cdot\|_{\mathrm{H}^\mathrm{s}(\Omega)}$. By $\mathbf{H}$ and $\mathbb{H}$ we will denote the corresponding vectorial and tensorial counterparts of a generic scalar functional space H. The $\mathrm{L}^2(\Omega)$ inner product for scalar, vector, or tensor valued functions is denoted by $(\cdot,\cdot)_\Omega$. The $\mathrm{L}^2(\Gamma)$ inner product or duality pairing is denoted by $\langle\cdot,\cdot\rangle_\Gamma$. Moreover, given a separable Banach space V endowed with the norm $\|\cdot\|_\mathrm{V}$, we let $\mathrm{L}^\mathrm{p}(0,T;\mathrm{V})$ be the space of classes of functions $f:(0,T)\to \mathrm{V}$ that are Bochner measurable and such that $\|f\|_{\mathrm{L}^\mathrm{p}(0,T;\mathrm{V})} < \infty$, with

$$\|f\|^{\mathrm{p}}_{\mathrm{L}^\mathrm{p}(0,T;\mathrm{V})} := \int_0^T \|f(t)\|^{\mathrm{p}}_{\mathrm{V}}\, dt\,, \quad \|f\|_{\mathrm{L}^\infty(0,T;\mathrm{V})} := \operatorname*{ess\,sup}_{t\in[0,T]} \|f(t)\|_{\mathrm{V}}\,.$$

In turn, for any vector field $\mathbf{v} := (v_i)_{i=1}^d$, we define the gradient, the symmetric part of the gradient, and the divergence operators as follows:

$$\nabla\mathbf{v} := \left(\frac{\partial v_i}{\partial x_j}\right)_{i,j=1,d}, \quad \mathbf{e}(\mathbf{v}) := \frac{1}{2}\big(\nabla\mathbf{v} + (\nabla\mathbf{v})^{\mathrm{t}}\big), \quad \text{and} \quad \mathrm{div}(\mathbf{v}) := \sum_{j=1}^d \frac{\partial v_j}{\partial x_j}.$$

In addition, for any tensor fields $\boldsymbol{\tau} = (\tau_{ij})_{i,j=1}^d$ and $\boldsymbol{\zeta} = (\zeta_{ij})_{i,j=1}^d$, we let $\mathbf{div}(\boldsymbol{\tau})$ be the divergence operator div acting along the rows of $\boldsymbol{\tau}$ and define the transpose, the trace, the tensor inner product and the deviatoric operator, respectively, as

$$\boldsymbol{\tau}^{\mathrm{t}} := (\tau_{ji})_{i,j=1}^d, \quad \mathrm{tr}(\boldsymbol{\tau}) := \sum_{i=1}^d \tau_{ii}, \quad \boldsymbol{\tau} : \boldsymbol{\zeta} := \sum_{i,j=1}^d \tau_{ij}\,\zeta_{ij} \quad \text{and} \quad \boldsymbol{\tau}^{\mathrm{d}} := \boldsymbol{\tau} - \frac{1}{d}\,\mathrm{tr}(\boldsymbol{\tau})\,\mathbb{I},$$

where $\mathbb{I}$ stands for the identity tensor. Furthermore, in the sequel, we will make use of the well-known Hölder inequality, given by

$$\int_\Omega |f\,g| \le \|f\|_{\mathrm{L}^{\mathrm{p}}(\Omega)}\,\|g\|_{\mathrm{L}^{\mathrm{q}}(\Omega)} \quad \forall\, f \in \mathrm{L}^{\mathrm{p}}(\Omega),\, \forall\, g \in \mathrm{L}^{\mathrm{q}}(\Omega), \quad \text{with} \quad \frac{1}{\mathrm{p}} + \frac{1}{\mathrm{q}} = 1,$$

and the Young inequality, which for all $a, b \ge 0$, $1/\mathrm{p} + 1/\mathrm{q} = 1$, and $\delta > 0$, establishes that

$$ab \le \frac{\delta^{\mathrm{p}/2}}{\mathrm{p}}\,a^{\mathrm{p}} + \frac{1}{\mathrm{q}\,\delta^{\mathrm{q}/2}}\,b^{\mathrm{q}}. \tag{1.1}$$

Next, for each $r \in [1, +\infty]$, we introduce the Banach space

$$\mathbb{H}(\mathbf{div}_r;\Omega) := \Big\{\boldsymbol{\tau} \in \mathbb{L}^2(\Omega) \;:\; \mathbf{div}(\boldsymbol{\tau}) \in \mathbf{L}^r(\Omega)\Big\},$$

endowed with the natural norm

$$\|\boldsymbol{\tau}\|_{\mathbb{H}(\mathbf{div}_r;\Omega)} := \|\boldsymbol{\tau}\|_{\mathbb{L}^2(\Omega)} + \|\mathbf{div}(\boldsymbol{\tau})\|_{\mathbf{L}^r(\Omega)} \quad \forall\,\boldsymbol{\tau} \in \mathbb{H}(\mathbf{div}_r;\Omega).$$

Additionally, we recall that, proceeding as in [27, eq. (1.43), Section 1.3.4], one can prove that for all $r \in \begin{cases} (1, +\infty] \text{ in } \mathrm{R}^2, \\ \big[\tfrac{6}{5}, +\infty\big] \text{ in } \mathrm{R}^3, \end{cases}$ there holds

$$\langle \boldsymbol{\tau}\mathbf{n}, \mathbf{v}\rangle = \int_\Omega \Big\{\boldsymbol{\tau} : \nabla\mathbf{v} + \mathbf{v}\cdot\mathbf{div}(\boldsymbol{\tau})\Big\} \quad \forall\,(\boldsymbol{\tau}, \mathbf{v}) \in \mathbb{H}(\mathbf{div}_r;\Omega) \times \mathbf{H}^1(\Omega). \tag{1.2}$$

In addition, for all $\mathrm{p} \ge \mathrm{q}$, let $i_{\mathrm{p,q}} : \mathrm{L}^{\mathrm{p}}(\Omega) \to \mathrm{L}^{\mathrm{q}}(\Omega)$ denote the continuous inclusion, which satisfies

$$\|i_{\mathrm{p,q}}\| = |\Omega|^{(\mathrm{p}-\mathrm{q})/(\mathrm{pq})}, \tag{1.3}$$

and we also denote by $\mathbf{i}_{\mathrm{p,q}}$ its vector-valued counterpart, which also satisfies (1.3) if we replace $i_{\mathrm{p,q}}$ by $\mathbf{i}_{\mathrm{p,q}}$. Finally, we recall that $\mathrm{H}^1(\Omega)$ is continuously embedded into $\mathrm{L}^{\mathrm{p}}(\Omega)$ for $\mathrm{p} \ge 1$ if $d = 2$, or $\mathrm{p} \in [1, 6]$ if $d = 3$. More precisely, we have the following inequality

$$\|w\|_{\mathrm{L}^{\mathrm{p}}(\Omega)} \le \|i_{\mathrm{p}}\|\,\|w\|_{\mathrm{H}^1(\Omega)} \quad \forall\, w \in \mathrm{H}^1(\Omega), \tag{1.4}$$

with $\|i_{\mathrm{p}}\| > 0$ depending only on $|\Omega|$ and p (see [36, Theorem 1.3.4]).

2 The model problem and its mixed formulation

In this section, we present the model of interest and develop its mixed formulation based on the stress tensor, the velocity, and the vorticity tensor.

2.1 The model problem

Our model of interest is given by the unsteady Brinkman equations with spatially varying porosity (see, for instance, [10,11,19,28]), which describes the transient flow of an incompressible fluid through a porous medium, combining viscous diffusion with a Darcy-type resistance term. The spatial variability of the porosity modifies the mass conservation law by weighting the storage of the fluid with the local pore volume, and leads to heterogeneous permeability effects. More precisely, given a porosity distribution $\rho : \Omega \to \mathrm{R}$, a body force $\mathbf{f} : \Omega \times [0,T] \to \mathrm{R}^d$, and a suitable initial datum $\mathbf{u}_0 : \Omega \to \mathrm{R}^d$, the system takes the form

$$
\begin{gathered}
\rho \frac{\partial \mathbf{u}}{\partial t} - \mathbf{div}(2\,\mu\,\rho\,\mathbf{e}(\mathbf{u})) + \mu\,\mathbf{K}^{-1}\,\mathbf{u} + \nabla p \,=\, \mathbf{f}\,, \quad \operatorname{div}(\rho\,\mathbf{u}) \,=\, 0 \quad \text{in} \quad \Omega \times (0,T]\,, \\
\mathbf{u} \,=\, \mathbf{0} \quad \text{on} \quad \Gamma \times (0,T]\,, \quad \mathbf{u}(0) \,=\, \mathbf{u}_0 \quad \text{in} \quad \Omega\,, \quad (p,1)_\Omega \,=\, 0 \quad \text{in} \quad (0,T]\,,
\end{gathered}
\tag{2.1}
$$

where the unknowns are the velocity field $\mathbf{u}$ and the scalar pressure p. The constant $\mu > 0$ represents the viscosity, and $\mathbf{K}$ denotes a symmetric permeability tensor whose inverse belongs to $\mathbb{L}^\infty(\Omega)$. The equations are supplemented with a homogeneous Dirichlet condition, and further insights into the non-homogeneous case are provided later in Remark 3.2. The last equation in (2.1) serves to eliminate the indeterminacy in the pressure, which is commonly imposed to ensure the uniqueness of the pressure field.

Regarding the permeability tensor, we assume that $\mathbf{K}^{-1}$ is uniformly coercive. Namely, there exists a constant $C_{\mathbf{K}} > 0$ such that, for all $\mathbf{v} \in \mathrm{R}^d$,

$$
\mathbf{v} \cdot \mathbf{K}^{-1}\mathbf{v} \,\geq\, C_{\mathbf{K}}\,|\mathbf{v}|^2 \quad \text{in} \quad \Omega\,. \tag{2.2}
$$

In turn, we suppose that the porosity is positive and bounded, meaning that there exist constants ρ_0 and ρ_1 such that

$$
0 < \rho_0 \leq \rho(\mathbf{x}) \leq \rho_1 \qquad \text{a.e.} \quad \text{in} \quad \Omega\,. \tag{2.3}
$$

Let us now introduce a new stress-velocity-vorticity formulation for (2.1). To this end, we first rewrite the mass conservation equation in (2.1) as $\rho\,\operatorname{div}(\mathbf{u}) + \nabla\rho \cdot \mathbf{u} = 0$, which immediately gives

$$
\operatorname{div}(\mathbf{u}) = -\left(\frac{\nabla \rho}{\rho} \cdot \mathbf{u}\right) \quad \text{in} \quad \Omega\,. \tag{2.4}
$$

Moreover, by integrating (2.4) over Ω and using the homogeneous Dirichlet condition from (2.1), we obtain the compatibility relation

$$
\left(\frac{\nabla \rho}{\rho} \cdot \mathbf{u}\,,\, 1\right)_\Omega = 0\,. \tag{2.5}
$$

We now define the Cauchy stress tensor $\widetilde{\boldsymbol{\sigma}}$ and the vorticity $\boldsymbol{\gamma}$ by

$$
\widetilde{\boldsymbol{\sigma}} \,:=\, 2\,\mu\,\rho\,\mathbf{e}(\mathbf{u}) - p\,\mathbb{I} \quad \text{and} \quad \boldsymbol{\gamma} \,:=\, \frac{1}{2}\left(\nabla \mathbf{u} - (\nabla \mathbf{u})^{\mathrm{t}}\right). \tag{2.6}
$$

Taking the divergence of $\widetilde{\boldsymbol{\sigma}}$ and substituting it into the first equation of (2.1), yields

$$
\rho\,\frac{\partial \mathbf{u}}{\partial t} + \mu\,\mathbf{K}^{-1}\,\mathbf{u} - \mathbf{div}(\widetilde{\boldsymbol{\sigma}}) = \mathbf{f} \quad \text{in} \quad \Omega\,. \tag{2.7}
$$

In turn, taking matrix trace to the stress tensor in (2.6) and using (2.4), we get

$$p = -\frac{1}{d}\left(2\,\mu\,(\nabla\rho\cdot\mathbf{u}) + \mathrm{tr}(\widetilde{\boldsymbol{\sigma}})\right), \tag{2.8}$$

so replacing this into the constitutive equation of $\widetilde{\boldsymbol{\sigma}}$ (cf. (2.6)), dividing by $2\mu\rho$, and writing $\mathbf{e}(\mathbf{u}) = \nabla\mathbf{u} - \boldsymbol{\gamma}$ according to the definition of the vorticity, we obtain

$$\frac{1}{2\mu\rho}\,\widetilde{\boldsymbol{\sigma}}^{\mathrm{d}} = \nabla\mathbf{u} - \boldsymbol{\gamma} + \frac{1}{d}\left(\frac{\nabla\rho}{\rho}\cdot\mathbf{u}\right)\mathbb{I} \quad \text{in} \quad \Omega\,. \tag{2.9}$$

Thus, from (2.7), (2.9), and using (2.8), we deduce that (2.1) can be equivalently rewritten as follows: Find $\widetilde{\boldsymbol{\sigma}}$, $\mathbf{u}$, and $\boldsymbol{\gamma}$, with $\widetilde{\boldsymbol{\sigma}}$ symmetric and $\boldsymbol{\gamma}$ skew-symmetric, in suitable spaces to be indicated below such that

$$\begin{gathered}\frac{1}{2\mu\rho}\,\widetilde{\boldsymbol{\sigma}}^{\mathrm{d}} \;=\; \nabla\mathbf{u} - \boldsymbol{\gamma} + \frac{1}{d}\left(\frac{\nabla\rho}{\rho}\cdot\mathbf{u}\right)\mathbb{I}\,, \quad \rho\frac{\partial\,\mathbf{u}}{\partial\,t} + \mu\,\mathbf{K}^{-1}\,\mathbf{u} - \mathbf{div}(\widetilde{\boldsymbol{\sigma}}) \;=\; \mathbf{f} \quad \text{in} \quad \Omega\times(0,T]\,,\\ \mathbf{u} \;=\; \mathbf{0} \quad \text{on} \quad \Gamma\times(0,T]\,, \quad \mathbf{u}(0) \;=\; \mathbf{u}_0 \quad \text{in} \quad \Omega\,,\\ \left(2\,\mu\,(\nabla\rho\cdot\mathbf{u}) + \mathrm{tr}(\widetilde{\boldsymbol{\sigma}})\,,\,1\right)_\Omega \;=\; 0 \quad \text{in} \quad (0,T]\,.\end{gathered} \tag{2.10}$$

We note that the pressure has been completely eliminated from our system, and it can be recovered from ρ, $\mathbf{u}$, and $\widetilde{\boldsymbol{\sigma}}$ according to (2.8). In this context, the last equation of (2.10) is equivalent to the pressure uniqueness condition $(p,1)_\Omega = 0$ (cf. (2.1)). Moreover, it is worth noting that the first equation in (2.10) allows the gradient $\nabla\mathbf{u}$ to be recovered via post-processing from ρ, $\widetilde{\boldsymbol{\sigma}}$, $\boldsymbol{\gamma}$, and $\mathbf{u}$. Finally, enforcing the symmetry of $\widetilde{\boldsymbol{\sigma}}$ and the skew-symmetry of $\boldsymbol{\gamma}$ in (2.10) enables the vorticity to be obtained as the skew-symmetric part of $\nabla\mathbf{u}$, as defined in (2.6), which shows that, in fact, (2.10) is equivalent to (2.1).

2.2 The stress-velocity-vorticity weak formulation

In order to derive a weak formulation of (2.10) we initially consider $\mathbf{u}$ in $\mathbf{H}^1(\Omega)$, test the constitutive equation against a tensor field $\boldsymbol{\tau}\in\mathbb{H}(\mathbf{div}_\ell;\Omega)$, where $\ell\in(1,+\infty)$ if $d=2$, or $\ell\in[6/5,+\infty)$ if $d=3$, so that we are able to apply integration by parts according to (1.2) with the homogeneous Dirichlet condition, arriving at

$$\frac{1}{2\,\mu}\left(\frac{1}{\rho}\,\widetilde{\boldsymbol{\sigma}}^{\mathrm{d}},\boldsymbol{\tau}^{\mathrm{d}}\right)_\Omega + (\mathbf{u},\mathbf{div}(\boldsymbol{\tau}))_\Omega + (\boldsymbol{\gamma},\boldsymbol{\tau})_\Omega - \frac{1}{d}\left(\frac{\nabla\rho}{\rho}\cdot\mathbf{u},\mathrm{tr}(\boldsymbol{\tau})\right)_\Omega = 0\,. \tag{2.11}$$

Since the gradient of the velocity was eliminated, the above equation remains meaningful even when $\mathbf{u}$ is sought in a space larger than $\mathbf{H}^1(\Omega)$. Specifically, the second term suggests that $\mathbf{u}$ must be in $\mathbf{L}^s(\Omega)$, where s is the Hölder conjugate of ℓ, i.e. $1/s+1/\ell=1$. Moreover, the fourth term in (2.11) is estimated by using triple Hölder inequality and the fact that $\|\mathrm{tr}(\boldsymbol{\tau})\|_{\mathrm{L}^2(\Omega)} \le \sqrt{d}\,\|\boldsymbol{\tau}\|_{\mathbb{L}^2(\Omega)} \le \sqrt{d}\,\|\boldsymbol{\tau}\|_{\mathbb{H}(\mathbf{div}_\ell;\Omega)}$, thus obtaining

$$\left(\frac{\nabla\rho}{\rho}\cdot\mathbf{u},\mathrm{tr}(\boldsymbol{\tau})\right)_\Omega \le \sqrt{d}\,\left\|\frac{\nabla\rho}{\rho}\right\|_{\mathbf{L}^r(\Omega)}\|\mathbf{u}\|_{\mathbf{L}^s(\Omega)}\,\|\boldsymbol{\tau}\|_{\mathbb{H}(\mathbf{div}_\ell;\Omega)}\,, \tag{2.12}$$

where $r := 2s/(s-2)\in(2,+\infty]$, assuming $s\ge 2$, with the convention that $r=+\infty$ if $s=2$. Although considering $\nabla\rho/\rho\in\mathbf{L}^r(\Omega)$ with $r<+\infty$ is feasible in view of (2.12), we emphasize that in the subsequent analysis we shall repeatedly require the specific assumption $r=+\infty$. Nevertheless, we aim to preserve the generality of the Banach setting, that is, we keep $\mathbf{u}\in\mathbf{L}^s(\Omega)$ with s not necessarily equal to 2, while assuming $\nabla\rho/\rho\in\mathbf{L}^\infty(\Omega)$. At the end of this section, we provide additional comments on this assumption. Under this setting, we slightly simplify (2.12) by applying Cauchy–Schwarz and the continuous inclusion $\mathbf{i}_{s,2}$ (cf. (1.3)), thus obtaining

$$\left(\frac{\nabla\rho}{\rho}\cdot\mathbf{u},\operatorname{tr}(\boldsymbol{\tau})\right)_\Omega \le \sqrt{d}\,\|\mathbf{i}_{s,2}\|\,\left\|\frac{\nabla\rho}{\rho}\right\|_{\mathbf{L}^\infty(\Omega)}\|\mathbf{u}\|_{\mathbf{L}^s(\Omega)}\,\|\boldsymbol{\tau}\|_{\mathbb{H}(\mathbf{div}_\ell;\Omega)}\,.$$

As a consequence of the previous discussion, the admissible ranges of s and ℓ are given by

$$s\in\left\{\begin{array}{ll}[2,+\infty) & \text{if } d=2\,,\\ [2,6] & \text{if } d=3\,,\end{array}\right.\qquad\text{and}\qquad \ell=\frac{s}{s-1}\in\left\{\begin{array}{ll}(1,2] & \text{if } d=2\,,\\ \big[6/5,2\big] & \text{if } d=3\,.\end{array}\right. \tag{2.13}$$

Now, returning to (2.11), we observe from the third term that it is enough to look for $\boldsymbol{\gamma}$ in $\mathbb{L}^2(\Omega)$ as $\boldsymbol{\tau}\in\mathbb{H}(\mathbf{div}_\ell;\Omega)$. Moreover, in order to enforce the required skew-symmetry, we further restrict $\boldsymbol{\gamma}\in\mathbb{L}^2_{\text{skew}}(\Omega)$, where

$$\mathbb{L}^2_{\text{skew}}(\Omega):=\Big\{\boldsymbol{\eta}\in\mathbb{L}^2(\Omega)\;:\;\;\boldsymbol{\eta}^{\rm t}=-\boldsymbol{\eta}\Big\}\,.$$

In turn, the symmetry of the stress tensor $\widetilde{\boldsymbol{\sigma}}\in\mathbb{L}^2(\Omega)$ is weakly enforced by

$$(\widetilde{\boldsymbol{\sigma}},\boldsymbol{\eta})_\Omega=0\qquad\forall\,\boldsymbol{\eta}\in\mathbb{L}^2_{\text{skew}}(\Omega)\,. \tag{2.14}$$

Next, we test the momentum equation in (2.10) against $\mathbf{v}\in\mathbf{L}^s(\Omega)$, thereby obtaining

$$(\rho\,\partial_t\,\mathbf{u},\mathbf{v})_\Omega+\mu\,(\mathbf{K}^{-1}\mathbf{u},\mathbf{v})_\Omega-(\mathbf{div}(\widetilde{\boldsymbol{\sigma}}),\mathbf{v})_\Omega=(\mathbf{f},\mathbf{v})_\Omega\qquad\forall\,\mathbf{v}\in\mathbf{L}^s(\Omega)\,. \tag{2.15}$$

Regarding the first term, using (2.3) and applying Cauchy–Schwarz inequality we find that

$$(\rho\,\partial_t\,\mathbf{u},\mathbf{v})_\Omega\le\rho_1\,\|\partial_t\,\mathbf{u}\|_{\mathbf{L}^2(\Omega)}\,\|\mathbf{v}\|_{\mathbf{L}^2(\Omega)}\,,$$

which is finite due to the fact that $\mathbf{L}^s(\Omega)\hookrightarrow\mathbf{L}^2(\Omega)$ for all $s\ge 2$. Similarly, recalling that $\mathbf{K}^{-1}\in\mathbb{L}^\infty(\Omega)$, the second term in (2.15) is also well-defined since $\mathbf{u},\mathbf{v}\in\mathbf{L}^s(\Omega)$ with $s\ge 2$. The third term in (2.15) forces the stress tensor $\widetilde{\boldsymbol{\sigma}}$ to belong to $\mathbb{H}(\mathbf{div}_\ell;\Omega)$. Despite the fact that the right-hand side of (2.15) is well defined under the sole assumption $\mathbf{f}\in\mathbf{L}^\ell(\Omega)$, we restrict ourselves to the smaller space $\mathbf{L}^2(\Omega)$, since this will be required in our analysis of the well-posedness of the weak formulation (cf. Theorems 3.8 and 3.9).

We now recall the decomposition $\mathbb{H}(\mathbf{div}_\ell;\Omega)=\mathbb{H}_0(\mathbf{div}_\ell;\Omega)\oplus\mathrm{R}\,\mathbb{I}$, where

$$\mathbb{H}_0(\mathbf{div}_\ell;\Omega):=\Big\{\boldsymbol{\tau}\in\mathbb{H}(\mathbf{div}_\ell;\Omega)\;:\;\;(\operatorname{tr}(\boldsymbol{\tau}),1)_\Omega=0\Big\}\,, \tag{2.16}$$

which means that, for all $\boldsymbol{\tau}\in\mathbb{H}(\mathbf{div}_\ell;\Omega)$, there exist unique components $\boldsymbol{\tau}_0\in\mathbb{H}_0(\mathbf{div}_\ell;\Omega)$ and $\lambda_{\boldsymbol{\tau}}\in\mathrm{R}$ such that $\boldsymbol{\tau}=\boldsymbol{\tau}_0+\lambda_{\boldsymbol{\tau}}\,\mathbb{I}$. Moreover, it is easy to verify that

$$\lambda_{\boldsymbol{\tau}}=\frac{1}{d\,|\Omega|}\,(\operatorname{tr}(\boldsymbol{\tau}),1)_\Omega\,. \tag{2.17}$$

Thus, applying this decomposition to the stress tensor, and using the last equation in (2.10) to simplify the scalar expression in (2.17), we deduce the existence of unique components $\boldsymbol{\sigma}\in\mathbb{H}_0(\mathbf{div}_\ell;\Omega)$ and $\lambda_{\boldsymbol{\sigma}}\in\mathrm{R}$ such that

$$\widetilde{\boldsymbol{\sigma}}=\boldsymbol{\sigma}+\lambda_{\boldsymbol{\sigma}}\,\mathbb{I}\quad\text{with}\quad\lambda_{\boldsymbol{\sigma}}=-\frac{2\mu}{d\,|\Omega|}\,(\nabla\rho,\mathbf{u})_\Omega\,. \tag{2.18}$$

In this regard, we notice that (2.11), (2.14) and (2.15) remain unaltered if $\widetilde{\boldsymbol{\sigma}}$ is replaced by $\boldsymbol{\sigma}$, and, hence, from now on we seek $\boldsymbol{\sigma}\in\mathbb{H}_0(\mathbf{div}_\ell;\Omega)$ instead of $\widetilde{\boldsymbol{\sigma}}$. The original stress tensor can be recovered through post-processing via (2.18). Furthermore, using (2.5) along with the fact that $\boldsymbol{\gamma} \in \mathbb{L}^2_{\text{skew}}(\Omega)$, we notice that (2.11) trivially holds when $\boldsymbol{\tau}$ is any multiple of the identity tensor. Therefore, we may restrict ourselves to test in $\mathbb{H}_0(\mathbf{div}_\ell;\Omega)$ instead of the whole space.

In order to rewrite our system in a more suitable way for the analysis to be developed in the following sections, we define the spaces

$$\mathbb{X} := \mathbb{H}_0(\mathbf{div}_\ell;\Omega) \quad \text{and} \quad \mathbf{Y} := \mathbf{L}^s(\Omega) \times \mathbb{L}^2_{\text{skew}}(\Omega)\,,$$

and set the notation

$$\underline{\mathbf{u}} := (\mathbf{u}, \boldsymbol{\gamma})\ ,\ \underline{\mathbf{v}} := (\mathbf{v}, \boldsymbol{\eta}) \in \mathbf{Y}\,.$$

Under these definitions, it is natural to endow $\mathbf{Y}$ with the product space norm:

$$\|\underline{\mathbf{v}}\|_{\mathbf{Y}} := \|\mathbf{v}\|_{\mathbf{L}^s(\Omega)} + \|\boldsymbol{\eta}\|_{\mathbb{L}^2(\Omega)} \qquad \forall\, \underline{\mathbf{v}} \in \mathbf{Y}\,.$$

Hence, according to (2.11), (2.14) and (2.15), the weak formulation associated with (2.10) reads: Given $\mathbf{f} : [0,T] \to \mathbf{L}^2(\Omega)$ and $\mathbf{u}_0 \in \mathbf{L}^s(\Omega)$, find $(\boldsymbol{\sigma}, \underline{\mathbf{u}}) : [0,T] \to \mathbb{X} \times \mathbf{Y}$ such that $\mathbf{u}(0) = \mathbf{u}_0$ and, for a.e. $t \in (0,T)$,

$$\begin{aligned} [\mathbf{A}(\boldsymbol{\sigma}(t)), \boldsymbol{\tau}] + [\mathbf{B}'(\underline{\mathbf{u}}(t)), \boldsymbol{\tau}] + [\mathbf{D}'_\rho(\underline{\mathbf{u}}(t)), \boldsymbol{\tau}] &= 0 && \forall\, \boldsymbol{\tau} \in \mathbb{X}\,, \\ \frac{\partial}{\partial t}[\mathbf{E}(\underline{\mathbf{u}}(t)), \underline{\mathbf{v}}] - [\mathbf{B}(\boldsymbol{\sigma}(t)), \underline{\mathbf{v}}] + [\mathbf{C}(\underline{\mathbf{u}}(t)), \underline{\mathbf{v}}] &= [\mathbf{F}(t), \underline{\mathbf{v}}] && \forall\, \underline{\mathbf{v}} \in \mathbf{Y}\,, \end{aligned} \tag{2.19}$$

where the operators $\mathbf{A} : \mathbb{X} \to \mathbb{X}'$, $\mathbf{B}, \mathbf{D}_\rho : \mathbb{X} \to \mathbf{Y}'$, $\mathbf{C}, \mathbf{E} : \mathbf{Y} \to \mathbf{Y}'$ are defined, respectively, as

$$[\mathbf{A}(\boldsymbol{\sigma}), \boldsymbol{\tau}] := \frac{1}{2\mu}\left(\frac{1}{\rho}\,\boldsymbol{\sigma}^{\mathrm{d}}, \boldsymbol{\tau}^{\mathrm{d}}\right)_\Omega\,, \tag{2.20a}$$

$$[\mathbf{B}(\boldsymbol{\tau}), \underline{\mathbf{v}}] := (\mathbf{v}, \mathbf{div}(\boldsymbol{\tau}))_\Omega + (\boldsymbol{\eta}, \boldsymbol{\tau})_\Omega\,, \tag{2.20b}$$

$$[\mathbf{D}_\rho(\boldsymbol{\tau}), \underline{\mathbf{v}}] := -\frac{1}{d}\left(\frac{\nabla\rho}{\rho}\cdot \mathbf{v}, \operatorname{tr}(\boldsymbol{\tau})\right)_\Omega\,, \tag{2.20c}$$

$$[\mathbf{C}(\underline{\mathbf{u}}), \underline{\mathbf{v}}] := \mu\,(\mathbf{K}^{-1}\,\mathbf{u}, \mathbf{v})_\Omega\,, \tag{2.20d}$$

$$[\mathbf{E}(\underline{\mathbf{u}}), \underline{\mathbf{v}}] := (\rho\,\mathbf{u}, \mathbf{v})_\Omega\,, \tag{2.20e}$$

and the right-hand side term $\mathbf{F} : [0,T] \to \mathbf{Y}'$ is given by

$$[\mathbf{F}(t), \underline{\mathbf{v}}] := (\mathbf{f}(t), \mathbf{v})_\Omega\,.$$

In all the terms above, $[\cdot,\cdot]$ denotes the duality pairing induced by the corresponding operators. Additionally, we let $\mathbf{B}' : \mathbf{Y} \to \mathbb{X}'$ be the operator defined by the relation $[\mathbf{B}'(\underline{\mathbf{v}}), \boldsymbol{\tau}] = [\mathbf{B}(\boldsymbol{\tau}), \underline{\mathbf{v}}]$ for all $(\boldsymbol{\tau}, \underline{\mathbf{v}}) \in \mathbb{X} \times \mathbf{Y}$. The operator $\mathbf{D}'_\rho : \mathbf{Y} \to \mathbb{X}'$ is defined analogously.

We conclude this section with additional comments on the assumptions considered herein. First, we note that the hypothesis $\nabla\rho/\rho \in \mathbf{L}^\infty(\Omega)$ is compatible both with the classical Hilbertian case $s = \ell = 2$ and with the Banach case $s, \ell \neq 2$ in (2.13). Although the more general assumption $\nabla\rho/\rho \in \mathbf{L}^r(\Omega)$ would be desirable, it cannot be accommodated within the techniques employed in this work. We refer to [21], where the authors study the stationary Stokes equations with variable density and impose a similar assumption, and to [19], which addresses the convective Brinkman–Forchheimer equations with variable porosity under a less restrictive setting, where $\nabla\rho/\rho$ is considered in $\mathbf{L}^r(\Omega)$ with $r < +\infty$. The techniques developed in the latter work, however, are not fully applicable here due to the unsteady nature of the model under consideration. In particular, the assumption $\nabla\rho/\rho \in \mathbf{L}^\infty(\Omega)$ is crucial in the proofs of Lemma 3.3 and Theorem 3.4.

On the other hand, it is also important to highlight that the use of Banach spaces rather than Hilbert spaces is motivated by the potential applicability of this work to the analysis of coupled models. For instance, the Brinkman model can be coupled with transport or heat equations. In fact, a similar stationary model is analyzed in [13], where the convective Brinkman–Forchheimer system is coupled with a nonlinear transport equation. In that setting, both the fluid velocity and the concentration of a chemical species transported by the flow are required to belong to a Lebesgue space L^p, with p necessarily greater than 2. In general, such couplings demand higher regularity of the shared unknowns, particularly when nonlinear interactions are involved. Further examples of couplings formulated in Banach space frameworks can be found in [16, 17, 29].

3 Well-posedness of the model

In this section, we establish the solvability of (2.19). To this aim, we first collect some preliminary results that will be used in the forthcoming analysis.

3.1 Preliminary results

In what follows, a linear operator $\mathcal{A}$ from a real vector space E to its algebraic dual $E^\star$ is symmetric and monotone if, respectively,

$$[\mathcal{A}(x), y] = [\mathcal{A}(y), x] \quad \forall\, x, y \in E\,, \quad \text{and} \quad [\mathcal{A}(x), x] \geq 0 \quad \forall\, x \in E\,.$$

In addition, let us denote by $R(\mathcal{A})$ the range of $\mathcal{A}$. We also recall that the dual of a seminormed space is the space of all linear functionals that are continuous with respect to the seminorm.

The following result is a slight simplification of [38, Theorem IV.6.1(b)], which will be used to establish the existence of a solution to (2.19).

Theorem 3.1. *Let the linear, symmetric and monotone operator $\mathcal{N}$ be given from the real vector space E to its algebraic dual $E^\star$, and let E'_b be the Hilbert space which is the topological dual of the seminormed space $(E, |\cdot|_b)$, where*

$$|x|_b = [\mathcal{N}(x), x]^{1/2} \qquad \forall\, x \in E\,. \tag{3.1}$$

Let $\mathcal{M} : E \to E'_b$ be an operator with domain $\mathcal{D} = \Big\{ x \in E \,:\, \mathcal{M}(x) \in E'_b \Big\}$. Assume that $\mathcal{M}$ is monotone and $R(\mathcal{N} + \mathcal{M}) = E'_b$. Then, for each $f \in \mathrm{W}^{1,1}(0, T; E'_b)$ and for each $u_0 \in \mathcal{D}$, there is a solution $u : [0, T] \to E$ of

$$\frac{\partial}{\partial t}\big(\mathcal{N}(u(t))\big) + \mathcal{M}\big(u(t)\big) \;=\; f(t) \quad \textit{for a.e.} \quad 0 < t < T\,, \tag{3.2}$$

with

$$\mathcal{N}(u) \in \mathrm{W}^{1,\infty}(0, T; E'_b)\,, \quad u(t) \in \mathcal{D} \quad \textit{for all } 0 \leq t \leq T\,, \quad \textit{and} \quad \mathcal{N}(u(0)) = \mathcal{N}(u_0)\,.$$

One would like to write (2.19) in the form given by (3.2) and use this result to prove its well-posedness. However, it turns out that this is not possible, since the operator arising from the terms without time derivatives in (2.19) is not monotone. For this reason, we introduce an auxiliary formulation equivalent to (2.19) by defining the linear operator $\widetilde{\mathbf{B}} : \mathbb{X} \to \mathbf{Y}'$ as

$$[\widetilde{\mathbf{B}}(\boldsymbol{\tau}), \underline{\mathbf{v}}] := [\mathbf{B}(\boldsymbol{\tau}), \underline{\mathbf{v}}] + [\mathbf{D}_\rho(\boldsymbol{\tau}), \underline{\mathbf{v}}] \qquad \forall\, \underline{\mathbf{v}} \in \mathbf{Y}\,,$$

and, for each $\boldsymbol{\zeta} \in \mathbb{X}$, we let $\widetilde{\mathbf{F}}_{\boldsymbol{\zeta}} : [0,T] \to \mathbf{Y}'$ be defined, for all $t \in [0,T]$, by

$$[\widetilde{\mathbf{F}}_{\boldsymbol{\zeta}}(t), \underline{\mathbf{v}}] := [\mathbf{F}(t), \underline{\mathbf{v}}] - [\mathbf{D}_\rho(\boldsymbol{\zeta}), \underline{\mathbf{v}}] \qquad \forall\, \underline{\mathbf{v}} \in \mathbf{Y}\,.$$

The following result states the auxiliary problem and establishes its equivalence with (2.19). The proof is straightforward and is therefore omitted.

Lemma 3.2. *Let $\mathbf{f} : [0,T] \to \mathbf{L}^2(\Omega)$ and $\mathbf{u}_0 \in \mathbf{L}^s(\Omega)$. Then, $(\boldsymbol{\sigma}, \underline{\mathbf{u}}) : [0,T] \to \mathbb{X} \times \mathbf{Y}$ is solution to (2.19) if and only if $\mathbf{u}(0) = \mathbf{u}_0$ and, for a.e. $t \in (0,T)$,*

$$\begin{aligned} [\mathbf{A}(\boldsymbol{\sigma}(t)), \boldsymbol{\tau}] + [\widetilde{\mathbf{B}}'(\underline{\mathbf{u}}(t)), \boldsymbol{\tau}] &= 0 && \forall\, \boldsymbol{\tau} \in \mathbb{X}\,, \\ \frac{\partial}{\partial t}\,[\mathbf{E}(\underline{\mathbf{u}}(t)), \underline{\mathbf{v}}] - [\widetilde{\mathbf{B}}(\boldsymbol{\sigma}(t)), \underline{\mathbf{v}}] + [\mathbf{C}(\underline{\mathbf{u}}(t)), \underline{\mathbf{v}}] &= [\widetilde{\mathbf{F}}_{\boldsymbol{\sigma}}(t), \underline{\mathbf{v}}] && \forall\, \underline{\mathbf{v}} \in \mathbf{Y}\,. \end{aligned} \tag{3.3}$$

Next, we establish stability properties of the operators involved in (2.19). In fact, employing Cauchy–Schwarz and Hölder inequalities, and the continuous inclusion $\mathbf{i}_{s,2}$ (cf. (1.3)), we find that

$$\big|[\mathbf{A}(\boldsymbol{\sigma}), \boldsymbol{\tau}]\big| \le \frac{1}{2\mu\rho_0}\,\|\boldsymbol{\sigma}\|_{\mathbb{X}}\,\|\boldsymbol{\tau}\|_{\mathbb{X}}\,, \quad \big|[\mathbf{B}(\boldsymbol{\tau}), \underline{\mathbf{v}}]\big| \le \|\boldsymbol{\tau}\|_{\mathbb{X}}\,\|\underline{\mathbf{v}}\|_{\mathbf{Y}}\,, \tag{3.4a}$$

$$\big|[\mathbf{D}_\rho(\boldsymbol{\tau}), \underline{\mathbf{v}}]\big| \le \frac{\|\mathbf{i}_{s,2}\|}{\sqrt{d}}\,\left\|\frac{\nabla\rho}{\rho}\right\|_{\mathbf{L}^\infty(\Omega)}\,\|\boldsymbol{\tau}\|_{\mathbb{X}}\,\|\underline{\mathbf{v}}\|_{\mathbf{Y}}\,, \tag{3.4b}$$

$$\big|[\mathbf{E}(\underline{\mathbf{u}}), \underline{\mathbf{v}}]\big| \le \rho_1\,\|\mathbf{i}_{s,2}\|\,\|\mathbf{u}\|_{\mathbf{L}^2(\Omega)}\,\|\mathbf{v}\|_{\mathbf{L}^s(\Omega)} \le \rho_1\,\|\mathbf{i}_{s,2}\|^2\,\|\underline{\mathbf{u}}\|_{\mathbf{Y}}\,\|\underline{\mathbf{v}}\|_{\mathbf{Y}}\,, \tag{3.4c}$$

$$\big|[\mathbf{C}(\underline{\mathbf{u}}), \underline{\mathbf{v}}]\big| \le \mu\,\|\mathbf{i}_{s,2}\|^2\,\|\mathbf{K}^{-1}\|_{\mathbb{L}^\infty(\Omega)}\,\|\underline{\mathbf{u}}\|_{\mathbf{Y}}\,\|\underline{\mathbf{v}}\|_{\mathbf{Y}}\,, \tag{3.4d}$$

$$\text{and} \quad \big|[\mathbf{F}(t), \underline{\mathbf{v}}]\big| \le \|\mathbf{i}_{s,2}\|\,\|\mathbf{f}(t)\|_{\mathbf{L}^2(\Omega)}\,\|\underline{\mathbf{v}}\|_{\mathbf{Y}}\,. \tag{3.4e}$$

On the other hand, from (2.2) and (2.3), it follows that $\mathbf{A}$, $\mathbf{C}$, and $\mathbf{E}$ are monotone. Indeed,

$$\big|[\mathbf{A}(\boldsymbol{\tau}), \boldsymbol{\tau}]\big| \ge \frac{1}{2\mu\rho_1}\|\boldsymbol{\tau}^{\mathrm{d}}\|^2_{\mathbb{L}^2(\Omega)}\,, \quad \big|[\mathbf{C}(\underline{\mathbf{v}}), \underline{\mathbf{v}}]\big| \ge \mu\,C_{\mathbf{K}}\,\|\mathbf{v}\|^2_{\mathbf{L}^2(\Omega)}\,, \tag{3.5a}$$

$$\text{and} \quad \big|[\mathbf{E}(\underline{\mathbf{v}}), \underline{\mathbf{v}}]\big| \ge \rho_0\,\|\mathbf{v}\|^2_{\mathbf{L}^2(\Omega)}\,. \tag{3.5b}$$

We continue by establishing some inf-sup conditions needed for the subsequent analysis. We begin with the following condition for $\mathbf{B}$: there exists a positive constant β such that

$$\sup_{0 \ne \boldsymbol{\tau} \in \mathbb{X}} \frac{[\mathbf{B}(\boldsymbol{\tau}), \underline{\mathbf{v}}]}{\|\boldsymbol{\tau}\|_{\mathbb{X}}} \ge \beta\,\|\underline{\mathbf{v}}\|_{\mathbf{Y}} \qquad \forall\, \underline{\mathbf{v}} \in \mathbf{Y}\,. \tag{3.6}$$

The proof follows from a straightforward generalization of [30, Lemma 3.5] (see also [29, Lemma 3.4]), where the case $s = 4$ and $\ell = 4/3$ was analyzed, and is therefore omitted here. We remark that, to apply the same arguments as in these references, the continuous embedding $\mathbf{H}^1(\Omega) \hookrightarrow \mathbf{L}^s(\Omega)$ (cf. (1.4)) is required. Since $s \in [2, +\infty)$ for $d = 2$ and $s \in [2, 6]$ for $d = 3$ (cf. (2.13)), this embedding holds in our setting.

Now, we let $\mathbb{V}$ denote the kernel of $\mathbf{B}$ (cf. (2.20b)), which is characterized by

$$\mathbb{V} := \Big\{ \boldsymbol{\tau} \in \mathbb{X} \ : \quad \mathbf{div}(\boldsymbol{\tau}) = 0 \quad \text{and} \quad \boldsymbol{\tau}^{\mathrm{t}} = \boldsymbol{\tau} \Big\} . \tag{3.7}$$

In turn, from a slight modification of [27, Lemma 2.3] (see also [15, Lemma 3.1]), there exists a positive constant c_ℓ such that

$$\|\boldsymbol{\tau}^{\mathrm{d}}\|_{\mathbb{L}^2(\Omega)} + \|\mathbf{div}(\boldsymbol{\tau})\|_{\mathbf{L}^\ell(\Omega)} \ \geq \ c_\ell \, \|\boldsymbol{\tau}\|_{\mathbb{L}^2(\Omega)} \qquad \forall\, \boldsymbol{\tau} \in \mathbb{X} . \tag{3.8}$$

Then, for each $\boldsymbol{\tau} \in \mathbb{V}$, we have that $\|\boldsymbol{\tau}^{\mathrm{d}}\|_{\mathbb{L}^2(\Omega)} \geq c_\ell \, \|\boldsymbol{\tau}\|_{\mathbb{L}^2(\Omega)} = c_\ell \, \|\boldsymbol{\tau}\|_{\mathbb{X}}$. Consequently, the monotonicity property of $\mathbf{A}$ (cf. (3.5a)) translates into a coercivity property in $\mathbb{V}$, meaning that

$$\big|[\mathbf{A}(\boldsymbol{\tau}), \boldsymbol{\tau}]\big| \geq \frac{c_\ell^2}{2\mu\rho_1} \, \|\boldsymbol{\tau}\|_{\mathbb{X}}^2 \qquad \forall\, \boldsymbol{\tau} \in \mathbb{V} . \tag{3.9}$$

Thus, noting that $\mathbf{A}$ and $\mathbf{C}$ are symmetric, having established (3.6) and (3.9), and bearing in mind that $\mathbf{C}$ is monotone (cf. (3.5a)), we can invoke [25, Theorem 3.4] to deduce that the following problem is well-posed: Given $(\mathcal{F}, \mathcal{G}) \in \mathbb{X}' \times \mathbf{Y}'$, find $(\boldsymbol{\sigma}, \underline{\mathbf{u}}) \in \mathbb{X} \times \mathbf{Y}$ such that

$$\begin{aligned} [\mathbf{A}(\boldsymbol{\sigma}), \boldsymbol{\tau}] + [\mathbf{B}'(\underline{\mathbf{u}}), \boldsymbol{\tau}] \ &= \ \mathcal{F}(\boldsymbol{\tau}) \quad \forall\, \boldsymbol{\tau} \in \mathbb{X} , \\ [\mathbf{B}(\boldsymbol{\sigma}), \underline{\mathbf{v}}] - [\mathbf{C}(\underline{\mathbf{u}}), \underline{\mathbf{v}}] \ &= \ \mathcal{G}(\underline{\mathbf{v}}) \quad \forall\, \underline{\mathbf{v}} \in \mathbf{Y} . \end{aligned}$$

This means that there exists a positive constant Λ, depending only on β, c_ℓ, μ, ρ_0, ρ_1, $\|\mathbf{K}^{-1}\|_{\mathbb{L}^\infty(\Omega)}$ and $|\Omega|$, such that, for all $(\boldsymbol{\zeta}, \underline{\mathbf{w}}) \in \mathbb{X} \times \mathbf{Y}$, there holds

$$\Lambda \, \|(\boldsymbol{\zeta}, \underline{\mathbf{w}})\|_{\mathbb{X} \times \mathbf{Y}} \leq \sup_{\mathbf{0} \neq (\boldsymbol{\tau}, \underline{\mathbf{v}}) \in \mathbb{X} \times \mathbf{Y}} \frac{[\mathbf{A}(\boldsymbol{\zeta}), \boldsymbol{\tau}] + [\mathbf{B}'(\underline{\mathbf{w}}), \boldsymbol{\tau}] + [\mathbf{B}(\boldsymbol{\zeta}), \underline{\mathbf{v}}] - [\mathbf{C}(\underline{\mathbf{w}}), \underline{\mathbf{v}}]}{\|(\boldsymbol{\tau}, \underline{\mathbf{v}})\|_{\mathbb{X} \times \mathbf{Y}}} . \tag{3.10}$$

3.2 Construction of compatible initial data and stability

In this section, we begin by constructing initial data $\boldsymbol{\gamma}_0$ and $\boldsymbol{\sigma}_0$ compatible with $\mathbf{u}_0$, a necessary step to apply Theorem 3.1 in the context of (3.3). We subsequently derive a stability result for problem (2.19).

Lemma 3.3. *Assume that the initial condition $\mathbf{u}_0$ belongs to $\mathbf{L}^s(\Omega) \cap \mathbf{H}$, where*

$$\mathbf{H} := \Big\{ \mathbf{v} \in \mathbf{H}_0^1(\Omega) \ : \quad \mathbf{div}(\rho\, \mathbf{e}(\mathbf{v})) \in \mathbf{L}^2(\Omega) \quad \textit{and} \quad \mathrm{div}(\rho\, \mathbf{v}) = 0 \quad \textit{in} \quad \Omega \Big\} . \tag{3.11}$$

Then there exist $\boldsymbol{\gamma}_0 \in \mathbb{L}^2_{\mathrm{skew}}(\Omega)$ and $\boldsymbol{\sigma}_0 \in \mathbb{X}$ such that, if we set $\underline{\mathbf{u}}_0 := (\mathbf{u}_0, \boldsymbol{\gamma}_0) \in \mathbf{Y}$, there holds

$$\begin{pmatrix} \mathbf{A} & \widetilde{\mathbf{B}}' \\ -\widetilde{\mathbf{B}} & \mathbf{C} \end{pmatrix} \begin{pmatrix} \boldsymbol{\sigma}_0 \\ \underline{\mathbf{u}}_0 \end{pmatrix} \in \{\mathbf{0}\} \times \big(\mathbf{L}^2(\Omega) \times \{\mathbf{0}\}\big) .$$

Proof. Given $\mathbf{u}_0 \in \mathbf{L}^s(\Omega) \cap \mathbf{H}$, we define

$$\boldsymbol{\sigma}_0 := 2\mu\, \rho\, \mathbf{e}(\mathbf{u}_0) + \kappa\, \mathbb{I} \quad \text{and} \quad \boldsymbol{\gamma}_0 := \nabla \mathbf{u}_0 - \mathbf{e}(\mathbf{u}_0) \quad \text{in} \quad \Omega , \tag{3.12}$$

with $\kappa \in \mathrm{R}$ chosen so that $(\mathrm{tr}(\boldsymbol{\sigma}_0), 1)_\Omega = 0$. Since $\mathbf{u}_0 \in \mathbf{H}$, we have $\mathrm{div}(\rho\, \mathbf{u}_0) = 0$ in Ω, which, as in (2.4), implies

$$\mathrm{div}(\mathbf{u}_0) = -\left(\frac{\nabla \rho}{\rho} \cdot \mathbf{u}_0 \right) \quad \text{in} \quad \Omega . \tag{3.13}$$

Then, noting that $\mathrm{tr}(\boldsymbol{\sigma}_0) = 2\mu\,\rho\,\mathrm{div}(\mathbf{u}_0) + d\,\kappa$ and using (3.13), we find that κ is certainly given by

$$\kappa = \frac{2\mu}{d\,|\Omega|}\big(\nabla\rho, \mathbf{u}_0\big)_\Omega\,.$$

Moreover, we observe that

$$\mathbf{div}(\boldsymbol{\sigma}_0) = 2\mu\,\mathbf{div}(\rho\,\mathbf{e}(\mathbf{u}_0)) \in \mathbf{L}^2(\Omega)\,,$$

so, consequently, $\boldsymbol{\sigma}_0 \in \mathbb{H}_0(\mathbf{div};\Omega) \subset \mathbb{X}$, where $\mathbb{H}_0(\mathbf{div};\Omega) := \mathbb{H}_0(\mathbf{div}_2;\Omega)$. In turn, using once more the fact that $\mathbf{u}_0 \in \mathbf{H}$, we deduce $\boldsymbol{\gamma}_0 \in \mathbb{L}^2_{\mathrm{skew}}(\Omega)$, with the skew-symmetry following directly from the definition of $\mathbf{e}(\mathbf{u}_0)$. In addition, from (3.12) we have $\frac{1}{2\mu\rho}\,\boldsymbol{\sigma}_0^{\mathrm{d}} = \mathbf{e}(\mathbf{u}_0)^{\mathrm{d}}$. Using this, the identity (3.13) and integrating by parts, which is valid since $\mathbf{u}_0 \in \mathbf{H}^1_0(\Omega)$, we then perform straightforward algebraic manipulations to readily obtain

$$[\mathbf{A}(\boldsymbol{\sigma}_0), \boldsymbol{\tau}] + [\widetilde{\mathbf{B}}'(\underline{\mathbf{u}}_0), \boldsymbol{\tau}] = 0 \qquad \forall\,\boldsymbol{\tau} \in \mathbb{X}\,. \tag{3.14}$$

In turn, one checks that

$$-[\widetilde{\mathbf{B}}(\boldsymbol{\sigma}_0), \underline{\mathbf{v}}] + [\mathbf{C}(\underline{\mathbf{u}}_0), \underline{\mathbf{v}}] = [\widetilde{\mathbf{G}}_0, \underline{\mathbf{v}}] \qquad \forall\,\underline{\mathbf{v}} \in \mathbf{L}^2(\Omega) \times \mathbb{L}^2_{\mathrm{skew}}(\Omega)\,, \tag{3.15}$$

where $\widetilde{\mathbf{G}}_0 = (\widetilde{\mathbf{g}}_0, \mathbf{0})$, with

$$[\widetilde{\mathbf{g}}_0, \mathbf{v}] = -2\mu\big(\mathbf{div}(\rho\,\mathbf{e}(\mathbf{u}_0)), \mathbf{v}\big)_\Omega + \frac{2\mu}{d}\,\big(\nabla\rho\cdot\mathbf{v}, \mathrm{div}(\mathbf{u}_0)\big)_\Omega + \kappa\left(\frac{\nabla\rho}{\rho}, \mathbf{v}\right)_\Omega + \mu(\mathbf{K}^{-1}\mathbf{u}_0, \mathbf{v})_\Omega\,.$$

Thus, according to (3.14) and (3.15), we have arrived at

$$\begin{pmatrix} \mathbf{A} & \widetilde{\mathbf{B}}' \\ -\widetilde{\mathbf{B}} & \mathbf{C} \end{pmatrix} \begin{pmatrix} \boldsymbol{\sigma}_0 \\ \underline{\mathbf{u}}_0 \end{pmatrix} = \begin{pmatrix} \mathbf{0} \\ \widetilde{\mathbf{G}}_0 \end{pmatrix}. \tag{3.16}$$

It remains to verify that $\widetilde{\mathbf{G}}_0$ belongs to $\mathbf{L}^2(\Omega) \times \{\mathbf{0}\}$. To this end, we apply the Cauchy–Schwarz inequality, use that $\nabla\rho/\rho \in \mathbf{L}^\infty(\Omega)$, exploit the identity (3.13), and then perform algebraic manipulations to obtain

$$\big|[\widetilde{\mathbf{g}}_0, \mathbf{v}]\big| \le \widetilde{C}_0 \left\{ \|\mathbf{div}(\rho\,\mathbf{e}(\mathbf{u}_0))\|_{\mathbf{L}^2(\Omega)} + \left(\left\|\frac{\nabla\rho}{\rho}\right\|^2_{\mathbf{L}^\infty(\Omega)} + \|\mathbf{K}^{-1}\|_{\mathbb{L}^\infty(\Omega)} \right) \|\mathbf{u}_0\|_{\mathbf{L}^2(\Omega)} \right\} \|\mathbf{v}\|_{\mathbf{L}^2(\Omega)}\,, \tag{3.17}$$

with $\widetilde{C}_0 := \mu\,\max\big\{2, 4\rho_1\,d^{-1} + 1\big\}$. This shows that $\widetilde{\mathbf{g}}_0$ is a linear and bounded functional on $\mathbf{L}^2(\Omega)$, and, therefore, $\widetilde{\mathbf{G}}_0 \in \mathbf{L}^2(\Omega) \times \{\mathbf{0}\}$, as desired. $\square$

Remark 3.1. *By a slight modification of the proof of Lemma 3.3, we also obtain compatible initial data for the original problem (2.19), constructed in the same way. More precisely, given $\mathbf{u}_0 \in \mathbf{L}^s(\Omega) \cap \mathbf{H}$, and taking $\boldsymbol{\sigma}_0$ and $\boldsymbol{\gamma}_0$ constructed as in (3.12), we have*

$$\begin{pmatrix} \mathbf{A} & \mathbf{B}' + \mathbf{D}'_\rho \\ -\mathbf{B} & \mathbf{C} \end{pmatrix} \begin{pmatrix} \boldsymbol{\sigma}_0 \\ \underline{\mathbf{u}}_0 \end{pmatrix} = \begin{pmatrix} \mathbf{0} \\ \mathbf{G}_0 \end{pmatrix}, \tag{3.18}$$

with $\mathbf{G}_0 := (\mathbf{g}_0, \mathbf{0})$, where

$$[\mathbf{g}_0, \mathbf{v}] := -2\mu\,\big(\mathbf{div}(\rho\,\mathbf{e}(\mathbf{u}_0)), \mathbf{v}\big)_\Omega + \mu\,\big(\mathbf{K}^{-1}\,\mathbf{u}_0, \mathbf{v}\big)_\Omega\,.$$

We next derive a stability result for the formulation (2.19), employing arguments that are similar in spirit to those in [23, Theorem 3.8] (see also [4, Theorem 3.9]).

Theorem 3.4. *Let $(\boldsymbol{\sigma}, \underline{\mathbf{u}}) : [0,T] \to \mathbb{X} \times \mathbf{Y}$ be a solution to (2.19), with $\mathbf{u}(0) = \mathbf{u}_0 \in \mathbf{L}^s(\Omega) \cap \mathbf{H}$ (cf. Lemma 3.3) and $\mathbf{f} \in \mathrm{L}^2(0,T;\mathbf{L}^2(\Omega))$. Suppose that the porosity satisfies*

$$\left\| \frac{\nabla \rho}{\rho} \right\|_{\mathbf{L}^\infty(\Omega)} \leq c_\rho \,, \quad \textit{with} \quad c_\rho := \frac{\sqrt{d}\,\Lambda}{2\,\|\mathbf{i}_{s,2}\|} \min\left\{ 1, \frac{\sqrt{\rho_0}}{4\rho_1} \right\}. \tag{3.19}$$

Then, $\boldsymbol{\sigma} \in \mathrm{L}^2(0,T;\mathbb{X})$, $\mathbf{u} \in \mathrm{H}^1(0,T;\mathbf{L}^2(\Omega)) \cap \mathrm{L}^2(0,T;\mathbf{L}^s(\Omega))$ and $\boldsymbol{\gamma} \in \mathrm{L}^2(0,T;\mathbb{L}^2_{\text{skew}}(\Omega))$. In addition, $\boldsymbol{\sigma}^{\mathrm{d}}(0) = \boldsymbol{\sigma}_0^{\mathrm{d}}$ and $\boldsymbol{\gamma}(0) = \boldsymbol{\gamma}_0$, where $\boldsymbol{\sigma}_0$ and $\boldsymbol{\gamma}_0$ are given in (3.12). Moreover, there exists a positive constant C_{B}, depending only on μ, ρ_0, ρ_1, $C_{\mathbf{K}}$, $\|\mathbf{K}^{-1}\|_{\mathbf{L}^\infty(\Omega)}$, Λ and $|\Omega|$, such that

$$\begin{aligned} &\|\boldsymbol{\sigma}\|^2_{\mathrm{L}^2(0,T;\mathbb{X})} + \|\mathbf{u}\|^2_{\mathrm{L}^2(0,T;\mathbf{L}^s(\Omega))} + \|\mathbf{u}\|^2_{\mathrm{L}^\infty(0,T;\mathbf{L}^2(\Omega))} + \|\boldsymbol{\gamma}\|^2_{\mathrm{L}^2(0,T;\mathbb{L}^2(\Omega))} \\ &\qquad \leq C_{\mathrm{B}} \left\{ \|\mathbf{f}\|^2_{\mathrm{L}^2(0,T;\mathbf{L}^2(\Omega))} + \|\mathbf{u}_0\|^2_{\mathbf{L}^2(\Omega)} + \|\mathbf{e}(\mathbf{u}_0)\|^2_{\mathbb{L}^2(\Omega)} \right\}. \end{aligned} \tag{3.20}$$

Proof. Let $(\boldsymbol{\sigma}, \underline{\mathbf{u}}) : [0,T] \to \mathbb{X} \times \mathbf{Y}$ be a solution to (2.19). Then, we have the identity

$$[\mathbf{A}(\boldsymbol{\sigma}), \boldsymbol{\tau}] + [\mathbf{B}'(\underline{\mathbf{u}}), \boldsymbol{\tau}] + [\mathbf{B}(\boldsymbol{\sigma}), \underline{\mathbf{v}}] - [\mathbf{C}(\underline{\mathbf{u}}), \underline{\mathbf{v}}] = -[\mathbf{D}'_\rho(\underline{\mathbf{u}}), \boldsymbol{\tau}] + [\partial_t \mathbf{E}(\underline{\mathbf{u}}), \underline{\mathbf{v}}] - [\mathbf{F}, \underline{\mathbf{v}}]\,,$$

for all $(\boldsymbol{\tau}, \underline{\mathbf{v}}) \in \mathbb{X} \times \mathbf{Y}$. Using this into (3.10), and then applying the estimates (3.4b), (3.4c), (3.4e), and (3.19), we arrive at

$$\begin{aligned} \Lambda\,\|(\boldsymbol{\sigma}, \underline{\mathbf{u}})\|_{\mathbb{X}\times\mathbf{Y}} &\leq \sup_{\mathbf{0} \neq (\boldsymbol{\tau}, \underline{\mathbf{v}}) \in \mathbb{X}\times\mathbf{Y}} \frac{[\partial_t \mathbf{E}(\underline{\mathbf{u}}), \underline{\mathbf{v}}] - [\mathbf{D}'_\rho(\underline{\mathbf{u}}), \boldsymbol{\tau}] - [\mathbf{F}, \underline{\mathbf{v}}]}{\|(\boldsymbol{\tau}, \underline{\mathbf{v}})\|_{\mathbb{X}\times\mathbf{Y}}} \\ &\leq \rho_1\,\|\mathbf{i}_{s,2}\|\,\|\partial_t \mathbf{u}\|_{\mathbf{L}^2(\Omega)} + \frac{c_\rho}{\sqrt{d}}\,\|\mathbf{i}_{s,2}\|\,\|\mathbf{u}\|_{\mathbf{L}^s(\Omega)} + \|\mathbf{i}_{s,2}\|\,\|\mathbf{f}\|_{\mathbf{L}^2(\Omega)}\,. \end{aligned}$$

Now, using the fact that $c_\rho \leq \sqrt{d}\,\Lambda/(2\,\|\mathbf{i}_{s,2}\|)$, squaring and integrating over $[0,T]$, we obtain

$$\begin{aligned} &C_1 \left(\|\boldsymbol{\sigma}\|^2_{\mathrm{L}^2(0,T;\mathbb{X})} + \|\mathbf{u}\|^2_{\mathrm{L}^2(0,T;\mathbf{L}^s(\Omega))} + \|\boldsymbol{\gamma}\|^2_{\mathrm{L}^2(0,T;\mathbb{L}^2(\Omega))} \right) \\ &\qquad \leq \int_0^T \|\partial_t \mathbf{u}\|^2_{\mathbf{L}^2(\Omega)}\,dt + \rho_1^{-2}\,\|\mathbf{f}\|^2_{\mathrm{L}^2(0,T;\mathbf{L}^2(\Omega))}\,, \end{aligned} \tag{3.21}$$

where $C_1 := \Lambda^2/(8\,\|\mathbf{i}_{s,2}\|^2\,\rho_1^2)$.

In order to bound the integral on the right-hand side of (3.21), we differentiate in time the first equation in (2.19), test the system against $(\boldsymbol{\sigma}, \partial_t \underline{\mathbf{u}})$, and, then, after summing both equations, applying the monotonicity properties (cf. (3.5a) and (3.5b)), and using Cauchy–Schwarz and Young's inequalities (cf. (1.1)), we get

$$\begin{aligned} &\partial_t \left(\frac{1}{4\mu} \left(\frac{1}{\rho}\,\boldsymbol{\sigma}^{\mathrm{d}}, \boldsymbol{\sigma}^{\mathrm{d}} \right)_\Omega + \frac{\mu}{2}\,(\mathbf{K}^{-1}\mathbf{u}, \mathbf{u})_\Omega \right) + \rho_0\,\|\partial_t \mathbf{u}\|^2_{\mathbf{L}^2(\Omega)} = (\mathbf{f}, \partial_t \mathbf{u})_\Omega + \frac{1}{d} \left(\frac{\nabla \rho}{\rho} \cdot \partial_t \mathbf{u}, \operatorname{tr}(\boldsymbol{\sigma}) \right)_\Omega \\ &\qquad \leq \frac{1}{2\delta}\,\|\mathbf{f}\|^2_{\mathbf{L}^2(\Omega)} + \frac{\delta}{2}\,\|\partial_t \mathbf{u}\|^2_{\mathbf{L}^2(\Omega)} + \frac{\tilde{\delta}}{2\sqrt{d}}\,c_\rho\,\|\partial_t \mathbf{u}\|^2_{\mathbf{L}^2(\Omega)} + \frac{c_\rho}{2\tilde{\delta}\sqrt{d}}\,\|\boldsymbol{\sigma}\|^2_{\mathbb{L}^2(\Omega)}\,, \end{aligned}$$

whence, by choosing $\delta = \rho_0$ and $\tilde{\delta} = \sqrt{d}\,\rho_0/(2\,c_\rho)$, it follows that

$$\partial_t \left(\frac{1}{2\mu} \left(\frac{1}{\rho}\,\boldsymbol{\sigma}^{\mathrm{d}}, \boldsymbol{\sigma}^{\mathrm{d}} \right)_\Omega + \mu\,(\mathbf{K}^{-1}\mathbf{u}, \mathbf{u})_\Omega \right) + \frac{\rho_0}{2}\,\|\partial_t \mathbf{u}\|^2_{\mathbf{L}^2(\Omega)} \leq \frac{1}{\rho_0}\,\|\mathbf{f}\|^2_{\mathbf{L}^2(\Omega)} + \frac{2\,c_\rho^2}{d\,\rho_0}\,\|\boldsymbol{\sigma}\|^2_{\mathbb{L}^2(\Omega)}\,. \tag{3.22}$$

Now, integrating from 0 to $t \in (0,T]$, and using (2.2), (2.3), together with the fact that $\mathbf{K}^{-1} \in \mathbb{L}^\infty(\Omega)$, we perform some algebraic manipulations so that the previous estimate becomes

$$\begin{aligned} &\frac{1}{\mu\rho_0\rho_1}\,\|\boldsymbol{\sigma}^{\mathrm{d}}(t)\|^2_{\mathbb{L}^2(\Omega)} + \frac{2\mu C_{\mathbf{K}}}{\rho_0}\,\|\mathbf{u}(t)\|^2_{\mathbf{L}^2(\Omega)} + \int_0^t \|\partial_t \mathbf{u}(\mathrm{s})\|^2_{\mathbf{L}^2(\Omega)}\,ds \\ &\quad \leq \frac{2}{\rho_0^2}\int_0^t \|\mathbf{f}(\mathrm{s})\|^2_{\mathbf{L}^2(\Omega)}\,ds + \frac{4c_\rho^2}{d\rho_0^2}\int_0^t \|\boldsymbol{\sigma}(\mathrm{s})\|^2_{\mathbb{L}^2(\Omega)}\,ds + \frac{1}{\mu\rho_0^2}\,\|\boldsymbol{\sigma}^{\mathrm{d}}(0)\|^2_{\mathbb{L}^2(\Omega)} \\ &\quad + \frac{2\mu}{\rho_0}\,\|\mathbf{K}^{-1}\|_{\mathbb{L}^\infty(\Omega)}\,\|\mathbf{u}(0)\|^2_{\mathbf{L}^2(\Omega)}\,, \end{aligned} \tag{3.23}$$

for all $t \in (0,T]$. We now use that $4c_\rho^2/(d\rho_0^2) \leq C_1/2$ (cf. (3.19)), and, by a straightforward application of the definition of the Bochner norms, (3.23) implies that

$$\begin{aligned} \int_0^T \|\partial_t \mathbf{u}(t)\|^2_{\mathbf{L}^2(\Omega)}\,dt &\leq \frac{2}{\rho_0^2}\,\|\mathbf{f}\|^2_{\mathrm{L}^2(0,T;\mathbf{L}^2(\Omega))} + \frac{C_1}{2}\,\|\boldsymbol{\sigma}\|^2_{\mathrm{L}^2(0,T,\mathbb{L}^2(\Omega))} + \frac{1}{\mu\rho_0^2}\,\|\boldsymbol{\sigma}^{\mathrm{d}}(0)\|^2_{\mathbb{L}^2(\Omega)} \\ &\quad + \frac{2\,\mu}{\rho_0}\,\|\mathbf{K}^{-1}\|_{\mathbb{L}^\infty(\Omega)}\,\|\mathbf{u}(0)\|^2_{\mathbf{L}^2(\Omega)} - \frac{2\,\mu\,C_{\mathbf{K}}}{\rho_0}\,\|\mathbf{u}\|^2_{\mathrm{L}^\infty(0,T;\mathbf{L}^2(\Omega))}\,, \end{aligned} \tag{3.24}$$

which proves that $\partial_t \mathbf{u} \in \mathrm{L}^2(0,T;\mathbf{L}^2(\Omega))$. We have neglected the first term in (3.23) in order to simplify the estimate.

Next, to bound the term $\|\boldsymbol{\sigma}^{\mathrm{d}}(0)\|^2_{\mathbb{L}^2(\Omega)}$ in (3.24), we first notice that the first equation in (2.19) implies that the left-hand side, as a function from $[0,T]$ to R, belongs to the same $\mathrm{L}^\infty(0,T)$-class as the null function. Consequently, the left-hand side can be viewed as a continuous function in time and we can let $t \to 0^+$ in the first equation of (2.19), use the fact that $\mathbf{u}(0) = \mathbf{u}_0$, and subtract it from the first row of (3.18) with $\boldsymbol{\sigma}_0$ and $\boldsymbol{\gamma}_0$ constructed as in (3.12), thus obtaining

$$[\mathbf{A}(\boldsymbol{\sigma}_0 - \boldsymbol{\sigma}(0)), \boldsymbol{\tau}] + (\boldsymbol{\gamma}_0 - \boldsymbol{\gamma}(0), \boldsymbol{\tau})_\Omega = 0 \qquad \forall\, \boldsymbol{\tau} \in \mathbb{X}\,. \tag{3.25}$$

In turn, by testing the second equation in (2.19) with $\underline{\mathbf{v}} = (\mathbf{0}, \boldsymbol{\eta}(t))$ and letting $t \to 0^+$, which is valid by the same reasoning mentioned above, we obtain that $\boldsymbol{\sigma}(0)$ is weakly symmetric. Since $\boldsymbol{\sigma}_0$ is also symmetric (cf. (3.12)), it follows that $\boldsymbol{\sigma}_0 - \boldsymbol{\sigma}(0)$ is weakly symmetric. Then, testing (3.25) with $\boldsymbol{\tau} = \boldsymbol{\sigma}_0 - \boldsymbol{\sigma}(0)$, and observing that the second term vanishes by weak symmetry, we get

$$[\mathbf{A}(\boldsymbol{\sigma}_0 - \boldsymbol{\sigma}(0)), \boldsymbol{\sigma}_0 - \boldsymbol{\sigma}(0)] = 0\,.$$

In view of the monotonicity of $\mathbf{A}$ (cf. (3.5a)), this implies $\boldsymbol{\sigma}^{\mathrm{d}}(0) = \boldsymbol{\sigma}_0^{\mathrm{d}}$. As a consequence, using the inf-sup condition (3.6) together with (3.25), we obtain directly that $\boldsymbol{\gamma}(0) = \boldsymbol{\gamma}_0$. Moreover, from (3.12) and (2.3), we also deduce that

$$\|\boldsymbol{\sigma}^{\mathrm{d}}(0)\|_{\mathbb{L}^2(\Omega)} = \|\boldsymbol{\sigma}_0^{\mathrm{d}}\|_{\mathbb{L}^2(\Omega)} \leq 2\mu\,\rho_1\,\|\mathbf{e}(\mathbf{u}_0)\|_{\mathbb{L}^2(\Omega)}\,.$$

Finally, replacing this into (3.24), and combining it with (3.21), gives (3.20), with constant

$$C_{\mathtt{B}} := \frac{2\,\max\left\{\rho_0^2 + 2\rho_1^2\,,\, 4\mu\,\rho_0^2\,\rho_1^2\,,\, 2\mu\,\rho_0\,\rho_1^2\,\|\mathbf{K}^{-1}\|_{\mathbb{L}^\infty(\Omega)}\right\}}{\min\left\{C_1\,\rho_0^2\,\rho_1^2\,,\, 4\mu\,C_{\mathbf{K}}\,\rho_0\,\rho_1^2\right\}}\,.$$

$\square$

3.3 A fixed-point strategy

In order to establish the well-posedness of (2.19), we shall prove that, under certain conditions on the porosity, the problem (3.3) has a unique solution. To that end, we propose a fixed-point strategy. Let $\mathcal{J} : \mathrm{L}^2(0,T;\mathbb{X}) \to \mathrm{L}^2(0,T;\mathbb{X})$ be the operator defined as

$$\mathcal{J}(\boldsymbol{\zeta}) := \boldsymbol{\sigma} \qquad \forall\, \boldsymbol{\zeta} \in \mathrm{L}^2(0,T;\mathbb{X})\,,$$

where $(\boldsymbol{\sigma}, \underline{\mathbf{u}})$ is the unique solution (to be confirmed below) to

$$\begin{aligned} [\mathbf{A}(\boldsymbol{\sigma}(t)), \boldsymbol{\tau}] + [\widetilde{\mathbf{B}}'(\underline{\mathbf{u}}(t)), \boldsymbol{\tau}] &= 0 && \forall\, \boldsymbol{\tau} \in \mathbb{X}\,, \\ \frac{\partial}{\partial t}\,[\mathbf{E}(\underline{\mathbf{u}}(t)), \underline{\mathbf{v}}] - [\widetilde{\mathbf{B}}(\boldsymbol{\sigma}(t)), \underline{\mathbf{v}}] + [\mathbf{C}(\underline{\mathbf{u}}(t)), \underline{\mathbf{v}}] &= [\widetilde{\mathbf{F}}_{\boldsymbol{\zeta}}(t), \underline{\mathbf{v}}] && \forall\, \underline{\mathbf{v}} \in \mathbf{Y}\,, \end{aligned} \tag{3.26}$$

for a.e. $t \in (0,T)$ and $\mathbf{u}(0) = \mathbf{u}_0$. We stress here that the operator $\mathcal{J}$ is naturally defined on $\mathrm{L}^2(0,T;\mathbb{X})$, as motivated by the stability result (cf. Theorem 3.4). Notice also that solving (3.3) is equivalent to finding a solution to the fixed-point equation

$$\mathcal{J}(\boldsymbol{\sigma}) = \boldsymbol{\sigma}\,. \tag{3.27}$$

Now, to show that $\mathcal{J}$ is well-defined, we shall prove that (3.26) admits a unique solution by employing Theorem 3.1. For this purpose, we observe that (3.26) can be written in the form of (3.2) with

$$E = \mathbb{X} \times \mathbf{Y}\,, \quad u = (\boldsymbol{\sigma}, \underline{\mathbf{u}})\,, \quad \mathcal{N} = \begin{pmatrix} \mathbf{0} & \mathbf{0} \\ \mathbf{0} & \mathbf{E} \end{pmatrix} \quad \text{and} \quad \mathcal{M} = \begin{pmatrix} \mathbf{A} & \widetilde{\mathbf{B}}' \\ -\widetilde{\mathbf{B}} & \mathbf{C} \end{pmatrix}. \tag{3.28}$$

Let E'_b denote the Hilbert space defined as the dual of $(\mathbb{X} \times \mathbf{Y}, |\cdot|_b)$, where $|\cdot|_b$ is the seminorm induced by $\mathbf{E}$ (cf. (3.1)), and is given by

$$|(\boldsymbol{\tau}, \underline{\mathbf{v}})|_b = (\rho\,\mathbf{v}, \mathbf{v})_\Omega^{1/2} \qquad \forall\,(\boldsymbol{\tau}, \underline{\mathbf{v}}) \in \mathbb{X} \times \mathbf{Y}\,.$$

Since ρ is positive and bounded (cf. (2.3)), it is straightforward to show that E'_b is isomorphic to $\{\mathbf{0}\} \times \big(\mathbf{L}^2(\Omega) \times \{\mathbf{0}\}\big)$. Accordingly, we are able to define the spaces

$$E'_b := \{\mathbf{0}\} \times \big(\mathbf{L}^2(\Omega) \times \{\mathbf{0}\}\big) \quad \text{and} \quad \mathcal{D} := \Big\{(\boldsymbol{\tau}, \underline{\mathbf{v}}) \in \mathbb{X} \times \mathbf{Y} :\; \mathcal{M}(\boldsymbol{\tau}, \underline{\mathbf{v}}) \in E'_b\Big\}\,.$$

Notice that the range condition in Theorem 3.1 is equivalent to prove the existence of a solution to the following resolvent system: Find $(\boldsymbol{\sigma}, \underline{\mathbf{u}}) \in \mathbb{X} \times \mathbf{Y}$ such that

$$\begin{aligned} [\mathbf{A}(\boldsymbol{\sigma}), \boldsymbol{\tau}] + [\widetilde{\mathbf{B}}'(\underline{\mathbf{u}}), \boldsymbol{\tau}] &= 0 && \forall\, \boldsymbol{\tau} \in \mathbb{X}\,, \\ [\widetilde{\mathbf{B}}(\boldsymbol{\sigma}), \underline{\mathbf{v}}] - [(\mathbf{E} + \mathbf{C})(\underline{\mathbf{u}}), \underline{\mathbf{v}}] &= -(\widehat{\mathbf{f}}, \mathbf{v})_\Omega && \forall\, \underline{\mathbf{v}} \in \mathbf{Y}\,, \end{aligned} \tag{3.29}$$

where $\widehat{\mathbf{f}} \in \mathbf{L}^2(\Omega)$ so that $(\mathbf{0}, (\widehat{\mathbf{f}}, \mathbf{0}))$ represents an arbitrary element of E'_b. In a similar way to how we proved the global inf-sup condition (3.10), we shall invoke [25, Theorem 3.4] to establish the well-posedness of (3.29). In this way, we now focus on verifying the hypotheses of this theorem, starting with the inf-sup condition of the operator $\widetilde{\mathbf{B}}$. Notice that, in order to relax the assumption on the datum ρ, in the following two intermediate lemmas we can suppose $\nabla\rho/\rho \in \mathbf{L}^r(\Omega)$ with $r = 2s/(s-2)$ as in (2.12).

Lemma 3.5. *Assume that the porosity satisfies*

$$\left\| \frac{\nabla \rho}{\rho} \right\|_{\mathbf{L}^r(\Omega)} \leq \frac{\sqrt{d}\, \beta}{2}\,, \tag{3.30}$$

with β as given in (3.6). Then, the following inf-sup condition holds:

$$\sup_{0 \neq \boldsymbol{\tau} \in \mathbb{X}} \frac{[\widetilde{\mathbf{B}}(\boldsymbol{\tau}), \underline{\mathbf{v}}]}{\|\boldsymbol{\tau}\|_{\mathbb{X}}} \geq \frac{\beta}{2} \, \|\underline{\mathbf{v}}\|_{\mathbf{Y}} \qquad \forall\, \underline{\mathbf{v}} \in \mathbf{Y}\,.$$

Proof. Since $\mathbf{L}^\infty(\Omega) \hookrightarrow \mathbf{L}^r(\Omega)$, we can use (2.12) to bound $\mathbf{D}_\rho$, and then employ the assumption (3.30) along with the inf-sup condition of $\mathbf{B}$ (cf. (3.6)), to obtain

$$\sup_{0 \neq \boldsymbol{\tau} \in \mathbb{X}} \frac{[\widetilde{\mathbf{B}}(\boldsymbol{\tau}), \underline{\mathbf{v}}]}{\|\boldsymbol{\tau}\|_{\mathbb{X}}} \geq \sup_{0 \neq \boldsymbol{\tau} \in \mathbb{X}} \frac{[\mathbf{B}(\boldsymbol{\tau}), \underline{\mathbf{v}}]}{\|\boldsymbol{\tau}\|_{\mathbb{X}}} - \frac{1}{\sqrt{d}} \left\| \frac{\nabla \rho}{\rho} \right\|_{\mathbf{L}^r(\Omega)} \|\underline{\mathbf{v}}\|_{\mathbf{Y}} \geq \frac{\beta}{2} \, \|\underline{\mathbf{v}}\|_{\mathbf{Y}}\,.$$

□

Let $\widetilde{\mathbb{V}}$ be the kernel of the operator $\widetilde{\mathbf{B}}$, which, by standard duality and orthogonality arguments, can be characterized as

$$\widetilde{\mathbb{V}} = \left\{ \boldsymbol{\tau} \in \mathbb{X} \;:\quad \mathbf{div}(\boldsymbol{\tau}) = \frac{1}{d} \frac{\nabla \rho}{\rho} \operatorname{tr}(\boldsymbol{\tau}) \quad \text{and} \quad \boldsymbol{\tau}^{\mathrm{t}} = \boldsymbol{\tau} \right\}. \tag{3.31}$$

Employing this subspace, we now establish an inf-sup condition for $\mathbf{A}$.

Lemma 3.6. *Let c_ℓ be as in (3.8), and assume that the porosity satisfies*

$$\left\| \frac{\nabla \rho}{\rho} \right\|_{\mathbf{L}^r(\Omega)} \leq \frac{\sqrt{d}\, c_\ell}{2}\,. \tag{3.32}$$

Then, there exists a positive constant α, depending only on μ, ρ_1 and c_ℓ, such that

$$\sup_{0 \neq \boldsymbol{\tau} \in \widetilde{\mathbb{V}}} \frac{[\mathbf{A}(\boldsymbol{\sigma}), \boldsymbol{\tau}]}{\|\boldsymbol{\tau}\|_{\mathbb{X}}} \geq \alpha \, \|\boldsymbol{\sigma}\|_{\mathbb{X}} \qquad \forall\, \boldsymbol{\sigma} \in \widetilde{\mathbb{V}}\,.$$

Proof. Given $\boldsymbol{\sigma} \in \widetilde{\mathbb{V}}$, we have $\mathbf{div}(\boldsymbol{\sigma}) = \frac{1}{d} (\nabla\rho/\rho) \operatorname{tr}(\boldsymbol{\sigma})$ (cf. (3.31)). From this identity, we apply Hölder's inequality, use (3.32) and the fact that $\|\operatorname{tr}(\boldsymbol{\sigma})\|_{\mathrm{L}^2(\Omega)} \leq \sqrt{d}\, \|\boldsymbol{\sigma}\|_{\mathbb{L}^2(\Omega)}$, to get

$$\|\mathbf{div}(\boldsymbol{\sigma})\|_{\mathbf{L}^\ell(\Omega)} \leq \frac{1}{d} \left\| \frac{\nabla \rho}{\rho} \right\|_{\mathbf{L}^r(\Omega)} \|\operatorname{tr}(\boldsymbol{\sigma})\|_{\mathrm{L}^2(\Omega)} \leq \frac{c_\ell}{2} \, \|\boldsymbol{\sigma}\|_{\mathbb{L}^2(\Omega)}\,. \tag{3.33}$$

Combining this estimate with (3.8) gives $\frac{c_\ell}{2} \|\boldsymbol{\sigma}\|_{\mathbb{L}^2(\Omega)} \leq \|\boldsymbol{\sigma}^{\mathrm{d}}\|_{\mathbb{L}^2(\Omega)}$. Then, adding to both sides $\frac{1}{2} \|\mathbf{div}(\boldsymbol{\sigma})\|_{\mathbf{L}^\ell(\Omega)}$ and using again (3.33), we obtain

$$\frac{c_\ell}{2} \, \|\boldsymbol{\sigma}\|_{\mathbb{L}^2(\Omega)} + \frac{1}{2} \, \|\mathbf{div}(\boldsymbol{\sigma})\|_{\mathbf{L}^\ell(\Omega)} \leq \|\boldsymbol{\sigma}^{\mathrm{d}}\|_{\mathbb{L}^2(\Omega)} + \frac{c_\ell}{4} \, \|\boldsymbol{\sigma}\|_{\mathbb{L}^2(\Omega)}\,.$$

Consequently,

$$\frac{1}{4} \, \min\{c_\ell, 2\} \, \|\boldsymbol{\sigma}\|_{\mathbb{X}} \leq \|\boldsymbol{\sigma}^{\mathrm{d}}\|_{\mathbb{L}^2(\Omega)}\,.$$

Hence, by using the boundedness of ρ (cf. (2.3)) together with the above estimate, we arrive at

$$\sup_{0 \neq \boldsymbol{\tau} \in \widetilde{\mathbb{V}}} \frac{[\mathbf{A}(\boldsymbol{\sigma}), \boldsymbol{\tau}]}{\|\boldsymbol{\tau}\|_{\mathbb{X}}} \geq \frac{\|\boldsymbol{\sigma}^{\mathrm{d}}\|^2_{\mathbb{L}^2(\Omega)}}{2\mu\rho_1 \, \|\boldsymbol{\sigma}\|_{\mathbb{X}}} \geq \frac{\min\{c_\ell^2, 4\}}{32\mu\rho_1} \, \|\boldsymbol{\sigma}\|_{\mathbb{X}}\,,$$

which completes the proof with $\alpha = \min\{c_\ell^2, 4\}/(32\mu\rho_1)$. □

Lemma 3.7. *Suppose that the porosity satisfies* (3.30) *and* (3.32). *Then, for all* $\widehat{\mathbf{f}} \in \mathbf{L}^2(\Omega)$, *there exists a unique solution to* (3.29).

Proof. It is clear from the definition of $\mathbf{A}$ and $\mathbf{E}+\mathbf{C}$ (cf. (2.20a), (2.20d) and (2.20e)) that they induce symmetric bilinear forms. Furthermore, from the monotonicity of $\mathbf{A}$, $\mathbf{E}$ and $\mathbf{C}$ (cf. (3.5a) and (3.5b)), we have

$$[\mathbf{A}(\boldsymbol{\tau}),\boldsymbol{\tau}] \geq \frac{1}{2\mu\rho_1}\,\|\boldsymbol{\tau}^{\mathrm{d}}\|^2_{\mathbb{L}^2(\Omega)} \geq 0 \quad \text{and} \quad [(\mathbf{E}+\mathbf{C})(\underline{\mathbf{v}}),\underline{\mathbf{v}}] \geq (\rho_0 + \mu\, C_{\mathbf{K}})\,\|\mathbf{v}\|^2_{\mathbf{L}^2(\Omega)} \geq 0\,,$$

for all $\boldsymbol{\tau} \in \mathbb{X}$ and $\underline{\mathbf{v}} \in \mathbf{Y}$, which means that $\mathbf{A}$ and $\mathbf{E}+\mathbf{C}$ induce positive semi-definite bilinear forms. On the other hand, by Lemmas 3.5 and 3.6, we also have the inf-sup conditions required by [25, Theorem 3.4]. Thus, applying this result in our context, we conclude that, for each $\widehat{\mathbf{f}} \in \mathbf{L}^2(\Omega)$, (3.29) is well-posed. □

With this result at hand, we are in a position to prove the well-posedness of (3.26), and hence that $\mathcal{J}$ is well-defined.

Theorem 3.8. *Suppose that the porosity* ρ *satisfies* (3.19), (3.30) *and* (3.32). *Furthermore, let* $\mathbf{f} \in \mathrm{W}^{1,1}(0,T;\mathbf{L}^2(\Omega)) \cap \mathrm{L}^2(0,T;\mathbf{L}^2(\Omega))$ *and* $\mathbf{u}_0 \in \mathbf{L}^s(\Omega) \cap \mathbf{H}$ *(cf.* (3.11)*) be given. Then, the operator* $\mathcal{J}$ *is well-defined. In particular, for each* $\boldsymbol{\zeta} \in \mathrm{L}^2(0,T;\mathbb{X})$, *there exists a unique solution* $(\boldsymbol{\sigma},\underline{\mathbf{u}})$ *to* (3.26) *such that* $\boldsymbol{\sigma} \in \mathrm{L}^2(0,T;\mathbb{X})$, $\mathbf{u} \in \mathrm{W}^{1,\infty}(0,T;\mathbf{L}^2(\Omega)) \cap \mathrm{L}^2(0,T;\mathbf{L}^s(\Omega))$, $\boldsymbol{\gamma} \in \mathrm{L}^2(0,T;\mathbb{L}^2_{\mathrm{skew}}(\Omega))$, $\mathbf{u}(0) = \mathbf{u}_0$, $\boldsymbol{\sigma}^{\mathrm{d}}(0) = \boldsymbol{\sigma}^{\mathrm{d}}_0$, $\boldsymbol{\gamma}(0) = \boldsymbol{\gamma}_0$ *(cf.* (3.12)*), and* $\mathcal{J}(\boldsymbol{\zeta}) = \boldsymbol{\sigma}$. *Moreover, there exist positive constants* $\widetilde{C}_{\mathrm{B}}$ *and* $C_{\mathcal{J}}$, *with* $\widetilde{C}_{\mathrm{B}}$ *depending only on* μ, ρ_0, ρ_1, $\|\mathbf{K}^{-1}\|_{\mathbb{L}^\infty(\Omega)}$, Λ, d *and* $|\Omega|$, *and* $C_{\mathcal{J}}$ *depending only on* ρ_0, ρ_1, Λ, d *and* $|\Omega|$, *such that*

$$\begin{aligned}\|\mathcal{J}(\boldsymbol{\zeta})\|_{\mathrm{L}^2(0,T;\mathbb{X})} \leq \widetilde{C}_{\mathrm{B}}\Big\{\|\mathbf{f}\|_{\mathrm{L}^2(0,T;\mathbf{L}^2(\Omega))} + \|\mathbf{u}_0\|_{\mathbf{L}^2(\Omega)} + \|\mathbf{e}(\mathbf{u}_0)\|_{\mathbb{L}^2(\Omega)}\Big\} \\ + C_{\mathcal{J}}\left\|\frac{\nabla\rho}{\rho}\right\|_{\mathbf{L}^\infty(\Omega)}\|\boldsymbol{\zeta}\|_{\mathrm{L}^2(0,T;\mathbb{X})}\,.\end{aligned} \tag{3.34}$$

Proof. Recalling the notation introduced in (3.28), we note that $\mathcal{N}$ is linear, symmetric, and monotone, which follow directly from the properties of $\mathbf{E}$. Similarly, $\mathcal{M}$ is monotone since both $\mathbf{A}$ and $\mathbf{C}$ are monotone. Moreover, by Lemma 3.7, for all $(\mathbf{0},(\widehat{\mathbf{f}},\mathbf{0})) \in E'_b$, there exists a unique $(\boldsymbol{\sigma},\underline{\mathbf{u}}) \in \mathbb{X}\times\mathbf{Y}$ such that $(\mathcal{N}+\mathcal{M})(\boldsymbol{\sigma},\underline{\mathbf{u}}) = (\mathbf{0},(\widehat{\mathbf{f}},\mathbf{0}))$. This implies that $E'_b = R(\mathcal{N}+\mathcal{M})$. Furthermore, owing to the fact that $\mathbf{u}_0 \in \mathbf{L}^s(\Omega)\cap\mathbf{H}$, Lemma 3.3 ensures the existence of compatible initial data such that $(\boldsymbol{\sigma}_0,\underline{\mathbf{u}}_0) \in \mathcal{D}$. Thus, by Theorem 3.1, we deduce the existence of a solution $(\boldsymbol{\sigma},\underline{\mathbf{u}})$ to (3.26), where $\mathbf{u} \in \mathrm{W}^{1,\infty}(0,T;\mathbf{L}^2(\Omega))$, $\mathcal{M}(\boldsymbol{\sigma}(t),\underline{\mathbf{u}}(t)) \in E'_b$, and $\mathbf{u}(0) = \mathbf{u}_0$. Moreover, by an argument similar to that in the proof of Theorem 3.4, we obtain $\boldsymbol{\sigma}^{\mathrm{d}}(0) = \boldsymbol{\sigma}^{\mathrm{d}}_0$, $\boldsymbol{\gamma}(0) = \boldsymbol{\gamma}_0$, and the desired regularity of the solution. In particular, proceeding as in (3.20), we get the following estimate for $\boldsymbol{\sigma}$:

$$\begin{aligned}\|\boldsymbol{\sigma}\|^2_{\mathrm{L}^2(0,T;\mathbb{X})} \leq C_1\Big\{\|\mathbf{f}\|^2_{\mathrm{L}^2(0,T;\mathbf{L}^2(\Omega))} + \|\mathbf{u}_0\|^2_{\mathbf{L}^2(\Omega)} + \|\mathbf{e}(\mathbf{u}_0)\|^2_{\mathbb{L}^2(\Omega)}\Big\} \\ + C_2\left\|\frac{\nabla\rho}{\rho}\right\|^2_{\mathbf{L}^\infty(\Omega)}\|\boldsymbol{\zeta}\|^2_{\mathrm{L}^2(0,T;\mathbb{X})}\,,\end{aligned} \tag{3.35}$$

where

$$C_1 := \frac{16\,\max\left\{\rho_0^2 + 2\rho_1^2\,,\, 4\mu\,\rho_0^2\,\rho_1^2\,,\, 2\mu\,\rho_0\,\rho_1^2\,\|\mathbf{K}^{-1}\|_{\mathbb{L}^\infty(\Omega)}\right\}}{\Lambda^2\,\rho_0^2\,\|\mathbf{i}_{s,2}\|^{-2}} \quad \text{and} \quad C_2 := \frac{16\,(\rho_0^2 + 4\rho_1^2)\,d^{-1}}{\Lambda^2\,\rho_0^2\,\|\mathbf{i}_{s,2}\|^{-2}}\,.$$

Then, by taking the square root in (3.35), some algebraic manipulations yield (3.34). To prove uniqueness of the solution, by linearity of the problem, it suffices to show that (3.26) admits only the trivial solution with the data $\mathbf{f} = \mathbf{0}$, $\mathbf{u}_0 = \mathbf{0}$, and $\boldsymbol{\zeta} = \mathbf{0}$. Certainly, one can establish estimates for $\mathbf{u}$ and $\boldsymbol{\gamma}$ similar to (3.35), once again relying on the arguments employed in the proof of Theorem 3.4. In this way, from (3.35), it turns out that if the data vanish, then the solution must be trivial. Therefore, (3.26) admits a unique solution, which implies that $\mathcal{J}$ is well-defined. This completes the proof. $\square$

We finally are able to prove that the fixed-point equation (3.27) has a unique solution under certain assumptions on the porosity.

Theorem 3.9. *Suppose that the porosity ρ satisfies (3.19), (3.30) and (3.32). Furthermore, assume that*

$$C_{\mathcal{J}} \left\| \frac{\nabla \rho}{\rho} \right\|_{\mathbf{L}^\infty(\Omega)} < 1 . \tag{3.36}$$

Then, given $\mathbf{f} \in \mathrm{W}^{1,1}(0,T;\mathbf{L}^2(\Omega)) \cap \mathrm{L}^2(0,T;\mathbf{L}^2(\Omega))$ and $\mathbf{u}_0 \in \mathbf{L}^s(\Omega) \cap \mathbf{H}$ (cf. (3.11)), there exists a unique $(\boldsymbol{\sigma}, \underline{\mathbf{u}})$ solution to (2.19) with $\mathbf{u}(0) = \mathbf{u}_0$, $\boldsymbol{\sigma}^{\mathrm{d}}(0) = \boldsymbol{\sigma}_0^{\mathrm{d}}$ and $\boldsymbol{\gamma}(0) = \boldsymbol{\gamma}_0$ (cf. (3.12)). Moreover, $\boldsymbol{\sigma} \in \mathrm{L}^2(0,T;\mathbb{X})$, $\mathbf{u} \in \mathrm{W}^{1,\infty}(0,T;\mathbf{L}^2(\Omega)) \cap \mathrm{L}^2(0,T;\mathbf{L}^s(\Omega))$ and $\boldsymbol{\gamma} \in \mathrm{L}^2(0,T;\mathbb{L}^2_{\mathrm{skew}}(\Omega))$, all of them satisfying (3.20) in Theorem 3.4.

Proof. We first notice that it is enough to prove that the fixed-point equation (3.27) has a unique solution. Once this is established, Lemma 3.2 ensures that (2.19) admits a unique solution, whose regularity then follows from Theorem 3.4. We therefore focus on the former. In this regard, by Theorem 3.8 the operator $\mathcal{J}$ is well-defined. We now show that $\mathcal{J}$ is Lipschitz continuous. Given $\boldsymbol{\zeta}_1, \boldsymbol{\zeta}_2 \in \mathrm{L}^2(0,T;\mathbb{X})$, since (3.26) is linear, we have that $\mathcal{J}(\boldsymbol{\zeta}_1) - \mathcal{J}(\boldsymbol{\zeta}_2)$ corresponds to the unique solution to (3.26) with $\mathbf{f} = \mathbf{0}$, $\mathbf{u}_0 = \mathbf{0}$ and $\boldsymbol{\zeta} = \boldsymbol{\zeta}_1 - \boldsymbol{\zeta}_2$. Thus, applying the estimate (3.34), we obtain

$$\|\mathcal{J}(\boldsymbol{\zeta}_1) - \mathcal{J}(\boldsymbol{\zeta}_2)\|_{\mathrm{L}^2(0,T;\mathbb{X})} \leq C_{\mathcal{J}} \left\| \frac{\nabla \rho}{\rho} \right\|_{\mathbf{L}^\infty(\Omega)} \|\boldsymbol{\zeta}_1 - \boldsymbol{\zeta}_2\|_{\mathrm{L}^2(0,T;\mathbb{X})} ,$$

which implies that $\mathcal{J}$ is Lipschitz continuous. Moreover, using (3.36), $\mathcal{J}$ is a contractive operator on the Banach space $\mathrm{L}^2(0,T;\mathbb{X})$, so that the Banach fixed-point theorem ensures that $\mathcal{J}$ admits a unique fixed-point. Hence, (3.27) has a unique solution, as desired. $\square$

Remark 3.2. *It is worth noting that our analysis can be readily extended to the case of a non-homogeneous Dirichlet boundary condition in (2.10), in a manner similar to [39, Section 2] (see also [20, Theorem 4.10]). Specifically, if we prescribe $\mathbf{u} = \mathbf{u}_{\mathrm{D}}$ on $\Gamma \times (0,T]$ for some time-dependent Dirichlet datum $\mathbf{u}_{\mathrm{D}} : [0,T] \to \mathbf{H}^{1/2}(\Gamma)$, a solution can be constructed as follows. Let $(\boldsymbol{\sigma}_\Gamma, \underline{\mathbf{u}}_\Gamma) \in \mathbb{X} \times \mathbf{Y}$ solve the problem*

$$\begin{aligned}
[\mathbf{A}(\boldsymbol{\sigma}_\Gamma(t)), \boldsymbol{\tau}] + [\mathbf{B}'(\underline{\mathbf{u}}_\Gamma(t)), \boldsymbol{\tau}] + [\mathbf{D}'_\rho(\underline{\mathbf{u}}_\Gamma(t)), \boldsymbol{\tau}] &= \langle \boldsymbol{\tau}\mathbf{n}, \mathbf{u}_{\mathrm{D}}(t) \rangle_\Gamma \quad \forall\, \boldsymbol{\tau} \in \mathbb{X} , \\
[\mathbf{E}(\underline{\mathbf{u}}_\Gamma(t)), \underline{\mathbf{v}}] - [\mathbf{B}(\boldsymbol{\sigma}_\Gamma(t)), \underline{\mathbf{v}}] + [\mathbf{C}(\underline{\mathbf{u}}_\Gamma(t)), \underline{\mathbf{v}}] &= [\mathbf{F}(t), \underline{\mathbf{v}}] \qquad\quad \forall\, \underline{\mathbf{v}} \in \mathbf{Y} ,
\end{aligned} \tag{3.37}$$

for all $t \in (0,T]$. Notice that for each fixed $t \in (0,T]$, the problem (3.37) is indeed well-posed owing to a slight modification of the structure studied in Lemma 3.7 (see also (3.29)). Then, having $\underline{\mathbf{u}}_\Gamma$ as data, we may define $(\boldsymbol{\sigma}_{\mathtt{H}}, \underline{\mathbf{u}}_{\mathtt{H}}) : [0,T] \to \mathbb{X} \times \mathbf{Y}$ as the solution of the problem

$$\begin{aligned}
[\mathbf{A}(\boldsymbol{\sigma}_{\mathtt{H}}(t)), \boldsymbol{\tau}] + [\mathbf{B}'(\underline{\mathbf{u}}_{\mathtt{H}}(t)), \boldsymbol{\tau}] + [\mathbf{D}'_\rho(\underline{\mathbf{u}}_{\mathtt{H}}(t)), \boldsymbol{\tau}] &= 0 \qquad\qquad\qquad\qquad\qquad \forall\, \boldsymbol{\tau} \in \mathbb{X} , \\
\partial_t\, [\mathbf{E}(\underline{\mathbf{u}}_{\mathtt{H}}(t)), \underline{\mathbf{v}}] - [\mathbf{B}(\boldsymbol{\sigma}_{\mathtt{H}}(t)), \underline{\mathbf{v}}] + [\mathbf{C}(\underline{\mathbf{u}}_{\mathtt{H}}(t)), \underline{\mathbf{v}}] &= [\mathbf{E}(\underline{\mathbf{u}}_\Gamma(t)) - \partial_t \mathbf{E}(\underline{\mathbf{u}}_\Gamma(t)), \underline{\mathbf{v}}] \quad \forall\, \underline{\mathbf{v}} \in \mathbf{Y} ,
\end{aligned} \tag{3.38}$$

which is also well-posed, as follows from the analysis developed in this section, by replacing the corresponding right-hand side in (2.19). *Consequently, taking into account the linearity of both* (3.37) *and* (3.38)*, it is straightforward to verify that* $(\boldsymbol{\sigma}, \underline{\mathbf{u}}) = (\boldsymbol{\sigma}_\Gamma, \underline{\mathbf{u}}_\Gamma) + (\boldsymbol{\sigma}_{\mathrm{H}}, \underline{\mathbf{u}}_{\mathrm{H}})$ *is indeed a solution to the weak formulation of* (2.10) *with non-homogeneous Dirichlet boundary conditions.*

4 Semidiscrete continuous-in-time approximation

In this section, we introduce and analyze the semidiscrete continuous-in-time approximation of (2.19). The solvability is established by adapting the arguments introduced in Section 3. Subsequently, we derive error estimates and identify the corresponding convergence rates.

4.1 Preliminaries

Let $\mathcal{T}_h$ be a shape-regular triangulation of Ω made up of triangles K (when $d = 2$) or tetrahedra K (when $d = 3$) of diameter h_K, and define the mesh-size $h := \max\left\{h_K \,:\, K \in \mathcal{T}_h\right\}$. For a given integer $k \geq 0$ and $K \in \mathcal{T}_h$, we let $\mathrm{P}_k(K)$ be the space of polynomials of total degree at most k defined on K. Its vector and tensorial counterparts are denoted by $\mathbf{P}_k(K) := [\mathrm{P}_k(K)]^d$ and $\mathbb{P}_k(K) := [\mathrm{P}_k(K)]^{d\times d}$, respectively. In addition, we let $\mathbf{RT}_k(K) := \mathbf{P}_k(K) + \mathrm{P}_k(K)\,\mathbf{x}$ be the local Raviart–Thomas space of order k defined on K, where $\mathbf{x}$ stands for a generic vector in R^d. We denote by $\mathbb{RT}_k(K)$ the tensor space of functions whose rows lie in $\mathbf{RT}_k(K)$. Furthermore, we let b_K be the bubble function on K, which is given by the product of its $d+1$ barycentric coordinates. The local bubble space of order k is then set as

$$\mathbf{B}_k(K) := \begin{cases} \mathbf{curl}(b_K\, \mathrm{P}_k(K)) & \text{if } d = 2\,, \\ \mathbf{curl}(b_K\, \mathbf{P}_k(K)) & \text{if } d = 3\,, \end{cases}$$

where the curl operators are defined as $\mathbf{curl}(v) := \left(\frac{\partial v}{\partial x_2}, -\frac{\partial v}{\partial x_1}\right)$ for $v : K \to \mathrm{R}$ (if $d = 2$), and $\mathbf{curl}(\mathbf{v}) := \nabla \times \mathbf{v}$ for $\mathbf{v} : K \to \mathrm{R}^3$ (if $d = 3$). Finally, $\mathbb{B}_k(K)$ denotes the space of tensor functions in which each row belongs to $\mathbf{B}_k(K)$. With these notations at hand, we introduce the following global finite element spaces:

$$\begin{aligned}
\mathbf{P}_k(\Omega) &:= \Big\{\mathbf{v}_h \in \mathbf{L}^2(\Omega) \ :\ \ \mathbf{v}_h|_K \in \mathbf{P}_k(K) \quad \forall\, K \in \mathcal{T}_h\Big\}\,, \\
\mathbb{P}_k(\Omega) &:= \Big\{\boldsymbol{\eta}_h \in \mathbb{L}^2(\Omega) \ :\ \ \boldsymbol{\eta}_h|_K \in \mathbb{P}_k(K) \quad \forall\, K \in \mathcal{T}_h\Big\}\,, \\
\mathbb{RT}_k(\Omega) &:= \Big\{\boldsymbol{\tau}_h \in \mathbb{H}(\mathbf{div};\Omega) \ :\ \ \boldsymbol{\tau}_h|_K \in \mathbb{RT}_k(K) \quad \forall\, K \in \mathcal{T}_h\Big\}\,, \\
\mathbb{B}_k(\Omega) &:= \Big\{\boldsymbol{\tau}_h \in \mathbb{H}(\mathbf{div};\Omega) \ :\ \ \boldsymbol{\tau}_h|_K \in \mathbb{B}_k(K) \quad \forall\, K \in \mathcal{T}_h\Big\}\,.
\end{aligned}$$

Let $\mathbb{X}_h \subset \mathbb{H}_0(\mathbf{div}_\ell;\Omega)$, $\mathbf{H}_h^{\mathbf{u}} \subset \mathbf{L}^s(\Omega)$ and $\mathbb{H}_h^\gamma \subset \mathbb{L}^2_{\mathrm{skew}}(\Omega)$ be finite-dimensional subspaces forming a stable finite element triplet for the Banach spaces-based mixed elasticity with weakly imposed stress symmetry. This means that there exists a positive constant $\beta_{\mathtt{d}}$, independent of h, such that

$$\sup_{0\neq\boldsymbol{\tau}_h\in\mathbb{X}_h} \frac{[\mathbf{B}(\boldsymbol{\tau}_h), \underline{\mathbf{v}}_h]}{\|\boldsymbol{\tau}_h\|_{\mathbb{X}}} \geq \beta_{\mathtt{d}}\, \|\underline{\mathbf{v}}_h\|_{\mathbf{Y}} \qquad \forall\, \underline{\mathbf{v}}_h := (\mathbf{v}_h, \boldsymbol{\eta}_h) \in \mathbf{Y}_h := \mathbf{H}_h^{\mathbf{u}} \times \mathbb{H}_h^\gamma\,. \tag{4.1}$$

We immediately stress that (4.1) is the discrete counterpart of the inf-sup condition (3.6). Furthermore, we point out that there exist several stable triples satisfying (4.1) with $s = \ell = 2$, which corresponds to the classical Hilbertian framework. Examples include the Amara–Thomas element [3], PEERS [7,35], Stenberg [40], Arnold–Falk–Winther [8], and Cockburn–Gopalakrishnan–Guzmán [24] families. As established in [30, Lemma 4.8], if a triplet of finite element subspaces of $\mathbb{H}(\mathbf{div};\Omega)$, $\mathbf{L}^2(\Omega)$, and $\mathbb{L}^2_{\mathrm{skew}}(\Omega)$ forms a stable triplet for linear elasticity in the Hilbertian setting, then, under certain assumptions detailed therein, these spaces also satisfy (4.1). That is, stability extends to the Banach setting. In particular, as shown in [30, Section 4.3.3], the Arnold–Falk–Winther and PEERS elements fulfill these assumptions. Therefore, we shall focus on these two families. To be precise, the Arnold–Falk–Winther element of order k, denoted AFW_k, consists of the following subspaces:

$$\widetilde{\mathbb{X}}_h := \mathbb{P}_{k+1}(\Omega)\cap\mathbb{H}(\mathbf{div};\Omega)\,,\quad \mathbf{H}^{\mathbf{u}}_h := \mathbf{P}_k(\Omega)\,,\quad \text{and}\quad \mathbb{H}^{\gamma}_h := \mathbb{L}^2_{\mathrm{skew}}(\Omega)\cap\mathbb{P}_k(\Omega)\,. \tag{4.2}$$

In turn, the plane elasticity element with reduced symmetry of order k, denoted by PEERS_k, is defined by

$$\begin{gathered}\widetilde{\mathbb{X}}_h := \mathbb{RT}_k(\Omega)\oplus\mathbb{B}_k(\Omega)\,,\quad \mathbf{H}^{\mathbf{u}}_h := \mathbf{P}_k(\Omega)\,,\\ \text{and}\quad \mathbb{H}^{\gamma}_h := \big[C(\overline{\Omega})\big]^{d\times d}\cap\mathbb{L}^2_{\mathrm{skew}}(\Omega)\cap\mathbb{P}_{k+1}(\Omega)\,.\end{gathered} \tag{4.3}$$

We notice that, even in the general framework where s and ℓ are not necessarily equal to 2, by setting $\mathbb{X}_h := \widetilde{\mathbb{X}}_h\cap\mathbb{H}_0(\mathbf{div}_\ell;\Omega)$ both for AFW_k and for PEERS_k, the triplet $(\mathbb{X}_h,\mathbf{H}^{\mathbf{u}}_h,\mathbb{H}^{\gamma}_h)$ is conforming with the continuous setting. Next, by letting $\underline{\mathbf{u}}_h := (\mathbf{u}_h,\gamma_h)\in\mathbf{Y}_h$, the semidiscrete continuous-in-time problem associated with (2.19) reads: Find $(\boldsymbol{\sigma}_h,\underline{\mathbf{u}}_h):[0,T]\to\mathbb{X}_h\times\mathbf{Y}_h$ such that, for a.e. $t\in(0,T)$,

$$\begin{aligned}[\mathbf{A}(\boldsymbol{\sigma}_h(t)),\boldsymbol{\tau}_h]+[\mathbf{B}'(\underline{\mathbf{u}}_h(t)),\boldsymbol{\tau}_h]+[\mathbf{D}'_\rho(\underline{\mathbf{u}}_h(t)),\boldsymbol{\tau}_h] &= 0 && \forall\,\boldsymbol{\tau}_h\in\mathbb{X}_h\,,\\ \frac{\partial}{\partial t}[\mathbf{E}(\underline{\mathbf{u}}_h(t)),\underline{\mathbf{v}}_h]-[\mathbf{B}(\boldsymbol{\sigma}_h(t)),\underline{\mathbf{v}}_h]+[\mathbf{C}(\underline{\mathbf{u}}_h(t)),\underline{\mathbf{v}}_h] &= [\mathbf{F}(t),\underline{\mathbf{v}}_h] && \forall\,\underline{\mathbf{v}}_h\in\mathbf{Y}_h\,,\end{aligned} \tag{4.4}$$

and $\mathbf{u}_h(0)=\mathbf{u}_{h,0}$, where $(\boldsymbol{\sigma}_{h,0},\underline{\mathbf{u}}_{h,0})=(\boldsymbol{\sigma}_{h,0},(\mathbf{u}_{h,0},\gamma_{h,0}))$ is a suitable approximation of $(\boldsymbol{\sigma}_0,\underline{\mathbf{u}}_0)$, which is the solution to (3.18). Namely, we choose $(\boldsymbol{\sigma}_{h,0},\underline{\mathbf{u}}_{h,0})\in\mathbb{X}_h\times\mathbf{Y}_h$ solving

$$\begin{aligned}[\mathbf{A}(\boldsymbol{\sigma}_{h,0}),\boldsymbol{\tau}_h]+[\mathbf{B}'(\underline{\mathbf{u}}_{h,0}),\boldsymbol{\tau}_h]+[\mathbf{D}'_\rho(\underline{\mathbf{u}}_{h,0}),\boldsymbol{\tau}_h] &= 0 && \forall\,\boldsymbol{\tau}_h\in\mathbb{X}_h\,,\\ -[\mathbf{B}(\boldsymbol{\sigma}_{h,0}),\underline{\mathbf{v}}_h]+[\mathbf{C}(\underline{\mathbf{u}}_{h,0}),\underline{\mathbf{v}}_h] &= [\mathbf{G}_0,\underline{\mathbf{v}}_h] && \forall\,\underline{\mathbf{v}}_h\in\mathbf{Y}_h\,,\end{aligned} \tag{4.5}$$

where $\mathbf{G}_0=(\mathbf{g}_0,\mathbf{0})$ is the linear functional defined as the right-hand side of (3.18). Notice that $\mathbf{G}_0\in\mathbf{Y}'$. In fact, by applying Cauchy–Schwarz inequality and the continuous embedding $\mathbf{i}_{s,2}$ (cf. (1.3)), we have

$$\big|[\mathbf{G}_0,\underline{\mathbf{v}}]\big|\le C_0\left\{\|\mathbf{div}(\rho\,\mathbf{e}(\mathbf{u}_0))\|_{\mathbf{L}^2(\Omega)}+\|\mathbf{u}_0\|_{\mathbf{L}^2(\Omega)}\right\}\|\underline{\mathbf{v}}\|_{\mathbf{Y}}\qquad\forall\,\underline{\mathbf{v}}\in\mathbf{Y}\,, \tag{4.6}$$

where $C_0:=2\mu\,\|\mathbf{i}_{s,2}\|\,\max\{1,\|\mathbf{K}^{-1}\|_{\mathbb{L}^\infty(\Omega)}\}$. We stress here that we are assuming the hypothesis of Lemma 3.3, that is, $\mathbf{u}_0\in\mathbf{L}^s(\Omega)\cap\mathbf{H}$. The well-posedness of (4.5) is established below, in Lemma 4.1.

4.2 Existence and uniqueness of a solution

Following the approach of the continuous formulation (cf. Section 3), we aim to prove the solvability of (4.4) by introducing a fixed-point strategy. To that end, we first let $\mathbb{V}_h$ be the discrete kernel of $\mathbf{B}$, which is given by

$$\mathbb{V}_h := \Big\{\boldsymbol{\tau}_h\in\mathbb{X}_h\ :\quad [\mathbf{B}(\boldsymbol{\tau}_h),\underline{\mathbf{v}}_h]=0\qquad\forall\,\underline{\mathbf{v}}_h\in\mathbf{Y}_h\Big\}\,.$$

In turn, from (4.2) and (4.3), we notice that $\mathbf{div}(\mathbb{X}_h)\subset\mathbf{H}^{\mathbf{u}}_h$. Thus, $\mathbb{V}_h$ can be characterized as

$$\mathbb{V}_h = \Big\{\boldsymbol{\tau}_h\in\mathbb{X}_h\ :\quad \mathbf{div}(\boldsymbol{\tau}_h)=0\quad\text{in}\quad\Omega\quad\text{and}\quad(\boldsymbol{\eta}_h,\boldsymbol{\tau}_h)_\Omega=0\quad\forall\,\boldsymbol{\eta}_h\in\mathbb{H}^{\gamma}_h\Big\}\,.$$

Notice that although $\mathbb{V}_h$ is not a subspace of $\mathbb{V}$ (cf. (3.7)), the coercivity of $\mathbf{A}$ also holds in the discrete kernel $\mathbb{V}_h$ (cf. (3.9)), since the divergence-free condition was the only property required in the argument. Consequently, bearing in mind (4.1) and following the same reasoning did it to prove (3.10), this time applying [25, Theorem 3.5], we obtain the existence of a positive constant $\Lambda_{\mathtt{d}}$, depending only on $\beta_{\mathtt{d}}$, c_ℓ, μ, ρ_0, ρ_1, $\|\mathbf{K}^{-1}\|_{\mathbb{L}^\infty(\Omega)}$ and $|\Omega|$, such that, for all $(\boldsymbol{\zeta}_h, \underline{\mathbf{w}}_h) \in \mathbb{X}_h \times \mathbf{Y}_h$, there holds

$$\Lambda_{\mathtt{d}} \, \|(\boldsymbol{\zeta}_h, \underline{\mathbf{w}}_h)\|_{\mathbb{X}\times\mathbf{Y}} \leq \sup_{\mathbf{0}\neq(\boldsymbol{\tau}_h,\underline{\mathbf{v}}_h)\in\mathbb{X}_h\times\mathbf{Y}_h} \frac{[\mathbf{A}(\boldsymbol{\zeta}_h), \boldsymbol{\tau}_h] + [\mathbf{B}'(\underline{\mathbf{w}}_h), \boldsymbol{\tau}_h] + [\mathbf{B}(\boldsymbol{\zeta}_h), \underline{\mathbf{v}}_h] - [\mathbf{C}(\underline{\mathbf{w}}_h), \underline{\mathbf{v}}_h]}{\|(\boldsymbol{\tau}_h, \underline{\mathbf{v}}_h)\|_{\mathbb{X}\times\mathbf{Y}}} \,. \tag{4.7}$$

Having established this inf-sup condition, we are in a position to prove the well-posedness of (4.5).

Lemma 4.1. *Assume that $\mathbf{u}_0 \in \mathbf{L}^s(\Omega) \cap \mathbf{H}$ (cf. (3.11)) and the porosity satisfies*

$$\left\| \frac{\nabla \rho}{\rho} \right\|_{\mathbf{L}^r(\Omega)} \leq \frac{\sqrt{d}\,\Lambda_{\mathtt{d}}}{2} \,. \tag{4.8}$$

Then, there exists a unique solution $(\boldsymbol{\sigma}_{h,0}, \underline{\mathbf{u}}_{h,0}) \in \mathbb{X}_h \times \mathbf{Y}_h$ to (4.5). Moreover, there exists a positive constant $C_{0,\mathtt{d}}$, depending only on $\Lambda_{\mathtt{d}}$ and C_0 (cf. (4.6)), such that

$$\|(\boldsymbol{\sigma}_{h,0}, \underline{\mathbf{u}}_{h,0})\|_{\mathbb{X}\times\mathbf{Y}} \leq C_{0,\mathtt{d}} \left\{ \|\mathbf{div}(\rho\,\mathbf{e}(\mathbf{u}_0))\|_{\mathbf{L}^2(\Omega)} + \|\mathbf{u}_0\|_{\mathbf{L}^2(\Omega)} \right\} . \tag{4.9}$$

Proof. Similarly to [12, eq. (4.17)–(4.18)], we employ the inf-sup condition (4.7), the stability property of $\mathbf{D}_\rho$ (cf. (3.4b)), and the assumption (4.8), to establish a global inf-sup condition analogous to (4.7), but incorporating $\mathbf{D}_\rho$. Similarly, it can be verified that this condition also holds when taking the supremum over the other component. Therefore, by invoking the Banach–Nečas–Babuška Theorem (see, e.g. [26, Theorem 25.15]), we conclude that (4.5) is well-posed, together with the corresponding *a priori* estimate. For the sake of brevity, we omit further details and refer the reader to [12, Lemma 4.3] for a similar analysis. □

Observe that (4.7) enables the stability of (4.4) to be established by following the same arguments as in the continuous case (cf. Theorem 3.4). Although the precise statement is deferred to Theorem 4.7, this observation motivates the introduction of a fixed-point operator $\mathcal{J}_{\mathtt{d}} : \mathrm{L}^2(0,T;\mathbb{X}_h) \to \mathrm{L}^2(0,T;\mathbb{X}_h)$ on the space $\mathrm{L}^2(0,T;\mathbb{X}_h)$, in a similar fashion as in (3.26). The operator $\mathcal{J}_{\mathtt{d}}$ is then defined by

$$\mathcal{J}_{\mathtt{d}}(\boldsymbol{\zeta}_h) := \boldsymbol{\sigma}_h \qquad \forall\, \boldsymbol{\zeta}_h \in \mathrm{L}^2(0,T;\mathbb{X}_h)\,,$$

where $(\boldsymbol{\sigma}_h, \underline{\mathbf{u}}_h) : [0,T] \to \mathbb{X}_h \times \mathbf{Y}_h$ is the unique solution (to be confirmed below) to

$$\begin{aligned} [\mathbf{A}(\boldsymbol{\sigma}_h(t)), \boldsymbol{\tau}_h] + [\widetilde{\mathbf{B}}'(\underline{\mathbf{u}}_h(t)), \boldsymbol{\tau}_h] &= 0 & \forall\, \boldsymbol{\tau}_h \in \mathbb{X}_h\,, \\ \frac{\partial}{\partial t}\,[\mathbf{E}(\underline{\mathbf{u}}_h(t)), \underline{\mathbf{v}}_h] - [\widetilde{\mathbf{B}}(\boldsymbol{\sigma}_h(t)), \underline{\mathbf{v}}_h] + [\mathbf{C}(\underline{\mathbf{u}}_h(t)), \underline{\mathbf{v}}_h] &= [\widetilde{\mathbf{F}}_{\boldsymbol{\zeta}_h}(t), \underline{\mathbf{v}}_h] & \forall\, \underline{\mathbf{v}}_h \in \mathbf{Y}_h\,, \end{aligned} \tag{4.10}$$

for a.e. $t \in (0,T)$ with $\mathbf{u}_h(0) = \mathbf{u}_{h,0}$, where $(\boldsymbol{\sigma}_{h,0}, \underline{\mathbf{u}}_{h,0}) \in \mathbb{X}_h \times \mathbf{Y}_h$ is the unique solution (to be confirmed in Lemma 4.5) to

$$\begin{aligned} [\mathbf{A}(\boldsymbol{\sigma}_{h,0}), \boldsymbol{\tau}_h] + [\widetilde{\mathbf{B}}'(\underline{\mathbf{u}}_{h,0}), \boldsymbol{\tau}_h] &= 0 & \forall\, \boldsymbol{\tau}_h \in \mathbb{X}_h\,, \\ -[\widetilde{\mathbf{B}}(\boldsymbol{\sigma}_{h,0}), \underline{\mathbf{v}}_h] + [\mathbf{C}(\underline{\mathbf{u}}_{h,0}), \underline{\mathbf{v}}_h] &= [\widetilde{\mathbf{G}}_0, \underline{\mathbf{v}}_h] & \forall\, \underline{\mathbf{v}}_h \in \mathbf{Y}_h\,, \end{aligned} \tag{4.11}$$

with $\widetilde{\mathbf{G}}_0 = (\widetilde{\mathbf{g}}_0, \mathbf{0})$ the linear functional on the right-hand side of (3.16). It follows from (3.17) and the continuous embedding $\mathbf{i}_{s,2}$ (cf. (1.3)) that $\widetilde{\mathbf{G}}_0 \in \mathbf{Y}'$. To prove the unique solvability of (4.10), we first establish the discrete counterpart of Lemma 3.5. The proof is analogous to the continuous case, employing the discrete inf-sup condition (4.1) in place of (3.6).

Lemma 4.2. *Assume that the porosity satisfies*

$$\left\|\frac{\nabla\rho}{\rho}\right\|_{\mathbf{L}^r(\Omega)} \leq \frac{\sqrt{d}\,\beta_{\mathtt{d}}}{2}\,, \tag{4.12}$$

with $\beta_{\mathtt{d}}$ as given in (4.1). Then, the following inf-sup condition holds:

$$\sup_{0\neq\boldsymbol{\tau}_h\in\mathbb{X}_h} \frac{[\widetilde{\mathbf{B}}(\boldsymbol{\tau}_h),\underline{\mathbf{v}}_h]}{\|\boldsymbol{\tau}_h\|_{\mathbb{X}}} \geq \frac{\beta_{\mathtt{d}}}{2}\,\|\underline{\mathbf{v}}_h\|_{\mathbf{Y}} \qquad \forall\,\underline{\mathbf{v}}_h\in\mathbf{Y}_h\,. \tag{4.13}$$

Next, we define $\widetilde{\mathbb{V}}_h$ as the discrete kernel of the operator $\widetilde{\mathbf{B}}$, namely

$$\widetilde{\mathbb{V}}_h := \Big\{\boldsymbol{\tau}_h\in\mathbb{X}_h \;\;:\;\; [\widetilde{\mathbf{B}}(\boldsymbol{\tau}_h),\underline{\mathbf{v}}_h] = 0 \qquad \forall\,\underline{\mathbf{v}}_h\in\mathbf{Y}_h\Big\}\,. \tag{4.14}$$

Then, we have the following result, which serves as the discrete counterpart of Lemma 3.6.

Lemma 4.3. *Let c_ℓ be as in (3.8) and assume that the porosity satisfies*

$$\left\|\frac{\nabla\rho}{\rho}\right\|_{\mathbf{L}^\infty(\Omega)} \leq \frac{\sqrt{d}\,c_\ell}{2\,\|\mathbf{i}_{s,2}\|}\,. \tag{4.15}$$

Then, with the same constant α as in Lemma 3.6, which is independent of h, it holds

$$\sup_{0\neq\boldsymbol{\tau}_h\in\widetilde{\mathbb{V}}_h} \frac{[\mathbf{A}(\boldsymbol{\sigma}_h),\boldsymbol{\tau}_h]}{\|\boldsymbol{\tau}_h\|_{\mathbb{X}}} \geq \alpha\,\|\boldsymbol{\sigma}_h\|_{\mathbb{X}} \qquad \forall\,\boldsymbol{\sigma}_h\in\widetilde{\mathbb{V}}_h\,. \tag{4.16}$$

Proof. Let $\boldsymbol{\sigma}_h\in\widetilde{\mathbb{V}}_h$. Since $\mathbf{div}(\boldsymbol{\sigma}_h)\in\mathbf{H}_h^{\mathbf{u}}$, we can use (4.14) with $\underline{\mathbf{v}}_h = (\mathbf{div}(\boldsymbol{\sigma}_h),\mathbf{0})\in\mathbf{Y}_h$. Then, we apply Cauchy–Schwarz inequality along with (4.15), thus obtaining

$$\|\mathbf{div}(\boldsymbol{\sigma}_h)\|^2_{\mathbf{L}^2(\Omega)} = \frac{1}{d}\left(\frac{\nabla\rho}{\rho}\cdot\mathbf{div}(\boldsymbol{\sigma}_h),\mathrm{tr}(\boldsymbol{\sigma}_h)\right)_\Omega \leq \frac{c_\ell}{2\,\|\mathbf{i}_{s,2}\|}\,\|\mathbf{div}(\boldsymbol{\sigma}_h)\|_{\mathbf{L}^2(\Omega)}\,\|\boldsymbol{\sigma}_h\|_{\mathbb{L}^2(\Omega)}\,.$$

Now, using this estimate and the continuous embedding $\mathbf{i}_{2,\ell}$, which satisfies $\|\mathbf{i}_{2,\ell}\| = |\Omega|^{(2-\ell)/(2\ell)} = |\Omega|^{(s-2)/(2s)} = \|\mathbf{i}_{s,2}\|$ (cf. (1.3)), we find that

$$\|\mathbf{div}(\boldsymbol{\sigma}_h)\|_{\mathbf{L}^\ell(\Omega)} \leq \|\mathbf{i}_{s,2}\|\,\|\mathbf{div}(\boldsymbol{\sigma}_h)\|_{\mathbf{L}^2(\Omega)} \leq \frac{c_\ell}{2}\,\|\boldsymbol{\sigma}_h\|_{\mathbb{L}^2(\Omega)}\,.$$

Having this established, the rest of the argument proceeds exactly as in the proof of Lemma 3.6, thereby showing that (4.16) holds with the same constant. We omit further details. □

Lemma 4.4. *Suppose that the porosity ρ satisfies (4.12) and (4.15). Then, for all $\widehat{\mathbf{f}}\in\mathbf{L}^2(\Omega)$, there exists a unique solution $(\boldsymbol{\sigma}_h,\underline{\mathbf{u}}_h)\in\mathbb{X}_h\times\mathbf{Y}_h$ to the problem*

$$\begin{aligned} [\mathbf{A}(\boldsymbol{\sigma}_h),\boldsymbol{\tau}_h] + [\widetilde{\mathbf{B}}'(\underline{\mathbf{u}}_h),\boldsymbol{\tau}_h] &= 0 && \forall\,\boldsymbol{\tau}_h\in\mathbb{X}_h\,,\\ [\widetilde{\mathbf{B}}(\boldsymbol{\sigma}_h),\underline{\mathbf{v}}_h] - [(\mathbf{E}+\mathbf{C})(\underline{\mathbf{u}}_h),\underline{\mathbf{v}}_h] &= -(\widehat{\mathbf{f}},\mathbf{v}_h)_\Omega && \forall\,\underline{\mathbf{v}}_h\in\mathbf{Y}_h\,, \end{aligned} \tag{4.17}$$

Proof. Bearing in mind Lemmas 4.2 and 4.3, and recalling that $\mathbf{A}$ and $\mathbf{E}+\mathbf{C}$ induce symmetric bilinear forms, we apply [25, Theorem 3.5] to conclude. □

Certainly, Lemma 4.4 proves the range condition of Theorem 3.1 in our discrete setting, thereby establishing the discrete counterpart of Lemma 3.7. Moreover, by neglecting the operator $\mathbf{E}$ in (4.17), we also prove that, under the same assumptions as in Lemma 4.4, the problem associated with the initial conditions (4.11) has a unique solution. We state this in the following result.

Lemma 4.5. *Assume that $\mathbf{u}_0 \in \mathbf{L}^s(\Omega) \cap \mathbf{H}$ (cf. Lemma 3.3) and that the porosity ρ satisfies (4.12) and (4.15). Then, the problem (4.11) has a unique solution $(\boldsymbol{\sigma}_{h,0}, \underline{\mathbf{u}}_{h,0}) \in \mathbb{X}_h \times \mathbf{Y}_h$. Moreover, there exists a positive constant $\widetilde{C}_{0,\mathtt{d}}$, depending only on α, $\beta_{\mathtt{d}}$, $\|\mathbf{K}^{-1}\|_{\mathbb{L}^\infty(\Omega)}$, ρ_0, and $\widetilde{C}_0$ (cf. (3.17)), and thus independent of h, such that*

$$\|\boldsymbol{\sigma}_{h,0}\|_{\mathbb{X}} + \|\underline{\mathbf{u}}_{h,0}\|_{\mathbf{Y}} \leq \widetilde{C}_{0,\mathtt{d}} \left\{ \|\mathbf{div}(\rho\, \mathbf{e}(\mathbf{u}_0))\|_{\mathbf{L}^2(\Omega)} + \|\mathbf{u}_0\|_{\mathbf{L}^2(\Omega)} \right\}. \tag{4.18}$$

Proof. Similarly to the proof of Lemma 4.4, we invoke [25, Theorem 3.5] to ensure existence and uniqueness of the solution. Moreover, we use the *a priori* estimate provided by the same result, together with the continuity of $\widetilde{\mathbf{G}}_0$ established in (3.17), to obtain (4.18). We omit further details. □

The following result shows that (4.10) has a unique solution, which means that $\mathcal{J}_{\mathtt{d}}$ is well-defined.

Theorem 4.6. *Suppose that the porosity ρ satisfies (4.12) and (4.15). Let $\mathbf{f} \in \mathrm{W}^{1,1}(0,T;\mathbf{L}^2(\Omega)) \cap \mathrm{L}^2(0,T;\mathbf{L}^2(\Omega))$ and $\mathbf{u}_0 \in \mathbf{L}^s(\Omega) \cap \mathbf{H}$ be given, and let $(\boldsymbol{\sigma}_{h,0}, \underline{\mathbf{u}}_{h,0})$ be solution to (4.5). Then, the operator $\mathcal{J}_{\mathtt{d}}$ is well-defined. In particular, for each $\boldsymbol{\zeta}_h \in \mathrm{L}^2(0,T;\mathbb{X}_h)$, there exists a unique solution $(\boldsymbol{\sigma}_h, \underline{\mathbf{u}}_h)$ to (4.10) such that $\boldsymbol{\sigma}_h \in \mathrm{L}^2(0,T;\mathbb{X}_h)$, $\mathbf{u}_h \in \mathrm{W}^{1,\infty}(0,T;\mathbf{H}_h^{\mathbf{u}})$, $\boldsymbol{\gamma}_h \in \mathrm{L}^2(0,T;\mathbb{H}_h^{\boldsymbol{\gamma}})$, $\mathbf{u}_h(0) = \mathbf{u}_{h,0}$, $\boldsymbol{\sigma}_h^{\mathrm{d}}(0) = \boldsymbol{\sigma}_{h,0}^{\mathrm{d}}$, $\boldsymbol{\gamma}_h(0) = \boldsymbol{\gamma}_{h,0}$, and $\mathcal{J}_{\mathtt{d}}(\boldsymbol{\zeta}_h) = \boldsymbol{\sigma}_h$. Moreover, there exist positive constants $\widetilde{C}_{\mathtt{B},\mathtt{d}}$ and $C_{\mathcal{J}_{\mathtt{d}}}$, with $\widetilde{C}_{\mathtt{B},\mathtt{d}}$ depending only on μ, ρ_0, ρ_1, $\|\mathbf{K}^{-1}\|_{\mathbb{L}^\infty(\Omega)}$, $\Lambda_{\mathtt{d}}$, $\widetilde{C}_{0,\mathtt{d}}$, d and $|\Omega|$, and $C_{\mathcal{J}_{\mathtt{d}}}$ depending only on ρ_0, ρ_1, $\Lambda_{\mathtt{d}}$, d and $|\Omega|$, such that*

$$\begin{aligned} \|\mathcal{J}_{\mathtt{d}}(\boldsymbol{\zeta}_h)\|_{\mathrm{L}^2(0,T;\mathbb{X})} \leq \widetilde{C}_{\mathtt{B},\mathtt{d}} & \left\{ \|\mathbf{f}\|_{\mathrm{L}^2(0,T;\mathbf{L}^2(\Omega))} + \|\mathbf{div}(\rho\, \mathbf{e}(\mathbf{u}_0))\|_{\mathbf{L}^2(\Omega)} + \|\mathbf{u}_0\|_{\mathbf{L}^2(\Omega)} \right\} \\ & + C_{\mathcal{J}_{\mathtt{d}}} \left\| \frac{\nabla\rho}{\rho} \right\|_{\mathbf{L}^\infty(\Omega)} \|\boldsymbol{\zeta}_h\|_{\mathrm{L}^2(0,T;\mathbb{X})}. \end{aligned} \tag{4.19}$$

Proof. Using the fact that $\mathbb{X}_h \subset \mathbb{X}$ and $\mathbf{Y}_h \subset \mathbf{Y}$, the proof is identical to the proof of Theorem 3.8, this time relying on the discrete inf-sup conditions established in this section (cf. (4.1), (4.13), and (4.16)), the discrete initial conditions (cf. (4.11)) and the bound (4.18) given in Lemma 4.5. □

We finally obtain the main result of this section, which is the existence and uniqueness of a solution to (4.4) along with the stability of the discrete problem.

Theorem 4.7. *Suppose that the porosity ρ satisfies (4.12), (4.15),*

$$\left\| \frac{\nabla\rho}{\rho} \right\|_{\mathbf{L}^\infty(\Omega)} \leq c_{\rho,\mathtt{d}} \quad \text{with} \quad c_{\rho,\mathtt{d}} := \frac{\sqrt{d}\,\Lambda_{\mathtt{d}}}{2\,\|\mathbf{i}_{s,2}\|} \min\left\{1, \frac{\sqrt{\rho_0}}{4\rho_1}\right\}, \tag{4.20}$$

and

$$C_{\mathcal{J}_{\mathtt{d}}} \left\| \frac{\nabla\rho}{\rho} \right\|_{\mathbf{L}^\infty(\Omega)} < 1. \tag{4.21}$$

Then, given $\mathbf{f} \in \mathrm{W}^{1,1}(0,T;\mathbf{L}^2(\Omega)) \cap \mathrm{L}^2(0,T;\mathbf{L}^2(\Omega))$ and $\mathbf{u}_0 \in \mathbf{L}^s(\Omega) \cap \mathbf{H}$, and denoting by $(\boldsymbol{\sigma}_{h,0}, \underline{\mathbf{u}}_{h,0})$ the unique solution to (4.5) (cf. Lemma 4.5), there exists a unique solution to (4.4) with $\boldsymbol{\sigma}_h \in \mathrm{L}^2(0,T;\mathbb{X}_h)$, $\mathbf{u}_h \in \mathrm{W}^{1,\infty}(0,T;\mathbf{H}_h^{\mathbf{u}})$, $\boldsymbol{\gamma}_h \in \mathrm{L}^2(0,T;\mathbb{H}_h^{\boldsymbol{\gamma}})$, $\mathbf{u}_h(0) = \mathbf{u}_{h,0}$, $\boldsymbol{\sigma}_h^{\mathrm{d}}(0) = \boldsymbol{\sigma}_{h,0}^{\mathrm{d}}$, $\boldsymbol{\gamma}_h(0) = \boldsymbol{\gamma}_{h,0}$.

Moreover, there exists a positive constant $C_{\mathtt{B},\mathtt{d}}$, depending only on μ, ρ_0, ρ_1, $C_{\mathbf{K}}$, $\|\mathbf{K}^{-1}\|_{\mathbb{L}^\infty(\Omega)}$, $\Lambda_{\mathtt{d}}$, $C_{0,\mathtt{d}}$, d and $|\Omega|$, such that

$$
\begin{aligned}
&\|\boldsymbol{\sigma}_h\|^2_{\mathrm{L}^2(0,T;\mathbb{X})} + \|\mathbf{u}_h\|^2_{\mathrm{L}^2(0,T;\mathbf{L}^s(\Omega))} + \|\mathbf{u}_h\|^2_{\mathrm{L}^\infty(0,T;\mathbf{L}^2(\Omega))} + \|\boldsymbol{\gamma}_h\|^2_{\mathrm{L}^2(0,T;\mathbb{L}^2(\Omega))} \\
&\qquad\qquad \leq C_{\mathtt{B},\mathtt{d}} \left\{ \|\mathbf{f}\|^2_{\mathrm{L}^2(0,T;\mathbf{L}^2(\Omega))} + \|\mathbf{div}(\rho\,\mathbf{e}(\mathbf{u}_0))\|^2_{\mathbf{L}^2(\Omega)} + \|\mathbf{u}_0\|^2_{\mathbf{L}^2(\Omega)} \right\}.
\end{aligned}
\tag{4.22}
$$

Proof. Employing the same arguments as in the proof of Theorem 3.9, from (4.19) one verifies that $\mathcal{J}_{\mathtt{d}}$ is Lipschitz continuous with constant $C_{\mathcal{J}_{\mathtt{d}}}\|\nabla\rho/\rho\|_{\mathbf{L}^\infty(\Omega)}$. Under the assumption (4.21), the fixed-point operator is a contraction, and the Banach fixed-point theorem yields the solvability of (4.4). The stability estimate (4.22) then follows by the same reasoning as in Theorem 3.4, this time relying on the discrete global inf-sup condition (4.7) and applying the assumption (4.20). Finally, in analogy with Lemma 3.2, it is straightforward to show that (4.4) is equivalent to (4.10) with $\boldsymbol{\zeta}_h = \boldsymbol{\sigma}_h$, and that the initial conditions coincide. We omit further details. $\square$

Remark 4.1. *The analysis developed in this section remains valid for any other triplet of finite element spaces satisfying (4.1), provided that the sole requirement $\mathbf{div}(\mathbb{X}_h) \subset \mathbf{H}_h^{\mathbf{u}}$ is fulfilled.*

4.3 Error analysis

We now proceed to establish the rates of convergence. For the sake of clarity, we restrict the analysis to the PEERS element (cf. (4.3)), and indicate at the end of this section, in Remark 4.2, the minor adjustments required for the AFW element (cf. (4.2)) or any other choice of triples. In this way, let $\boldsymbol{\mathcal{P}}_h^k : \mathbf{L}^s(\Omega) \to \mathbf{H}_h^{\mathbf{u}}$ and $\boldsymbol{\mathcal{P}}_h^{k+1} : \mathbb{L}^2_{\text{skew}}(\Omega) \to \mathbb{H}_h^{\gamma}$ be the L^2-projection operators, satisfying

$$
\begin{aligned}
\big(\mathbf{u} - \boldsymbol{\mathcal{P}}_h^k(\mathbf{u}), \mathbf{v}_h\big)_\Omega = 0 \quad \forall\, \mathbf{v}_h \in \mathbf{H}_h^{\mathbf{u}}, \\
\big(\boldsymbol{\gamma} - \boldsymbol{\mathcal{P}}_h^{k+1}(\boldsymbol{\gamma}), \boldsymbol{\eta}_h\big)_\Omega = 0 \quad \forall\, \boldsymbol{\eta}_h \in \mathbb{H}_h^{\gamma},
\end{aligned}
\tag{4.23}
$$

and, given $\mathrm{p} \geq 2\,d/(d+2)$, we consider the space

$$
\mathbb{H}_{\mathrm{p}} := \Big\{ \boldsymbol{\tau} \in \mathbb{X} \;:\; \boldsymbol{\tau}|_K \in \mathbb{W}^{1,\mathrm{p}}(K) \qquad \forall\, K \in \mathcal{T}_h \Big\},
$$

so that we may define $\boldsymbol{\Pi}_h^k : \mathbb{H}_{\mathrm{p}} \to \mathbb{RT}_k(\Omega)$ as the tensorial counterpart of the Raviart–Thomas interpolation operator, which satisfies the well-known commuting diagram property (cf. [9, Section 2.5.2] or [27, Section 3.4.1])

$$
\mathbf{div}(\boldsymbol{\Pi}_h^k(\boldsymbol{\tau})) = \boldsymbol{\mathcal{P}}_h^k(\mathbf{div}(\boldsymbol{\tau})) \qquad \forall\, \boldsymbol{\tau} \in \mathbb{H}_{\mathrm{p}}. \tag{4.24}
$$

Furthermore, recalling the decomposition (2.16), let us define $\boldsymbol{\Pi}_{h,0}^k : \mathbb{H}_{\mathrm{p}} \to \mathbb{RT}_k(\Omega) \cap \mathbb{H}_0(\mathbf{div}_\ell;\Omega)$ such that, for each $\boldsymbol{\tau} \in \mathbb{H}_{\mathrm{p}}$, $\boldsymbol{\Pi}_{h,0}^k(\boldsymbol{\tau})$ is the $\mathbb{H}_0(\mathbf{div}_\ell;\Omega)$-component of $\boldsymbol{\Pi}_h^k(\boldsymbol{\tau})$. Then, we notice that the range of $\boldsymbol{\Pi}_{h,0}$ is contained in $\mathbb{X}_h$, as $\mathbb{RT}_k(\Omega) \cap \mathbb{H}_0(\mathbf{div}_\ell;\Omega) \subset \mathbb{X}_h$. Moreover, one readily checks that the property (4.24) also holds when $\boldsymbol{\Pi}_h^k$ is replaced by $\boldsymbol{\Pi}_{h,0}^k$.

Now, let us define the errors $\mathbf{e}_{\boldsymbol{\sigma}} := \boldsymbol{\sigma} - \boldsymbol{\sigma}_h$ and $\mathbf{e}_{\underline{\mathbf{u}}} := (\mathbf{e}_{\mathbf{u}}, \mathbf{e}_{\boldsymbol{\gamma}}) = (\mathbf{u} - \mathbf{u}_h, \boldsymbol{\gamma} - \boldsymbol{\gamma}_h)$, and consider the decompositions

$$
\mathbf{e}_{\boldsymbol{\sigma}} = \boldsymbol{\delta}_{\boldsymbol{\sigma}} + \boldsymbol{\theta}_{\boldsymbol{\sigma}} \quad \text{and} \quad \mathbf{e}_{\underline{\mathbf{u}}} = \boldsymbol{\delta}_{\underline{\mathbf{u}}} + \boldsymbol{\theta}_{\underline{\mathbf{u}}} = (\boldsymbol{\delta}_{\mathbf{u}} + \boldsymbol{\theta}_{\mathbf{u}}, \boldsymbol{\delta}_{\boldsymbol{\gamma}} + \boldsymbol{\theta}_{\boldsymbol{\gamma}}), \tag{4.25}
$$

where

$$
\begin{gathered}
\boldsymbol{\delta}_{\boldsymbol{\sigma}} := \boldsymbol{\sigma} - \boldsymbol{\Pi}_{h,0}^k(\boldsymbol{\sigma}), \quad \boldsymbol{\theta}_{\boldsymbol{\sigma}} := \boldsymbol{\Pi}_{h,0}^k(\boldsymbol{\sigma}) - \boldsymbol{\sigma}_h, \quad \boldsymbol{\delta}_{\mathbf{u}} := \mathbf{u} - \boldsymbol{\mathcal{P}}_h^k(\mathbf{u}), \quad \boldsymbol{\theta}_{\mathbf{u}} := \boldsymbol{\mathcal{P}}_h^k(\mathbf{u}) - \mathbf{u}_h, \\
\boldsymbol{\delta}_{\boldsymbol{\gamma}} := \boldsymbol{\gamma} - \boldsymbol{\mathcal{P}}_h^{k+1}(\boldsymbol{\gamma}), \quad \text{and} \quad \boldsymbol{\theta}_{\boldsymbol{\gamma}} := \boldsymbol{\mathcal{P}}_h^{k+1}(\boldsymbol{\gamma}) - \boldsymbol{\gamma}_h.
\end{gathered}
$$

Subtracting the discrete problem (4.4) from the continuous one (2.19), we obtain the following error system:

$$\begin{aligned} [\mathbf{A}(\mathbf{e}_{\boldsymbol{\sigma}}),\boldsymbol{\tau}_h] + [\mathbf{B}'(\mathbf{e}_{\underline{\mathbf{u}}}),\boldsymbol{\tau}_h] + [\mathbf{D}'_\rho(\mathbf{e}_{\underline{\mathbf{u}}}),\boldsymbol{\tau}_h] &= 0 \quad \forall\,\boldsymbol{\tau}_h\in\mathbb{X}_h\,,\\ \frac{\partial}{\partial t}[\mathbf{E}(\mathbf{e}_{\underline{\mathbf{u}}}),\underline{\mathbf{v}}_h] - [\mathbf{B}(\mathbf{e}_{\boldsymbol{\sigma}}),\underline{\mathbf{v}}_h] + [\mathbf{C}(\mathbf{e}_{\underline{\mathbf{u}}}),\underline{\mathbf{v}}_h] &= 0 \quad \forall\,\underline{\mathbf{v}}_h\in\mathbf{Y}_h\,. \end{aligned} \tag{4.26}$$

In turn, using the projection properties (4.23) and (4.24), we find that

$$[\mathbf{B}'(\boldsymbol{\delta}_{\underline{\mathbf{u}}}),\boldsymbol{\tau}_h] = (\boldsymbol{\tau}_h,\boldsymbol{\delta}_{\boldsymbol{\gamma}})_\Omega \quad \forall\,\boldsymbol{\tau}_h\in\mathbb{X}_h\,,\quad\text{and}\quad [\mathbf{B}(\boldsymbol{\delta}_{\boldsymbol{\sigma}}),\underline{\mathbf{v}}_h] = (\boldsymbol{\delta}_{\boldsymbol{\sigma}},\boldsymbol{\eta}_h)_\Omega \quad \forall\,\underline{\mathbf{v}}_h\in\mathbf{Y}_h\,.$$

Hence, the error system (4.26) can be rewritten as

$$\begin{aligned} [\mathbf{A}(\boldsymbol{\theta}_{\boldsymbol{\sigma}}),\boldsymbol{\tau}_h] + [\mathbf{B}'(\boldsymbol{\theta}_{\underline{\mathbf{u}}}),\boldsymbol{\tau}_h] + [\mathbf{D}'_\rho(\boldsymbol{\theta}_{\underline{\mathbf{u}}}),\boldsymbol{\tau}_h] &= -[\mathbf{A}(\boldsymbol{\delta}_{\boldsymbol{\sigma}}),\boldsymbol{\tau}_h] - (\boldsymbol{\tau}_h,\boldsymbol{\delta}_{\boldsymbol{\gamma}})_\Omega - [\mathbf{D}'_\rho(\boldsymbol{\delta}_{\underline{\mathbf{u}}}),\boldsymbol{\tau}_h]\,,\\ \frac{\partial}{\partial t}[\mathbf{E}(\boldsymbol{\theta}_{\underline{\mathbf{u}}}),\underline{\mathbf{v}}_h] - [\mathbf{B}(\boldsymbol{\theta}_{\boldsymbol{\sigma}}),\underline{\mathbf{v}}_h] + [\mathbf{C}(\boldsymbol{\theta}_{\underline{\mathbf{u}}}),\underline{\mathbf{v}}_h] &= -\frac{\partial}{\partial t}[\mathbf{E}(\boldsymbol{\delta}_{\underline{\mathbf{u}}}),\underline{\mathbf{v}}_h] + (\boldsymbol{\delta}_{\boldsymbol{\sigma}},\boldsymbol{\eta}_h)_\Omega - [\mathbf{C}(\boldsymbol{\delta}_{\underline{\mathbf{u}}}),\underline{\mathbf{v}}_h]\,, \end{aligned} \tag{4.27}$$

for all $(\boldsymbol{\tau}_h,\underline{\mathbf{v}}_h)\in\mathbb{X}_h\times\mathbf{Y}_h$.

On the other hand, similar notation is introduced for the discrete initial conditions system (4.5). Let us consider $\mathbf{e}_{\boldsymbol{\sigma}_0} := \boldsymbol{\sigma}_0 - \boldsymbol{\sigma}_{h,0}$ and $\mathbf{e}_{\underline{\mathbf{u}}_0} := (\mathbf{e}_{\mathbf{u}_0},\mathbf{e}_{\gamma_0}) = (\mathbf{u}_0-\mathbf{u}_{h,0},\gamma_0-\gamma_{h,0})$, with the corresponding decompositions

$$\mathbf{e}_{\boldsymbol{\sigma}_0} = \boldsymbol{\delta}_{\boldsymbol{\sigma}_0} + \boldsymbol{\theta}_{\boldsymbol{\sigma}_0} \quad\text{and}\quad \mathbf{e}_{\underline{\mathbf{u}}_0} = \boldsymbol{\delta}_{\underline{\mathbf{u}}_0} + \boldsymbol{\theta}_{\underline{\mathbf{u}}_0} = (\boldsymbol{\delta}_{\mathbf{u}_0}+\boldsymbol{\theta}_{\mathbf{u}_0},\boldsymbol{\delta}_{\gamma_0}+\boldsymbol{\theta}_{\gamma_0})\,, \tag{4.28}$$

where

$$\begin{gathered} \boldsymbol{\delta}_{\boldsymbol{\sigma}_0} := \boldsymbol{\sigma}_0 - \boldsymbol{\Pi}^k_{h,0}(\boldsymbol{\sigma}_0)\,,\quad \boldsymbol{\theta}_{\boldsymbol{\sigma}_0} := \boldsymbol{\Pi}^k_{h,0}(\boldsymbol{\sigma}_0) - \boldsymbol{\sigma}_{h,0}\,,\quad \boldsymbol{\delta}_{\mathbf{u}_0} := \mathbf{u}_0 - \boldsymbol{\mathcal{P}}^k_h(\mathbf{u}_0)\,,\quad \boldsymbol{\theta}_{\mathbf{u}_0} := \boldsymbol{\mathcal{P}}^k_h(\mathbf{u}_0) - \mathbf{u}_{h,0}\,,\\ \boldsymbol{\delta}_{\gamma_0} := \gamma_0 - \mathbb{P}^{k+1}_h(\gamma_0)\,,\quad\text{and}\quad \boldsymbol{\theta}_{\gamma_0} := \mathbb{P}^{k+1}_h(\gamma_0) - \gamma_{h,0}\,. \end{gathered}$$

Thus, by subtracting the discrete initial conditions system (4.5) from the continuous one (3.18), we obtain the error system

$$\begin{aligned} [\mathbf{A}(\mathbf{e}_{\boldsymbol{\sigma}_0}),\boldsymbol{\tau}_h] + [\mathbf{B}'(\mathbf{e}_{\underline{\mathbf{u}}_0}),\boldsymbol{\tau}_h] + [\mathbf{D}'_\rho(\mathbf{e}_{\underline{\mathbf{u}}_0}),\boldsymbol{\tau}_h] &= 0 \quad \forall\,\boldsymbol{\tau}_h\in\mathbb{X}_h\,,\\ -[\mathbf{B}(\mathbf{e}_{\boldsymbol{\sigma}_0}),\underline{\mathbf{v}}_h] + [\mathbf{C}(\mathbf{e}_{\underline{\mathbf{u}}_0}),\underline{\mathbf{v}}_h] &= 0 \quad \forall\,\underline{\mathbf{v}}_h\in\mathbf{Y}_h\,. \end{aligned} \tag{4.29}$$

We now establish the main result of this section.

Theorem 4.8. *Assume that the hypotheses of Theorems 3.9 and 4.7 hold. Furthermore, suppose that the porosity satisfies*

$$\left\|\frac{\nabla\rho}{\rho}\right\|_{\mathbf{L}^\infty(\Omega)} \le \frac{\sqrt{d}\,\rho_0\,\Lambda_{\mathbf{d}}}{8\sqrt{2}\,\rho_1\,\|\mathbf{i}_{s,2}\|}\,. \tag{4.30}$$

Let $(\boldsymbol{\sigma},\underline{\mathbf{u}})$ *and* $(\boldsymbol{\sigma}_h,\underline{\mathbf{u}}_h)$ *be the unique solutions of the continuous and semidiscrete problems (2.19) and (4.4), respectively, with the regularity specified in Theorems 3.9 and 4.7. Assume further that* $\boldsymbol{\sigma}\in\mathbb{H}_{\mathrm{p}}$ *for some* $\mathrm{p}\ge 2d/(d+2)$*. Then, there exists a positive constant* $\mathcal{C}$*, independent of* h*, such that*

$$\|\mathbf{e}_{\boldsymbol{\sigma}}\|^2_{\mathrm{L}^2(0,T;\mathbb{X})} + \|\mathbf{e}_{\mathbf{u}}\|^2_{\mathrm{L}^2(0,T;\mathbf{L}^s(\Omega))} + \|\mathbf{e}_{\mathbf{u}}\|^2_{\mathrm{L}^\infty(0,T;\mathbf{L}^2(\Omega))} + \|\mathbf{e}_{\boldsymbol{\gamma}}\|^2_{\mathrm{L}^2(0,T;\mathbb{L}^2(\Omega))} \le \mathcal{C}\,\mathrm{E}_{\boldsymbol{\delta}}\,, \tag{4.31}$$

where

$$\begin{aligned} \mathrm{E}_{\boldsymbol{\delta}} := {}& \|\boldsymbol{\delta}_{\boldsymbol{\sigma}}\|^2_{\mathrm{L}^2(0,T;\mathbb{X})} + \|\boldsymbol{\delta}_{\mathbf{u}}\|^2_{\mathrm{L}^2(0,T;\mathbf{L}^s(\Omega))} + \|\boldsymbol{\delta}_{\boldsymbol{\gamma}}\|^2_{\mathrm{L}^2(0,T;\mathbb{L}^2(\Omega))} + \|\partial_t\boldsymbol{\delta}_{\boldsymbol{\sigma}}\|^2_{\mathrm{L}^2(0,T;\mathbb{L}^2(\Omega))}\\ &+ \|\partial_t\boldsymbol{\delta}_{\mathbf{u}}\|^2_{\mathrm{L}^2(0,T;\mathbf{L}^2(\Omega))} + \|\partial_t\boldsymbol{\delta}_{\boldsymbol{\gamma}}\|^2_{\mathrm{L}^2(0,T;\mathbb{L}^2(\Omega))} + \|\boldsymbol{\delta}_{\boldsymbol{\sigma}}\|^2_{\mathrm{L}^\infty(0,T;\mathbb{X})} + \|\boldsymbol{\delta}_{\mathbf{u}}\|^2_{\mathrm{L}^\infty(0,T;\mathbf{L}^s(\Omega))}\\ &+ \|\boldsymbol{\delta}_{\boldsymbol{\gamma}}\|^2_{\mathrm{L}^\infty(0,T;\mathbb{L}^2(\Omega))} + \|\boldsymbol{\delta}_{\boldsymbol{\sigma}}(0)\|^2_{\mathbb{X}} + \|\boldsymbol{\delta}_{\boldsymbol{\sigma}_0}\|^2_{\mathbb{X}} + \|\boldsymbol{\delta}_{\mathbf{u}_0}\|^2_{\mathbf{L}^s(\Omega)} + \|\boldsymbol{\delta}_{\gamma_0}\|^2_{\mathbb{L}^2(\Omega)}\,. \end{aligned}$$

Proof. First, notice that since $\boldsymbol{\sigma} \in \mathbb{H}_{\mathrm{p}}$, $\boldsymbol{\Pi}_{h,0}^{k}(\boldsymbol{\sigma})$ is well-defined. Then, proceeding similarly as in the proof of Theorem 3.4, we use the discrete inf-sup condition (4.7), the error system (4.27), and the assumption $\|\nabla\rho/\rho\|_{\mathbf{L}^\infty(\Omega)} \leq \sqrt{d}\,\Lambda_{\mathtt{d}}/(2\,\|\mathbf{i}_{s,2}\|)$ (cf. (4.20)), so that we obtain

$$\begin{aligned}\frac{\Lambda_{\mathtt{d}}}{2}\,\|(\boldsymbol{\theta}_{\boldsymbol{\sigma}},\boldsymbol{\theta}_{\underline{\mathbf{u}}})\|_{\mathbb{X}\times\mathbf{Y}} \leq C_1\,\big(\|\boldsymbol{\delta}_{\boldsymbol{\sigma}}\|_{\mathbb{X}} + \|\boldsymbol{\delta}_{\mathbf{u}}\|_{\mathbf{L}^s(\Omega)} + \|\boldsymbol{\delta}_{\boldsymbol{\gamma}}\|_{\mathbb{L}^2(\Omega)} + \|\partial_t\,\boldsymbol{\delta}_{\mathbf{u}}\|_{\mathbf{L}^2(\Omega)}\big) \\ + \rho_1\,\|\mathbf{i}_{s,2}\|\,\|\partial_t\boldsymbol{\theta}_{\mathbf{u}}\|_{\mathbf{L}^2(\Omega)}\,,\end{aligned} \tag{4.32}$$

where C_1 is a positive constant depending only on μ, ρ_0, ρ_1, $|\Omega|$, $\|\mathbf{K}^{-1}\|_{\mathbb{L}^\infty(\Omega)}$, and $\|\nabla\rho/\rho\|_{\mathbf{L}^r(\Omega)}$. By squaring (4.32), integrating from 0 to $t \in (0,T]$, and performing some algebraic manipulations, we arrive at

$$\begin{aligned}&\frac{\Lambda_{\mathtt{d}}^2}{8\,\rho_1^2\,\|\mathbf{i}_{s,2}\|^2}\int_0^t \Big\{\|\boldsymbol{\theta}_{\boldsymbol{\sigma}}(\mathrm{s})\|_{\mathbb{X}}^2 + \|\boldsymbol{\theta}_{\mathbf{u}}(\mathrm{s})\|_{\mathbf{L}^s(\Omega)}^2 + \|\boldsymbol{\theta}_{\boldsymbol{\gamma}}(\mathrm{s})\|_{\mathbb{L}^2(\Omega)}^2\Big\}\,d\mathrm{s} \\ &\quad\leq \widetilde{C}_1\int_0^t \Big\{\|\boldsymbol{\delta}_{\boldsymbol{\sigma}}(\mathrm{s})\|_{\mathbb{X}}^2 + \|\boldsymbol{\delta}_{\mathbf{u}}(\mathrm{s})\|_{\mathbf{L}^s(\Omega)}^2 + \|\boldsymbol{\delta}_{\boldsymbol{\gamma}}(\mathrm{s})\|_{\mathbb{L}^2(\Omega)}^2 + \|\partial_t\,\boldsymbol{\delta}_{\mathbf{u}}(\mathrm{s})\|_{\mathbf{L}^2(\Omega)}^2\Big\}\,d\mathrm{s} \\ &\qquad + \int_0^t \|\partial_t\,\boldsymbol{\theta}_{\mathbf{u}}(\mathrm{s})\|_{\mathbf{L}^2(\Omega)}^2\,d\mathrm{s}\,,\end{aligned} \tag{4.33}$$

with $\widetilde{C}_1$ having the same dependence on the data and parameters as C_1.

In order to bound the last term in (4.33), we differentiate in time the first row of (4.27), test with $(\boldsymbol{\tau}_h,\underline{\mathbf{v}}_h) = (\boldsymbol{\theta}_{\boldsymbol{\sigma}},\partial_t\,\boldsymbol{\theta}_{\underline{\mathbf{u}}})$, and use the identity $(\boldsymbol{\delta}_{\boldsymbol{\sigma}},\partial_t\,\boldsymbol{\theta}_{\boldsymbol{\gamma}})_\Omega = \partial_t\,(\boldsymbol{\delta}_{\boldsymbol{\sigma}},\boldsymbol{\theta}_{\boldsymbol{\gamma}})_\Omega - (\partial_t\,\boldsymbol{\delta}_{\boldsymbol{\sigma}},\boldsymbol{\theta}_{\boldsymbol{\gamma}})_\Omega$, thus obtaining

$$\begin{aligned}&\frac{1}{2\,\mu}\left(\frac{1}{\rho}\,\partial_t\,\boldsymbol{\theta}_{\boldsymbol{\sigma}}^{\mathrm{d}},\boldsymbol{\theta}_{\boldsymbol{\sigma}}^{\mathrm{d}}\right)_\Omega + \big(\rho\,\partial_t\,\boldsymbol{\theta}_{\mathbf{u}},\partial_t\,\boldsymbol{\theta}_{\mathbf{u}}\big)_\Omega + \mu\,\big(\mathbf{K}^{-1}\,\boldsymbol{\theta}_{\mathbf{u}},\partial_t\,\boldsymbol{\theta}_{\mathbf{u}}\big)_\Omega \\ &\quad = -\frac{1}{2\mu}\left(\frac{1}{\rho}\,\partial_t\,\boldsymbol{\delta}_{\boldsymbol{\sigma}}^{\mathrm{d}},\boldsymbol{\theta}_{\boldsymbol{\sigma}}^{\mathrm{d}}\right)_\Omega - \big(\rho\,\partial_t\,\boldsymbol{\delta}_{\mathbf{u}},\partial_t\,\boldsymbol{\theta}_{\mathbf{u}}\big)_\Omega - (\boldsymbol{\theta}_{\boldsymbol{\sigma}},\partial_t\,\boldsymbol{\delta}_{\boldsymbol{\gamma}})_\Omega + \partial_t\,(\boldsymbol{\delta}_{\boldsymbol{\sigma}},\boldsymbol{\theta}_{\boldsymbol{\gamma}})_\Omega \\ &\qquad - (\partial_t\,\boldsymbol{\delta}_{\boldsymbol{\sigma}},\boldsymbol{\theta}_{\boldsymbol{\gamma}})_\Omega + \frac{1}{d}\left(\frac{\nabla\rho}{\rho}\cdot\partial_t\,\mathbf{e}_{\mathbf{u}},\mathrm{tr}(\boldsymbol{\theta}_{\boldsymbol{\sigma}})\right)_\Omega - \mu\,\big(\mathbf{K}^{-1}\,\boldsymbol{\delta}_{\mathbf{u}},\partial_t\,\boldsymbol{\theta}_{\mathbf{u}}\big)_\Omega\,.\end{aligned}$$

Now we use the monotonicity properties (cf. (3.5a) and (3.5b)), Cauchy–Schwarz and Young's inequalities (cf. (1.1)), so that, after some algebraic manipulations, the previous estimate becomes

$$\begin{aligned}&\frac{1}{4\,\mu}\,\partial_t\left(\frac{1}{\rho}\,\boldsymbol{\theta}_{\boldsymbol{\sigma}}^{\mathrm{d}},\boldsymbol{\theta}_{\boldsymbol{\sigma}}^{\mathrm{d}}\right)_\Omega + \frac{\rho_0}{8}\,\|\partial_t\,\boldsymbol{\theta}_{\mathbf{u}}\|_{\mathbf{L}^2(\Omega)}^2 + \frac{\mu}{2}\,\partial_t\,\big(\mathbf{K}^{-1}\,\boldsymbol{\theta}_{\mathbf{u}},\boldsymbol{\theta}_{\mathbf{u}}\big)_\Omega \\ &\quad\leq C_2\,\Big(\|\partial_t\,\boldsymbol{\delta}_{\boldsymbol{\sigma}}\|_{\mathbb{L}^2(\Omega)}^2 + \|\partial_t\,\boldsymbol{\delta}_{\mathbf{u}}\|_{\mathbf{L}^2(\Omega)}^2 + \|\boldsymbol{\delta}_{\mathbf{u}}\|_{\mathbf{L}^s(\Omega)}^2 + \|\partial_t\,\boldsymbol{\delta}_{\boldsymbol{\gamma}}\|_{\mathbb{L}^2(\Omega)}^2\Big) \\ &\qquad + \delta_1\,\|\boldsymbol{\theta}_{\boldsymbol{\sigma}}\|_{\mathbb{X}}^2 + \delta_2\,\|\boldsymbol{\theta}_{\boldsymbol{\gamma}}\|_{\mathbb{L}^2(\Omega)}^2 + \frac{1}{d\,\rho_0}\left\|\frac{\nabla\rho}{\rho}\right\|_{\mathbf{L}^\infty(\Omega)}^2\,\|\boldsymbol{\theta}_{\boldsymbol{\sigma}}\|_{\mathbb{X}}^2 + \partial_t\,(\boldsymbol{\delta}_{\boldsymbol{\sigma}},\boldsymbol{\theta}_{\boldsymbol{\gamma}})_\Omega\,,\end{aligned} \tag{4.34}$$

with C_2 depending only on μ, ρ_0, ρ_1, $\|\mathbf{K}^{-1}\|_{\mathbb{L}^\infty(\Omega)}$, and δ_1,δ_2 arbitrary positive numbers to be chosen later. Then, integrating (4.34) from 0 to $t \in (0,T]$, and using the assumption (4.30), we get

$$
\begin{aligned}
&\frac{1}{4\,\mu\,\rho_1}\,\|\boldsymbol{\theta}^{\mathrm{d}}_{\boldsymbol{\sigma}}(t)\|^2_{\mathbb{L}^2(\Omega)} + \frac{\mu\,C_{\mathbf{K}}}{2}\,\|\boldsymbol{\theta}_{\mathbf{u}}(t)\|^2_{\mathbf{L}^2(\Omega)} + \frac{\rho_0}{8}\int_0^t \|\partial_t\,\boldsymbol{\theta}_{\mathbf{u}}(\mathrm{s})\|^2_{\mathbf{L}^2(\Omega)}\,ds \\
&\quad\leq C_2\int_0^t \Big(\|\partial_t\,\boldsymbol{\delta}_{\boldsymbol{\sigma}}(\mathrm{s})\|^2_{\mathbb{L}^2(\Omega)} + \|\partial_t\,\boldsymbol{\delta}_{\mathbf{u}}(\mathrm{s})\|^2_{\mathbf{L}^2(\Omega)} + \|\boldsymbol{\delta}_{\mathbf{u}}(\mathrm{s})\|^2_{\mathbf{L}^s(\Omega)} + \|\partial_t\,\boldsymbol{\delta}_{\boldsymbol{\gamma}}(\mathrm{s})\|^2_{\mathbb{L}^2(\Omega)}\Big)\,ds \\
&\qquad + \int_0^t \big(\delta_1\,\|\boldsymbol{\theta}_{\boldsymbol{\sigma}}(\mathrm{s})\|^2_{\mathbb{X}} + \delta_2\,\|\boldsymbol{\theta}_{\boldsymbol{\gamma}}(\mathrm{s})\|^2_{\mathbb{L}^2(\Omega)}\big)\,ds + \frac{\rho_0\,\Lambda^2_{\mathtt{d}}}{128\,\rho_1^2\,\|\mathbf{i}_{s,2}\|^2}\int_0^t \|\boldsymbol{\theta}_{\boldsymbol{\sigma}}(\mathrm{s})\|^2_{\mathbb{X}}\,ds \\
&\qquad + \|\boldsymbol{\delta}_{\boldsymbol{\sigma}}(t)\|_{\mathbb{L}^2(\Omega)}\,\|\boldsymbol{\theta}_{\boldsymbol{\gamma}}(t)\|_{\mathbb{L}^2(\Omega)} + \|\boldsymbol{\delta}_{\boldsymbol{\sigma}}(0)\|_{\mathbb{L}^2(\Omega)}\,\|\boldsymbol{\theta}_{\boldsymbol{\gamma}}(0)\|_{\mathbb{L}^2(\Omega)} + \frac{1}{4\mu\,\rho_0}\,\|\boldsymbol{\theta}^{\mathrm{d}}_{\boldsymbol{\sigma}}(0)\|^2_{\mathbb{L}^2(\Omega)} \\
&\qquad + \frac{\mu}{2}\,\|\mathbf{K}^{-1}\|_{\mathbb{L}^\infty(\Omega)}\,\|\boldsymbol{\theta}_{\mathbf{u}}(0)\|^2_{\mathbf{L}^2(\Omega)}\,.
\end{aligned}
\tag{4.35}
$$

To bound the term $\|\boldsymbol{\theta}_{\boldsymbol{\gamma}}(t)\|_{\mathbb{L}^2(\Omega)}$, we observe from the first equation in (4.27) that

$$
[\widetilde{\mathbf{B}}'(\boldsymbol{\theta}_{\underline{\mathbf{u}}}),\boldsymbol{\tau}_h] = -[\mathbf{A}(\mathbf{e}_{\boldsymbol{\sigma}}),\boldsymbol{\tau}_h] - (\boldsymbol{\delta}_{\boldsymbol{\gamma}},\boldsymbol{\tau}_h)_\Omega - [\mathbf{D}'_\rho(\boldsymbol{\delta}_{\underline{\mathbf{u}}}),\boldsymbol{\tau}_h] \qquad \forall\,\boldsymbol{\tau}_h\in\mathbb{X}_h\,.
$$

Then, applying the discrete inf-sup condition of $\widetilde{\mathbf{B}}$ (cf. (4.13)), together with the Cauchy–Schwarz inequality, yields

$$
\begin{aligned}
\|\boldsymbol{\theta}_{\boldsymbol{\gamma}}(t)\|_{\mathbb{L}^2(\Omega)} &\leq \frac{1}{\beta_{\mathtt{d}}\,\mu\,\rho_0}\,\|\boldsymbol{\theta}^{\mathrm{d}}_{\boldsymbol{\sigma}}(t)\|_{\mathbb{L}^2(\Omega)} + \frac{1}{\beta_{\mathtt{d}}\,\mu\,\rho_0}\,\|\boldsymbol{\delta}^{\mathrm{d}}_{\boldsymbol{\sigma}}(t)\|_{\mathbb{L}^2(\Omega)} \\
&\quad + \frac{2}{\beta_{\mathtt{d}}}\,\|\boldsymbol{\delta}_{\boldsymbol{\gamma}}(t)\|_{\mathbb{L}^2(\Omega)} + \frac{2}{\sqrt{d}\,\beta_{\mathtt{d}}}\,\left\|\frac{\nabla\rho}{\rho}\right\|_{\mathbf{L}^r(\Omega)}\|\boldsymbol{\delta}_{\mathbf{u}}(t)\|_{\mathbf{L}^s(\Omega)}\,.
\end{aligned}
$$

Consequently, by suitably applying Young's inequality (cf. (1.1)), we obtain

$$
\|\boldsymbol{\delta}_{\boldsymbol{\sigma}}(t)\|_{\mathbb{L}^2(\Omega)}\,\|\boldsymbol{\theta}_{\boldsymbol{\gamma}}(t)\|_{\mathbb{L}^2(\Omega)} \leq \frac{1}{4\mu\,\rho_1}\,\|\boldsymbol{\theta}^{\mathrm{d}}_{\boldsymbol{\sigma}}(t)\|^2_{\mathbb{L}^2(\Omega)} + C_3\Big(\|\boldsymbol{\delta}_{\boldsymbol{\sigma}}(t)\|^2_{\mathbb{X}} + \|\boldsymbol{\delta}_{\mathbf{u}}(t)\|^2_{\mathbf{L}^s(\Omega)} + \|\boldsymbol{\delta}_{\boldsymbol{\gamma}}(t)\|^2_{\mathbb{L}^2(\Omega)}\Big)\,, \tag{4.36}
$$

with $C_3>0$ depending only on $\beta_{\mathtt{d}}$, μ, ρ_0, ρ_1 and $\|\nabla\rho/\rho\|_{\mathbf{L}^r(\Omega)}$.

On the other hand, to bound the last three terms in (4.35), we first observe that, similarly as in (4.32), by using the discrete global inf-sup condition (4.7), together with Cauchy–Schwarz and Young's inequalities, and assumption (4.20), it follows from (4.29) that

$$
\|\boldsymbol{\theta}_{\boldsymbol{\sigma}_0}\|^2_{\mathbb{X}} + \|\boldsymbol{\theta}_{\mathbf{u}_0}\|^2_{\mathbf{L}^s(\Omega)} + \|\boldsymbol{\theta}_{\boldsymbol{\gamma}_0}\|^2_{\mathbb{L}^2(\Omega)} \leq C_4\Big(\|\boldsymbol{\delta}_{\boldsymbol{\sigma}_0}\|^2_{\mathbb{X}} + \|\boldsymbol{\delta}_{\mathbf{u}_0}\|^2_{\mathbf{L}^s(\Omega)} + \|\boldsymbol{\delta}_{\boldsymbol{\gamma}_0}\|^2_{\mathbb{L}^2(\Omega)}\Big)\,, \tag{4.37}
$$

with $C_4>0$ depending only on $\Lambda_{\mathtt{d}}$, μ, $|\Omega|$, $\|\nabla\rho/\rho\|_{\mathbf{L}^\infty(\Omega)}$, $\|\mathbf{K}^{-1}\|_{\mathbb{L}^\infty(\Omega)}$ and ρ_0. In turn, we recall from Theorems 3.9 and 4.7 that $\boldsymbol{\sigma}^{\mathrm{d}}(0)=\boldsymbol{\sigma}^{\mathrm{d}}_0$ and $\boldsymbol{\sigma}^{\mathrm{d}}_h(0)=\boldsymbol{\sigma}^{\mathrm{d}}_{h,0}$, which allows us to estimate

$$
\begin{aligned}
\|\boldsymbol{\theta}^{\mathrm{d}}_{\boldsymbol{\sigma}}(0)\|_{\mathbb{L}^2(\Omega)} &= \big\|\boldsymbol{\Pi}^k_{h,0}(\boldsymbol{\sigma}(0))^{\mathrm{d}} - \boldsymbol{\sigma}^{\mathrm{d}}(0) + \boldsymbol{\sigma}^{\mathrm{d}}_0 - \boldsymbol{\Pi}^k_{h,0}(\boldsymbol{\sigma}_0)^{\mathrm{d}} + \boldsymbol{\Pi}^k_{h,0}(\boldsymbol{\sigma}_0)^{\mathrm{d}} - \boldsymbol{\sigma}^{\mathrm{d}}_{h,0}\big\|_{\mathbb{L}^2(\Omega)} \\
&\leq \|\boldsymbol{\delta}^{\mathrm{d}}_{\boldsymbol{\sigma}}(0)\|_{\mathbb{L}^2(\Omega)} + \|\boldsymbol{\delta}^{\mathrm{d}}_{\boldsymbol{\sigma}_0}\|_{\mathbb{L}^2(\Omega)} + \|\boldsymbol{\theta}^{\mathrm{d}}_{\boldsymbol{\sigma}_0}\|_{\mathbb{L}^2(\Omega)} \leq \|\boldsymbol{\delta}_{\boldsymbol{\sigma}}(0)\|_{\mathbb{X}} + \|\boldsymbol{\delta}_{\boldsymbol{\sigma}_0}\|_{\mathbb{X}} + \|\boldsymbol{\theta}_{\boldsymbol{\sigma}_0}\|_{\mathbb{X}}\,.
\end{aligned}
\tag{4.38}
$$

Moreover, by the same results, $\mathbf{u}(0)=\mathbf{u}_0$, $\boldsymbol{\gamma}(0)=\boldsymbol{\gamma}_0$, $\mathbf{u}_h(0)=\mathbf{u}_{h,0}$, and $\boldsymbol{\gamma}_h(0)=\boldsymbol{\gamma}_{h,0}$, which implies that $\boldsymbol{\theta}_{\mathbf{u}_0}=\boldsymbol{\theta}_{\mathbf{u}}(0)$ and $\boldsymbol{\theta}_{\boldsymbol{\gamma}_0}=\boldsymbol{\theta}_{\boldsymbol{\gamma}}(0)$. Hence, substituting these facts into (4.37), and then combining it with (4.38), we obtain that

$$
\|\boldsymbol{\theta}^{\mathrm{d}}_{\boldsymbol{\sigma}}(0)\|^2_{\mathbb{L}^2(\Omega)} + \|\boldsymbol{\theta}_{\mathbf{u}}(0)\|^2_{\mathbf{L}^s(\Omega)} + \|\boldsymbol{\theta}_{\boldsymbol{\gamma}}(0)\|^2_{\mathbb{L}^2(\Omega)} \leq C_5\,\mathrm{E}_{\boldsymbol{\delta},0}\,, \tag{4.39}
$$

where $C_5 > 0$ depends only on C_4, and $\mathrm{E}_{\boldsymbol{\delta},0}$ is defined as

$$\mathrm{E}_{\boldsymbol{\delta},0} := \|\boldsymbol{\delta}_{\boldsymbol{\sigma}}(0)\|_{\mathbb{X}}^2 + \|\boldsymbol{\delta}_{\boldsymbol{\sigma}_0}\|_{\mathbb{X}}^2 + \|\boldsymbol{\delta}_{\mathbf{u}_0}\|_{\mathbf{L}^s(\Omega)}^2 + \|\boldsymbol{\delta}_{\gamma_0}\|_{\mathbb{L}^2(\Omega)}^2 .$$

Thus, by replacing (4.36) and (4.39) into (4.35), and then applying Young's inequality (cf. (1.1)) together with some algebraic manipulations, we deduce that

$$\begin{aligned}
&\frac{\mu\, C_{\mathbf{K}}}{2}\,\|\boldsymbol{\theta}_{\mathbf{u}}(t)\|_{\mathbf{L}^2(\Omega)}^2 + \frac{\rho_0}{8}\int_0^t \|\partial_t\boldsymbol{\theta}_{\mathbf{u}}(\mathrm{s})\|_{\mathbf{L}^2(\Omega)}^2\, d\mathrm{s} \\
&\le C_2 \int_0^t \Big(\|\partial_t\, \boldsymbol{\delta}_{\boldsymbol{\sigma}}(\mathrm{s})\|_{\mathbb{L}^2(\Omega)}^2 + \|\partial_t\, \boldsymbol{\delta}_{\mathbf{u}}(\mathrm{s})\|_{\mathbf{L}^2(\Omega)}^2 + \|\boldsymbol{\delta}_{\mathbf{u}}(\mathrm{s})\|_{\mathbf{L}^s(\Omega)}^2 + \|\partial_t\, \boldsymbol{\delta}_{\boldsymbol{\gamma}}(\mathrm{s})\|_{\mathbb{L}^2(\Omega)}^2\Big)\, d\mathrm{s} \\
&+ C_6 \Big(\|\boldsymbol{\delta}_{\boldsymbol{\sigma}}(t)\|_{\mathbb{X}}^2 + \|\boldsymbol{\delta}_{\mathbf{u}}(t)\|_{\mathbf{L}^s(\Omega)}^2 + \|\boldsymbol{\delta}_{\boldsymbol{\gamma}}(t)\|_{\mathbb{L}^2(\Omega)}^2 + \mathrm{E}_{\boldsymbol{\delta},0}\Big) \\
&+ \int_0^t \big(\delta_1\,\|\boldsymbol{\theta}_{\boldsymbol{\sigma}}(\mathrm{s})\|_{\mathbb{X}}^2 + \delta_2\,\|\boldsymbol{\theta}_{\boldsymbol{\gamma}}(\mathrm{s})\|_{\mathbb{L}^2(\Omega)}^2\big)\, d\mathrm{s} + \frac{\rho_0\,\Lambda_{\mathtt{d}}^2}{128\,\rho_1^2\,\|\mathbf{i}_{s,2}\|^2}\int_0^t \|\boldsymbol{\theta}_{\boldsymbol{\sigma}}(\mathrm{s})\|_{\mathbb{X}}^2\, d\mathrm{s}\,,
\end{aligned} \tag{4.40}$$

with $C_6 > 0$ depending only on C_3 and C_5. Then, we substitute (4.40) into (4.33), and choose δ_1 and δ_2 sufficiently small, thereby yielding

$$\begin{aligned}
&\int_0^t \Big(\|\boldsymbol{\theta}_{\boldsymbol{\sigma}}(\mathrm{s})\|_{\mathbb{X}}^2 + \|\boldsymbol{\theta}_{\mathbf{u}}(\mathrm{s})\|_{\mathbf{L}^s(\Omega)}^2 + \|\boldsymbol{\theta}_{\boldsymbol{\gamma}}(\mathrm{s})\|_{\mathbb{L}^2(\Omega)}^2\Big) d\mathrm{s} + \|\boldsymbol{\theta}_{\mathbf{u}}(t)\|_{\mathbf{L}^2(\Omega)}^2 \\
&\quad \le \widehat{C}_1 \Bigg\{ \int_0^t \Big(\|\boldsymbol{\delta}_{\boldsymbol{\sigma}}(\mathrm{s})\|_{\mathbb{X}}^2 + \|\boldsymbol{\delta}_{\mathbf{u}}(\mathrm{s})\|_{\mathbf{L}^s(\Omega)}^2 + \|\boldsymbol{\delta}_{\boldsymbol{\gamma}}(\mathrm{s})\|_{\mathbb{L}^2(\Omega)}^2\Big)\, d\mathrm{s} \\
&\qquad + \int_0^t \Big(\|\partial_t\boldsymbol{\delta}_{\mathbf{u}}(\mathrm{s})\|_{\mathbf{L}^2(\Omega)}^2 + \|\partial_t\boldsymbol{\delta}_{\boldsymbol{\sigma}}(\mathrm{s})\|_{\mathbb{L}^2(\Omega)}^2 + \|\partial_t\boldsymbol{\delta}_{\boldsymbol{\gamma}}(\mathrm{s})\|_{\mathbb{L}^2(\Omega)}^2\Big)\, ds \Bigg\} \\
&\quad + \widehat{C}_2 \Big(\|\boldsymbol{\delta}_{\boldsymbol{\sigma}}(t)\|_{\mathbb{X}}^2 + \|\boldsymbol{\delta}_{\mathbf{u}}(t)\|_{\mathbf{L}^s(\Omega)}^2 + \|\boldsymbol{\delta}_{\boldsymbol{\gamma}}(t)\|_{\mathbb{L}^2(\Omega)}^2 + \mathrm{E}_{\boldsymbol{\delta},0}\Big)\,,
\end{aligned} \tag{4.41}$$

with $\widehat{C}_1$ and $\widehat{C}_2$ depending on the previous constants, physical parameters and data. Finally, by using the error decompositions (4.25) together with (4.41), we obtain (4.31), as desired. □

Next, in order to obtain the theoretical rates of convergence for the semidiscrete scheme (4.4), we recall the approximation properties associated with the finite element spaces (cf. (4.2) and (4.3)), and the operators $\boldsymbol{\mathcal{P}}_h^k$, $\boldsymbol{\mathcal{P}}_h^{k+1}$, and $\boldsymbol{\Pi}_h^k$. These properties basically follow from classical interpolation estimates of Sobolev spaces and the commuting diagram property (cf. (4.24)). For details we refer to [27, Section 3.4.4], [9, Section 2.5.5], or [15, Section 4.2.1].

($\mathbf{AP}_h^{\boldsymbol{\sigma}}$) There exists a positive constant C, independent of h, such that for each $\vartheta \in (0, k+1]$ and for each $\boldsymbol{\tau} \in \mathbb{H}^{\vartheta}(\Omega) \cap \mathbb{X}$, with $\mathbf{div}(\boldsymbol{\tau}) \in \mathbf{W}^{\vartheta,\ell}(\Omega)$, there holds

$$\|\boldsymbol{\tau} - \boldsymbol{\Pi}_h^k(\boldsymbol{\tau})\|_{\mathbb{X}} \le C\, h^{\vartheta} \Big\{\|\boldsymbol{\tau}\|_{\mathbb{H}^{\vartheta}(\Omega)} + \|\mathbf{div}(\boldsymbol{\tau})\|_{\mathbf{W}^{\vartheta,\ell}(\Omega)}\Big\}.$$

($\mathbf{AP}_h^{\mathbf{u}}$) There exists a positive constant C, independent of h, such that for each $\vartheta \in [0, k+1]$ and for each $\mathbf{v} \in \mathbf{W}^{\vartheta,s}(\Omega)$, there holds

$$\|\mathbf{v} - \boldsymbol{\mathcal{P}}_h^k(\mathbf{v})\|_{\mathbf{L}^s(\Omega)} \le C\, h^{\vartheta}\, \|\mathbf{v}\|_{\mathbf{W}^{\vartheta,s}(\Omega)} .$$

($\mathbf{AP}_h^{\gamma}$) There exists a positive constant C, independent of h, such that for each $\vartheta \in [0, k+1]$ and for each $\boldsymbol{\eta} \in \mathbb{H}^{\vartheta}(\Omega) \cap \mathbb{L}^2_{\mathrm{skew}}(\Omega)$, there holds

$$\|\boldsymbol{\eta} - \boldsymbol{\mathcal{P}}_h^{k+1}(\boldsymbol{\eta})\|_{\mathbb{L}^2(\Omega)} \le C\, h^{\vartheta}\, \|\boldsymbol{\eta}\|_{\mathbb{H}^{\vartheta}(\Omega)} .$$

It is worth noting that $(\mathbf{AP}_h^{\boldsymbol{\sigma}})$ is stated in terms of $\boldsymbol{\Pi}_h^k$ instead of $\boldsymbol{\Pi}_{h,0}^k$. However, it is not difficult to prove that, for all $\boldsymbol{\tau} \in \mathbb{H}^{\vartheta}(\Omega) \cap \mathbb{X}$,

$$\|\boldsymbol{\tau} - \boldsymbol{\Pi}_{h,0}^k(\boldsymbol{\tau})\|_{\mathbb{X}} \leq (1 + d^2\,|\Omega|^2)^{1/2}\,\|\boldsymbol{\tau} - \boldsymbol{\Pi}_h^k(\boldsymbol{\tau})\|_{\mathbb{X}}\,,$$

so the approximation property also holds for this operator, up to a multiplicative constant independent of h. In this way, it follows that, under an extra regularity assumption on the exact solution, there exist positive constants $C(\boldsymbol{\sigma})$, $C(\mathbf{u})$, $C(\boldsymbol{\gamma})$, $C(\partial_t\boldsymbol{\sigma})$, $C(\partial_t\mathbf{u})$, and $C(\partial_t\boldsymbol{\gamma})$, whose explicit expression are obtained from the right-hand side of the foregoing approximation properties, such that

$$\begin{gathered}
\|\boldsymbol{\delta}_{\boldsymbol{\sigma}}\|_{\mathbb{X}} \leq C(\boldsymbol{\sigma})\,h^{\vartheta}\,, \quad \|\boldsymbol{\delta}_{\mathbf{u}}\|_{\mathbf{L}^s(\Omega)} \leq C(\mathbf{u})\,h^{\vartheta}\,, \quad \|\boldsymbol{\delta}_{\boldsymbol{\gamma}}\|_{\mathbb{L}^2(\Omega)} \leq C(\boldsymbol{\gamma})\,h^{\vartheta}\,, \\
\|\partial_t\boldsymbol{\delta}_{\boldsymbol{\sigma}}\|_{\mathbb{L}^2(\Omega)} \leq C(\partial_t\boldsymbol{\sigma})\,h^{\vartheta}\,, \quad \|\partial_t\boldsymbol{\delta}_{\mathbf{u}}\|_{\mathbf{L}^2(\Omega)} \leq C(\partial_t\mathbf{u})\,h^{\vartheta}\,, \quad \|\partial_t\boldsymbol{\delta}_{\boldsymbol{\gamma}}\|_{\mathbb{L}^2(\Omega)} \leq C(\partial_t\boldsymbol{\gamma})\,h^{\vartheta}\,.
\end{gathered} \tag{4.42}$$

The following result establishes the theoretical rates of convergence of the semidiscrete continuous-in-time scheme (4.4).

Theorem 4.9. *Assume the same hypotheses as in Theorem 4.8. Furthermore, suppose that there exists $\vartheta \in (0, k+1]$ such that $\boldsymbol{\sigma} \in \mathbb{H}^{\vartheta}(\Omega)$, $\mathbf{div}(\boldsymbol{\sigma}) \in \mathbf{W}^{\vartheta,\ell}(\Omega)$, $\mathbf{u} \in \mathbf{W}^{\vartheta,s}(\Omega)$ and $\boldsymbol{\gamma} \in \mathbb{H}^{\vartheta}(\Omega)$. Then, there exists a positive constant $\mathcal{C}(\boldsymbol{\sigma}, \underline{\mathbf{u}})$, depending only on $\mathcal{C}$ (cf. Theorem 4.8) and the constants defined in (4.42), such that*

$$\|\mathbf{e}_{\boldsymbol{\sigma}}\|_{\mathrm{L}^2(0,T;\mathbb{X})} + \|\mathbf{e}_{\mathbf{u}}\|_{\mathrm{L}^2(0,T;\mathbf{L}^s(\Omega))} + \|\mathbf{e}_{\mathbf{u}}\|_{\mathrm{L}^\infty(0,T;\mathbf{L}^2(\Omega))} + \|\mathbf{e}_{\boldsymbol{\gamma}}\|_{\mathrm{L}^2(0,T;\mathbb{L}^2(\Omega))} \leq \mathcal{C}(\boldsymbol{\sigma}, \underline{\mathbf{u}})\,h^{\vartheta}\,. \tag{4.43}$$

Proof. It follows from using (4.42) into (4.31), and performing some algebraic manipulations. We omit further details. □

Remark 4.2. *The error analysis remains valid for any triplet of finite element spaces that are stable for the semidiscrete continuous-in-time scheme (cf. (4.4)), provided that the orthogonal projectors $\boldsymbol{\mathcal{P}}_h^k$ and $\boldsymbol{\mathcal{P}}_h^{k+1}$ are available, and that a mixed interpolation operator satisfying the commuting diagram property (4.24) exists. In particular, for the choice of AFW elements (cf. (4.2)), we can employ the BDM interpolation operator (cf. [9, Section 2.5.1]), which also satisfies (4.24). Furthermore, since property $(\mathbf{AP}_h^{\boldsymbol{\sigma}})$ also holds for this operator (cf. [9, Proposition 2.5.4]), Theorem 4.9 remains unchanged.*

5 Fully discrete approximation

In this section, we introduce and analize a fully discrete approximation of (2.19). For this purpose, we employ the backward Euler method for the time discretization. Let Δt be the time step, $T = N\Delta t$, and let $t_n = n\Delta t$, for each $n \in \{0, \ldots, N\}$. Let $d_t u^n = (\Delta t)^{-1}\,(u^n - u^{n-1})$ be the first order (backward) discrete time derivative, where $u^n := u(t_n)$. Then, the fully discrete method reads: Given $\mathbf{f}^n \in \mathbf{L}^2(\Omega)$ and $(\boldsymbol{\sigma}_h^0, \underline{\mathbf{u}}_h^0) = (\boldsymbol{\sigma}_{h,0}, (\mathbf{u}_{h,0}, \boldsymbol{\gamma}_{h,0}))$ satisfying (4.5), find $(\boldsymbol{\sigma}_h^n, \underline{\mathbf{u}}_h^n) := (\boldsymbol{\sigma}_h^n, (\mathbf{u}_h^n, \boldsymbol{\gamma}_h^n)) \in \mathbb{X}_h \times \mathbf{Y}_h$, for $n \in \{1, \ldots, N\}$, such that

$$\begin{aligned}
[\mathbf{A}(\boldsymbol{\sigma}_h^n), \boldsymbol{\tau}_h] + [\mathbf{B}'(\underline{\mathbf{u}}_h^n), \boldsymbol{\tau}_h] + [\mathbf{D}'_\rho(\underline{\mathbf{u}}_h^n), \boldsymbol{\tau}_h] &= 0 && \forall\, \boldsymbol{\tau}_h \in \mathbb{X}_h\,, \\
d_t\,[\mathbf{E}(\underline{\mathbf{u}}_h^n), \underline{\mathbf{v}}_h] - [\mathbf{B}(\boldsymbol{\sigma}_h^n), \underline{\mathbf{v}}_h] + [\mathbf{C}(\underline{\mathbf{u}}_h^n), \underline{\mathbf{v}}_h] &= [\mathbf{F}^n, \underline{\mathbf{v}}_h] && \forall\, \underline{\mathbf{v}}_h \in \mathbf{Y}_h\,,
\end{aligned} \tag{5.1}$$

where $[\mathbf{F}^n, \underline{\mathbf{v}}_h] := (\mathbf{f}^n, \mathbf{v}_h)_\Omega$.

In what follows, for a separable Banach space V equipped with the norm $\|\cdot\|_V$, we define the following discrete-in-time norms:

$$\|u\|^2_{\ell^2(0,T;V)} := \Delta t \sum_{n=1}^{N} \|u^n\|^2_V \quad \text{and} \quad \|u\|_{\ell^\infty(0,T;V)} := \max_{1\le n\le N} \|u^n\|_V \,.$$

Endowed with these norms, we define the Banach spaces $\ell^2(0,T;V)$ and $\ell^\infty(0,T;V)$ respectively as

$$\ell^2(0,T;V) := \Big\{ u = (u^1,\dots,u^N) \in V^N \;:\; \|u\|_{\ell^2(0,T;V)} < +\infty \Big\}, \quad \text{and}$$
$$\ell^\infty(0,T;V) := \Big\{ u = (u^1,\dots,u^N) \in V^N \;:\; \|u\|_{\ell^\infty(0,T;V)} < +\infty \Big\}.$$

We begin our analysis of the fully discrete scheme (5.1) by establishing a stability result.

Theorem 5.1. *Suppose that the hypotheses of Theorem 3.9 and Lemma 4.1 hold. Assume further that the porosity satisfies*

$$\left\| \frac{\nabla\rho}{\rho} \right\|_{\mathbf{L}^\infty(\Omega)} \le \frac{\sqrt{d}\,\Lambda_{\mathtt{d}}\,\rho_0}{8\,\rho_1\,\|\mathbf{i}_{s,2}\|} \,. \tag{5.2}$$

Let $(\boldsymbol{\sigma}_h^n, \underline{\mathbf{u}}_h^n) = (\boldsymbol{\sigma}_h^n, (\mathbf{u}_h^n, \boldsymbol{\gamma}_h^n)) \in \mathbb{X}_h \times \mathbf{Y}_h$ *be a solution to* (5.1) *with* $(\boldsymbol{\sigma}_h^0, \underline{\mathbf{u}}_h^0) = (\boldsymbol{\sigma}_{h,0}, (\mathbf{u}_{h,0}, \boldsymbol{\gamma}_{h,0}))$ *satisfying* (4.5), *and* $\mathbf{f}^n \in \mathbf{L}^2(\Omega)$ *with* $n \in \{1,\dots,N\}$. *Then, there exists a positive constant* $\widehat{C}_{\mathtt{B}}$, *depending only on* μ, ρ_0, ρ_1, $C_{\mathbf{K}}$, $\Lambda_{\mathtt{d}}$, $C_{0,\mathtt{d}}$ *(cf.* (4.9)*)*, $\|\mathbf{K}^{-1}\|_{\mathbb{L}^\infty(\Omega)}$ *and* $|\Omega|$, *such that*

$$\begin{aligned}
&\|\boldsymbol{\sigma}_h\|^2_{\ell^2(0,T;\mathbb{X})} + \|\mathbf{u}_h\|^2_{\ell^2(0,T;\mathbf{L}^s(\Omega))} + \|\mathbf{u}_h\|^2_{\ell^\infty(0,T;\mathbf{L}^2(\Omega))} + \|\boldsymbol{\gamma}_h\|^2_{\ell^2(0,T;\mathbb{L}^2(\Omega))} \\
&\quad \le \widehat{C}_{\mathtt{B}} \Big\{ \|\mathbf{f}\|^2_{\ell^2(0,T;\mathbf{L}^2(\Omega))} + \|\mathbf{div}(\rho\,\mathbf{e}(\mathbf{u}_0))\|^2_{\mathbf{L}^2(\Omega)} + \|\mathbf{u}_0\|^2_{\mathbf{L}^2(\Omega)} \Big\}.
\end{aligned} \tag{5.3}$$

Proof. Following a similar approach to that in Theorem 3.4, we first apply the discrete global inf-sup condition (4.7), use the system (5.1), and recall that $\|\nabla\rho/\rho\|_{\mathbf{L}^r(\Omega)} \le \sqrt{d}\,\Lambda_{\mathtt{d}}/2$ (cf. (4.8)), to obtain

$$\frac{\Lambda_{\mathtt{d}}}{2}\, \|(\boldsymbol{\sigma}_h^n, \underline{\mathbf{u}}_h^n)\|_{\mathbb{X}\times\mathbf{Y}} \le \rho_1\,\|\mathbf{i}_{s,2}\|\,\|d_t\mathbf{u}_h^n\|_{\mathbf{L}^2(\Omega)} + \|\mathbf{i}_{s,2}\|\,\|\mathbf{f}^n\|_{\mathbf{L}^2(\Omega)}\,,$$

which, upon squaring, summing over the time steps $n \in \{1,\dots,N\}$, and multiplying by Δt, becomes the discrete counterpart of (3.21),

$$\begin{aligned}
&\widehat{C}_1 \Big\{ \|\boldsymbol{\sigma}_h\|^2_{\ell^2(0,T;\mathbb{X})} + \|\mathbf{u}_h\|^2_{\ell^2(0,T;\mathbf{L}^s(\Omega))} + \|\boldsymbol{\gamma}_h\|^2_{\ell^2(0,T;\mathbb{L}^2(\Omega))} \Big\} \\
&\quad \le \|d_t\mathbf{u}_h\|^2_{\ell^2(0,T;\mathbf{L}^2(\Omega))} + \rho_1^{-2}\,\|\mathbf{f}\|^2_{\ell^2(0,T;\mathbf{L}^2(\Omega))}\,,
\end{aligned} \tag{5.4}$$

where $\widehat{C}_1 := \Lambda_{\mathtt{d}}^2/(8\,\|\mathbf{i}_{s,2}\|^2\,\rho_1^2)$.

In order to bound the first term on the right-hand side of (5.4), we note that a discrete time differentiation of the first equation in (5.1) can be obtained merely through algebraic manipulations, which yield

$$[\mathbf{A}(d_t\boldsymbol{\sigma}_h^n), \boldsymbol{\tau}_h] + [\mathbf{B}'(d_t\underline{\mathbf{u}}_h^n), \boldsymbol{\tau}_h] + [\mathbf{D}'_\rho(d_t\underline{\mathbf{u}}_h^n), \boldsymbol{\tau}_h] = 0 \qquad \forall\,\boldsymbol{\tau}_h \in \mathbb{X}_h\,. \tag{5.5}$$

In particular, testing with $\boldsymbol{\tau}_h = \boldsymbol{\sigma}_h^n$ and using the second row of (5.1) with $\underline{\mathbf{v}}_h = d_t\underline{\mathbf{u}}_h^n$ to handle the second term of (5.5), we arrive at

$$[\mathbf{A}(d_t\boldsymbol{\sigma}_h^n), \boldsymbol{\sigma}_h^n] + [\mathbf{E}(d_t\underline{\mathbf{u}}_h^n), d_t\underline{\mathbf{u}}_h^n] + [\mathbf{C}(\underline{\mathbf{u}}_h^n), d_t\underline{\mathbf{u}}_h^n] = [\mathbf{F}^n, d_t\underline{\mathbf{u}}_h^n] - [\mathbf{D}'_\rho(d_t\underline{\mathbf{u}}_h^n), \boldsymbol{\sigma}_h^n]\,. \tag{5.6}$$

In turn, owing to the linearity of $\mathbf{A}$ and $\mathbf{C}$, simple algebraic manipulations show that

$$\begin{aligned} [\mathbf{A}(d_t\boldsymbol{\sigma}_h^n), \boldsymbol{\sigma}_h^n] &= \frac{1}{2}\, d_t[\mathbf{A}(\boldsymbol{\sigma}_h^n), \boldsymbol{\sigma}_h^n] + \frac{\Delta t}{2}\, [\mathbf{A}(d_t\boldsymbol{\sigma}_h^n), d_t\boldsymbol{\sigma}_h^n]\,, \\ [\mathbf{C}(\underline{\mathbf{u}}_h^n), d_t\underline{\mathbf{u}}_h^n] &= \frac{1}{2}\, d_t[\mathbf{C}(\underline{\mathbf{u}}_h^n), \underline{\mathbf{u}}_h^n] + \frac{\Delta t}{2}\, [\mathbf{C}(d_t\underline{\mathbf{u}}_h^n), d_t\underline{\mathbf{u}}_h^n]\,, \end{aligned} \tag{5.7}$$

so, substituting (5.7) into (5.6) and using the monotonicity properties (cf. (3.5a) and (3.5b)), together with Cauchy–Schwarz and Young's inequalities, leads to the discrete version of (3.22),

$$\begin{aligned} \left(\frac{\rho_0}{4} + \frac{\mu\, C_{\mathbf{K}}\,\Delta t}{2}\right) \|d_t\mathbf{u}_h^n\|^2_{\mathbf{L}^2(\Omega)} + \frac{\Delta t}{4\mu\,\rho_1}\, \|(d_t\boldsymbol{\sigma}_h^n)^{\mathrm{d}}\|^2_{\mathbb{L}^2(\Omega)} + \frac{1}{2}\, d_t\Big\{[\mathbf{A}(\boldsymbol{\sigma}_h^n), \boldsymbol{\sigma}_h^n] + [\mathbf{C}(\underline{\mathbf{u}}_h^n), \underline{\mathbf{u}}_h^n]\Big\} \\ \leq \frac{1}{d\rho_0} \left\|\frac{\nabla\rho}{\rho}\right\|^2_{\mathbf{L}^\infty(\Omega)} \|\boldsymbol{\sigma}_h^n\|^2_{\mathbb{L}^2(\Omega)} + \frac{1}{2\,\rho_0}\, \|\mathbf{f}^n\|^2_{\mathbf{L}^2(\Omega)}\,. \end{aligned} \tag{5.8}$$

Next, using (5.2) to bound $\|\nabla\rho/\rho\|^2_{\mathbf{L}^\infty(\Omega)}/(d\rho_0) \leq (\rho_0\widehat{C}_1)/8$, summing over the time steps $n \in \{1,\dots,m\}$, with $m \in \{1,\dots,N\}$, multiplying by Δt, and invoking once more the monotonicity of $\mathbf{A}$ and $\mathbf{C}$ (cf. (3.5a)) together with the stability properties (cf. (3.4a) and (3.4d)), we obtain

$$\begin{aligned} \left(\frac{\rho_0}{4} + \frac{\mu\, C_{\mathbf{K}}\,\Delta t}{2}\right) \Delta t \sum_{n=1}^{m} \|d_t\mathbf{u}_h^n\|^2_{\mathbf{L}^2(\Omega)} + \frac{1}{4\mu\rho_1}\, \|(\boldsymbol{\sigma}_h^m)^{\mathrm{d}}\|^2_{\mathbb{L}^2(\Omega)} + \frac{\mu\, C_{\mathbf{K}}}{2}\, \|\mathbf{u}_h^m\|^2_{\mathbf{L}^2(\Omega)} \\ \leq \frac{\rho_0\widehat{C}_1\,\Delta t}{8} \sum_{n=1}^{m} \|\boldsymbol{\sigma}_h^n\|^2_{\mathbb{X}} + \frac{\Delta t}{2\rho_0} \sum_{n=1}^{m} \|\mathbf{f}^n\|^2_{\mathbf{L}^2(\Omega)} + \frac{1}{4\mu\rho_0}\, \|\boldsymbol{\sigma}_h^0\|^2_{\mathbb{X}} \\ + \frac{\mu}{2\,\|\mathbf{i}_{s,2}\|^2}\, \|\mathbf{K}^{-1}\|_{\mathbb{L}^\infty(\Omega)}\, \|\mathbf{u}_h^0\|^2_{\mathbf{L}^s(\Omega)}\,. \end{aligned}$$

Notice that we have neglected the second term in (5.8). We now use the fact that $\boldsymbol{\sigma}_h^0 = \boldsymbol{\sigma}_{h,0}$ and $\mathbf{u}_h^0 = \mathbf{u}_{h,0}$, together with the estimate (4.18), and after some algebraic manipulations, and the omission of some terms for clarity, we obtain the discrete counterpart of (3.23),

$$\begin{aligned} \Delta t \sum_{n=1}^{m} \|d_t\mathbf{u}_h^n\|^2_{\mathbf{L}^2(\Omega)} + \frac{2\mu\, C_{\mathbf{K}}}{\rho_0}\, \|\mathbf{u}_h^m\|^2_{\mathbf{L}^2(\Omega)} \leq \frac{2\Delta t}{\rho_0^2} \sum_{n=1}^{m} \|\mathbf{f}^n\|^2_{\mathbf{L}^2(\Omega)} + \frac{\widehat{C}_1\,\Delta t}{2} \sum_{n=1}^{m} \|\boldsymbol{\sigma}_h^n\|^2_{\mathbb{X}} \\ + \widehat{C}_2 \left\{\|\mathbf{div}(\rho\,\mathbf{e}(\mathbf{u}_0))\|^2_{\mathbf{L}^2(\Omega)} + \|\mathbf{u}_0\|^2_{\mathbf{L}^2(\Omega)}\right\}, \end{aligned} \tag{5.9}$$

with $\widehat{C}_2$ depending only on $C_{0,\mathtt{d}}$ (cf. (4.18)), μ, ρ_0, $|\Omega|$ and $\|\mathbf{K}^{-1}\|_{\mathbb{L}^\infty(\Omega)}$. Since $m \in \{1,\dots,N\}$ is arbitrary, (5.9) implies

$$\begin{aligned} \|d_t\mathbf{u}_h\|^2_{\ell^2(0,T;\mathbf{L}^2(\Omega))} + \frac{2\mu\, C_{\mathbf{K}}}{\rho_0}\, \|\mathbf{u}_h\|^2_{\ell^\infty(0,T;\mathbf{L}^2(\Omega))} \leq \frac{2}{\rho_0^2}\, \|\mathbf{f}\|^2_{\ell^2(0,T;\mathbf{L}^2(\Omega))} + \frac{\widehat{C}_1}{2}\, \|\boldsymbol{\sigma}_h\|^2_{\ell^2(0,T;\mathbb{X})} \\ + \widehat{C}_2 \left\{\|\mathbf{div}(\rho\,\mathbf{e}(\mathbf{u}_0))\|^2_{\mathbf{L}^2(\Omega)} + \|\mathbf{u}_0\|^2_{\mathbf{L}^2(\Omega)}\right\}. \end{aligned} \tag{5.10}$$

Thus, substituting (5.10) into (5.4) yields (5.3) with constant

$$\widehat{C}_{\mathtt{B}} := \frac{\max\left\{\rho_1^{-2} + 2\,\rho_0^{-2}, \widehat{C}_2\right\}}{\min\{\widehat{C}_1/2, 2\mu C_{\mathbf{K}}\,\rho_0^{-1}\}}\,.$$

□

Certainly, one possible way to prove the well-posedness of (5.1) is to use an induction argument to handle the discrete time derivative and to follow a similar approach to that in Lemma 4.5. This consists in establishing the well-posedness of (5.1) while neglecting the operator $\mathbf{D}'_{\rho}$, deducing a global inf-sup condition, and then assuming that $\|\nabla\rho/\rho\|_{\mathbf{L}^\infty(\Omega)}$ is sufficiently small, depending on the global inf-sup constant, to incorporate the term associated with $\mathbf{D}'_{\rho}$. However, this constant depends on the time step Δt, which in turn implies that $\|\nabla\rho/\rho\|_{\mathbf{L}^\infty(\Omega)}$ must be smaller than a constant depending on the time step. To overcome this difficulty, we proceed similarly to Sections 3 and 4, introducing an auxiliary problem and a fixed-point strategy to establish the well-posedness of (5.1). In fact, let $\widehat{\mathcal{J}}_{\mathtt{d}} : \ell^2(0,T;\mathbb{X}_h) \to \ell^2(0,T;\mathbb{X}_h)$ be the operator defined by

$$\widehat{\mathcal{J}}_{\mathtt{d}}(\boldsymbol{\zeta}_h) := \boldsymbol{\sigma}_h\,,$$

where $(\boldsymbol{\sigma}_h, \underline{\mathbf{u}}_h)$ is the unique solution (to be confirmed below) to

$$\begin{aligned} [\mathbf{A}(\boldsymbol{\sigma}_h^n), \boldsymbol{\tau}_h] + [\widetilde{\mathbf{B}}'(\underline{\mathbf{u}}_h^n), \boldsymbol{\tau}_h] &= 0 && \forall\, \boldsymbol{\tau}_h \in \mathbb{X}_h\,, \\ d_t\, [\mathbf{E}(\underline{\mathbf{u}}_h^n), \underline{\mathbf{v}}_h] - [\widetilde{\mathbf{B}}(\boldsymbol{\sigma}_h^n), \underline{\mathbf{v}}_h] + [\mathbf{C}(\underline{\mathbf{u}}_h^n), \underline{\mathbf{v}}_h] &= [\widetilde{\mathbf{F}}^n_{\boldsymbol{\zeta}_h}, \underline{\mathbf{v}}_h] && \forall\, \underline{\mathbf{v}}_h \in \mathbf{Y}_h\,, \end{aligned} \tag{5.11}$$

for all $n \in \{1, \ldots, N\}$ with $(\boldsymbol{\sigma}_h^0, \underline{\mathbf{u}}_h^0)$ given by (4.5). Here, $[\widetilde{\mathbf{F}}^n_{\boldsymbol{\zeta}_h}, \underline{\mathbf{v}}_h] := (\mathbf{f}^n, \mathbf{v}_h)_\Omega - [\mathbf{D}(\boldsymbol{\zeta}_h^n), \underline{\mathbf{v}}_h]$.

Now, we notice that establishing the well-posedness of (5.1) is equivalent to prove that there exists a unique solution to the fixed-point equation

$$\widehat{\mathcal{J}}_{\mathtt{d}}(\boldsymbol{\sigma}_h) = \boldsymbol{\sigma}_h\,. \tag{5.12}$$

The following result asserts that (5.11) is well-posed and a stability result for the fixed-point system.

Theorem 5.2. *Suppose that the hypotheses of Theorem 3.9 and Lemma 4.5 hold. Then, $\widehat{\mathcal{J}}_{\mathtt{d}}$ is well-defined. More precisely, given $\boldsymbol{\zeta}_h \in \ell^2(0,T;\mathbb{X}_h)$, there exists a unique solution $(\boldsymbol{\sigma}_h, \underline{\mathbf{u}}_h)$ to (5.11), with $\boldsymbol{\sigma}_h \in \ell^2(0,T;\mathbb{X}_h)$, $\mathbf{u}_h \in \ell^\infty(0,T;\mathbf{H}_h^{\mathbf{u}})$, and $\boldsymbol{\gamma}_h \in \ell^2(0,T;\mathbb{H}_h^{\boldsymbol{\gamma}})$. Moreover, there exist positive constants $\widehat{C}_{\mathtt{B},\mathtt{d}}$ and $C_{\widehat{\mathcal{J}}_{\mathtt{d}}}$, with $\widehat{C}_{\mathtt{B},\mathtt{d}}$ depending only on μ, ρ_0, ρ_1, $\|\mathbf{K}^{-1}\|_{\mathbb{L}^\infty(\Omega)}$, $\Lambda_{\mathtt{d}}$, $\widetilde{C}_{0,\mathtt{d}}$ (cf. (4.18)), d and $|\Omega|$, and $C_{\widehat{\mathcal{J}}_{\mathtt{d}}}$ depending only on ρ_0, ρ_1, $\Lambda_{\mathtt{d}}$, d and $|\Omega|$, such that*

$$\begin{aligned} \|\widehat{\mathcal{J}}_{\mathtt{d}}(\boldsymbol{\zeta}_h)\|_{\ell^2(0,T;\mathbb{X})} \leq \widehat{C}_{\mathtt{B},\mathtt{d}} &\Big\{ \|\mathbf{f}\|_{\ell^2(0,T;\mathbf{L}^2(\Omega))} + \|\mathbf{div}(\rho\,\mathbf{e}(\mathbf{u}_0))\|_{\mathbf{L}^2(\Omega)} + \|\mathbf{u}_0\|_{\mathbf{L}^2(\Omega)} \Big\} \\ &+ C_{\widehat{\mathcal{J}}_{\mathtt{d}}} \left\| \frac{\nabla\rho}{\rho} \right\|_{\mathbf{L}^\infty(\Omega)} \|\boldsymbol{\zeta}_h\|_{\ell^2(0,T;\mathbb{X}_h)}\,. \end{aligned} \tag{5.13}$$

Proof. Let $\boldsymbol{\zeta}_h \in \ell^2(0,T;\mathbb{X}_h)$ be given and recall from Lemma 4.5 that we have the discrete initial conditions $(\boldsymbol{\sigma}_h^0, \underline{\mathbf{u}}_h^0)$ satisfying (4.18). We then proceed to establish the well-posedness of (5.11) at each time step by induction. In fact, assuming that $\mathbf{u}_h^{n-1}$ is known, we prove the existence and uniqueness of the problem by following the same arguments as in Lemma 4.4. Consequently, we obtain the existence and uniqueness of $\boldsymbol{\sigma}_h \in (\mathbb{X}_h)^N$ and $\underline{\mathbf{u}}_h \in (\mathbf{Y}_h)^N$ satisfying (5.11). In turn, to prove (5.13), one proceeds as in the proof of Theorem 5.1, arriving at (5.13) with a constant independent of h and Δt. Further details are omitted. $\square$

Theorem 5.3. *Suppose that the hypotheses of Theorems 5.1 and 5.2 hold. Assume further that the porosity satisfies*

$$C_{\widehat{\mathcal{J}}_{\mathtt{d}}} \left\| \frac{\nabla\rho}{\rho} \right\|_{\mathbf{L}^\infty(\Omega)} < 1\,. \tag{5.14}$$

Then, given $(\boldsymbol{\sigma}_h^0, \underline{\mathbf{u}}_h^0) = (\boldsymbol{\sigma}_{h,0}, (\mathbf{u}_{h,0}, \boldsymbol{\gamma}_{h,0}))$ satisfying (4.5) and $\mathbf{f}^n \in \mathbf{L}^2(\Omega)$ with $n \in \{1, \ldots, N\}$, there exists a unique solution $(\boldsymbol{\sigma}_h^n, \underline{\mathbf{u}}_h^n)$ to the fully discrete scheme (5.1). Moreover, the solution satisfy the stability estimate (5.3).

Proof. The existence and uniqueness is achieved by arguments similar to those of the proof of Theorems 3.9 and 4.7. In fact, it is straightforward to verify that $\widehat{\mathcal{J}}_{\mathtt{d}}$ is Lipschitz continuous with constant $C_{\widehat{\mathcal{J}}_{\mathtt{d}}} \|\nabla\rho/\rho\|_{\mathbf{L}^\infty(\Omega)}$. Then, by (5.14), it follows that $\widehat{\mathcal{J}}_{\mathtt{d}}$ is a contractive operator in the Banach space $\ell^2(0,T;\mathbb{X}_h)$. Thus, by the Banach fixed-point theorem, there exists a unique solution to (5.12), which is equivalent to the existence and uniqueness of solution to (5.1). The stability follows from Theorem 5.1. This completes the proof. □

Remark 5.1. *We emphasize that the fully discrete scheme (5.1) yields exact conservation of momentum when ρ, $\mathbf{K}$ and $\mathbf{f}^n$, for each $n \in \{1,\dots,N\}$, are piecewise constant. In this case, $\rho\, d_t\mathbf{u}_h^n$, $\mathbf{K}^{-1}\mathbf{u}_n^n$, and $\mathbf{f}^n$ all belong to $\mathbf{H}_h^{\mathbf{u}}$. This fact, together with the inclusion $\mathbf{div}(\mathbb{X}_h) \subset \mathbf{H}_h^{\mathbf{u}}$, implies from the second equation in (5.1) that, for every $n \in \{1,\dots,N\}$,*

$$\rho\, d_t\mathbf{u}_h^n + \mu\, \mathbf{K}^{-1}\, \mathbf{u}_h^n - \mathbf{div}(\boldsymbol{\sigma}_h^n) = \mathbf{f}^n \quad \textit{in} \quad \Omega\,. \tag{5.15}$$

Furthermore, if the data are not piecewise constant, (5.15) can only be obtained in an approximate sense, by replacing $\rho\, d_t\mathbf{u}_h^n$, $\mathbf{K}^{-1}\,\mathbf{u}_h^n$ and $\mathbf{f}^n$ with $\boldsymbol{\mathcal{P}}_h^k(\rho\, d_t\mathbf{u}_h^n)$, $\boldsymbol{\mathcal{P}}_h^k(\mathbf{K}^{-1}\,\mathbf{u}_h^n)$ and $\boldsymbol{\mathcal{P}}_h^k(\mathbf{f}^n)$, where $\boldsymbol{\mathcal{P}}_h^k$ is defined as in (4.23). The numerical verification of this property is illustrated in Section 6.

In what follows, we establish the rates of convergence associated with the fully discrete scheme (5.1). To this end, we subtract the fully discrete system (5.1) from its continuous counterpart (2.19) at each time step $n \in \{1,\dots,N\}$, yielding the following error system:

$$\begin{aligned} [\mathbf{A}(\boldsymbol{\sigma}^n - \boldsymbol{\sigma}_h^n), \boldsymbol{\tau}_h] + [\mathbf{B}'(\underline{\mathbf{u}}^n - \underline{\mathbf{u}}_h^n), \boldsymbol{\tau}_h] + [\mathbf{D}'_\rho(\underline{\mathbf{u}}^n - \underline{\mathbf{u}}_h^n), \boldsymbol{\tau}_h] &= 0 \\ (\rho\, d_t(\mathbf{u}^n - \mathbf{u}_h^n), \mathbf{v}_h)_\Omega - [\mathbf{B}(\boldsymbol{\sigma}^n - \boldsymbol{\sigma}_h^n), \underline{\mathbf{v}}_h] + [\mathbf{C}(\underline{\mathbf{u}}^n - \underline{\mathbf{u}}_h^n), \underline{\mathbf{v}}_h] &= (\rho\, \mathbf{r}_n(\mathbf{u}), \mathbf{v}_h)_\Omega \end{aligned}$$

for all $(\boldsymbol{\tau}_h, \underline{\mathbf{v}}_h) \in \mathbb{X}_h \times \mathbf{Y}_h$, where $\mathbf{r}_n$ is the difference between the continuous and discrete time derivatives, that is,

$$\mathbf{r}_n(\mathbf{u}) := d_t\mathbf{u}^n - \partial_t\mathbf{u}(t_n)\,.$$

Additionally, we recall from [14, Lemma 4] that, if $\mathbf{u} \in \mathrm{H}^2(0,T;\mathbf{L}^2(\Omega))$, there holds

$$\Delta t \sum_{n=1}^N \|\mathbf{r}_n(\mathbf{u})\|^2_{\mathbf{L}^2(\Omega)} \leq C(\partial_{tt}\mathbf{u})\,(\Delta t)^2\,, \quad \text{with} \quad C(\partial_{tt}\mathbf{u}) := C\,\|\partial_{tt}\mathbf{u}\|^2_{\mathrm{L}^2(0,T;\mathbf{L}^2(\Omega))}\,,$$

for some positive constant C, independent of Δt. Thus, we now state the theoretical rates of convergence associated with the fully discrete scheme (5.1). The proof follows the same structure as that of Theorem 4.8, relying on the approximation properties detailed in Section 4, and more precisely in (4.42), thereby yielding a result analogous to Theorem 4.9. Naturally, all arguments must be adapted to the discrete-in-time setting, in a way similar to the proof of Theorem 5.1. For the sake of brevity, we omit further details and restrict ourselves to stating the result.

Theorem 5.4. *Suppose that there exists $\vartheta \in (0, k+1]$ such that the assumptions of Theorem 4.9 hold. Assume further that the hypotheses of Theorem 5.3 hold and that $\mathbf{u} \in \mathrm{H}^2(0,T;\mathbf{L}^2(\Omega))$. Then, for the solution of the fully discrete scheme (5.1), there exists a positive constant $\widehat{\mathcal{C}}(\boldsymbol{\sigma}, \underline{\mathbf{u}})$, independent of h and Δt, but depending on the exact solutions and $\widehat{C}_{\mathtt{B}}$ (cf. (5.3)), such that*

$$\|\mathbf{e}_{\boldsymbol{\sigma}}\|_{\ell^2(0,T;\mathbb{X})} + \|\mathbf{e}_{\mathbf{u}}\|_{\ell^2(0,T;\mathbf{L}^s(\Omega))} + \|\mathbf{e}_{\mathbf{u}}\|_{\ell^\infty(0,T;\mathbf{L}^2(\Omega))} + \|\mathbf{e}_{\boldsymbol{\gamma}}\|_{\ell^2(0,T;\mathbb{L}^2(\Omega))} \leq \widehat{\mathcal{C}}(\boldsymbol{\sigma}, \underline{\mathbf{u}})\,(h^\vartheta + \Delta t)\,.$$

Finally, inspired by the first equation in (2.10), (2.8), and (2.18), we observe that the gradient of the velocity $\nabla\mathbf{u}$, the pressure p, and the original stress tensor $\widetilde{\boldsymbol{\sigma}}$, can be approximated through a post-processing procedure as

$$\begin{gathered}[\nabla\mathbf{u}]_h^n := \frac{1}{2\mu\rho}\,(\boldsymbol{\sigma}_h^n)^{\mathrm{d}} + \boldsymbol{\gamma}_h^n - \frac{1}{d}\left(\frac{\nabla\rho}{\rho}\cdot\mathbf{u}_h^n\right)\mathbb{I}\,,\quad p_h^n := -\frac{1}{d}\left\{2\mu\,(\nabla\rho\cdot\mathbf{u}_h^n) + \mathrm{tr}(\boldsymbol{\sigma}_h^n)\right\} - \lambda_{\boldsymbol{\sigma}_h^n}\,,\\ \text{and}\quad \widetilde{\boldsymbol{\sigma}}_h^n := \boldsymbol{\sigma}_h^n + \lambda_{\boldsymbol{\sigma}_h^n}\,\mathbb{I}\,,\quad \text{with}\quad \lambda_{\boldsymbol{\sigma}_h^n} := -\frac{2\mu}{d\,|\Omega|}\,(\nabla\rho,\mathbf{u}_h^n)_\Omega\,,\end{gathered}\tag{5.16}$$

for all $n\in\{1,\ldots,N\}$, where $[\nabla\mathbf{u}]_h$, p_h and $\widetilde{\boldsymbol{\sigma}}_h$ denote the respective approximations of the variables of interest. Consequently, from the rates of convergence of $\boldsymbol{\sigma}$, $\mathbf{u}$, and $\boldsymbol{\gamma}$ established in the previous theorem, it follows directly that the same rates are inherited by $[\nabla\mathbf{u}]_h$, p_h and $\widetilde{\boldsymbol{\sigma}}_h$.

Lemma 5.5. *Suppose the same assumptions as in Theorem 5.4. Then, there exists a positive constant $\widetilde{\mathcal{C}}(\boldsymbol{\sigma},\underline{\mathbf{u}})$, independent of h and Δt, but depending on the exact solutions and $\widehat{C}_{\mathtt{B}}$ (cf. (5.3)), such that*

$$\|\mathbf{e}_{\nabla\mathbf{u}}\|_{\ell^2(0,T;\mathbb{L}^2(\Omega))} + \|\mathbf{e}_p\|_{\ell^2(0,T;\mathrm{L}^2(\Omega))} + \|\mathbf{e}_{\widetilde{\boldsymbol{\sigma}}}\|_{\ell^2(0,T;\mathbb{X})} \le \widetilde{\mathcal{C}}(\boldsymbol{\sigma},\underline{\mathbf{u}})\,(h^\vartheta + \Delta t)\,,$$

where $\mathbf{e}_{\nabla\mathbf{u}} := \nabla\mathbf{u} - [\nabla\mathbf{u}]_h$, $\mathbf{e}_p := p - p_h$, and $\mathbf{e}_{\widetilde{\boldsymbol{\sigma}}} := \widetilde{\boldsymbol{\sigma}} - \widetilde{\boldsymbol{\sigma}}_h$.

Remark 5.2. *In the fully discrete scheme (5.1), we restrict ourselves to the backward Euler method merely for simplicity. Nevertheless, the analysis in Section 5 can be readily extended to other time discretizations, including BDF schemes and the Crank–Nicholson method.*

6 Numerical results

In this section, we present three numerical experiments that illustrate the performance of the fully discrete method (5.1). The implementation was carried out using the open-source finite element library `FEniCS` [1]. We consider quasi-uniform triangulations and the finite element subspaces associated with PEERS_k and AFW_k, as described in Section 4. Examples 1 and 2 aim to verify the expected rates of convergence in two- and three-dimensional domains, respectively, and to corroborate numerically that the conservation of momentum (5.15) holds. In these cases, the total simulation time is set to $T = 10^{-2}$ with a time step of $\Delta t = 10^{-3}$, which is sufficiently small to ensure that the temporal discretization error does not influence the observed convergence rates. Finally, Example 3 examines the flow of a free fluid around a porous obstacle under various operating conditions, highlighting the applicability of the proposed method to complex geometries and diverse physical scenarios.

For the first two examples, in addition to the errors in the velocity and vorticity, we also compute the errors associated with the original Cauchy stress tensor and the pressure obtained from (5.16) and Lemma 5.5, while omitting the computation of the velocity gradient for simplicity. In addition, we compute the error associated with the conservation of momentum (5.15) as

$$\mathbf{e}_{\mathtt{m},k} := \boldsymbol{\mathcal{P}}_h^k(\rho\,d_t\mathbf{u}_h) + \mu\,\boldsymbol{\mathcal{P}}_h^k(\mathbf{K}^{-1}\,\mathbf{u}_h) - \mathbf{div}(\boldsymbol{\sigma}_h) - \boldsymbol{\mathcal{P}}_h^k(\mathbf{f})\,.$$

We recall that the experimental rates of convergence are defined as

$$r_\diamond := \frac{\log(\mathbf{e}_\diamond/\mathbf{e}'_\diamond)}{\log(h/h')}\qquad \text{for } \diamond\in\{\widetilde{\boldsymbol{\sigma}},\mathbf{u},\boldsymbol{\gamma},p\}\,,$$

where h and h' denote two consecutive mesh sizes with errors $\mathbf{e}_\diamond$ and $\mathbf{e}'_\diamond$.

Finally, we remark that the zero-mean constraint on $\mathrm{tr}(\boldsymbol{\sigma}_h)$ over Ω is imposed via a scalar Lagrange multiplier, which amounts to adding one row and one column to the matrix system corresponding to (5.1).

Example 1: Convergence against smooth exact solutions in a 2D domain

In this test, we analyze the convergence with respect to the spatial discretization using a manufactured solution. The computational domain is the square $\Omega := (0,1)^2$, and we set $s = 4$, which yields $\ell = 4/3$ (cf. (2.13)). The viscosity is fixed at $\mu = 1$, and the permeability tensor is given by $\mathbf{K} := 10^{-2}\,\mathbb{I}$. Following [19], the porosity function is defined through an exponential profile, while the source term $\mathbf{f}$ is adjusted so that the manufactured solution coincides with the prescribed analytical functions (cf. (2.1)). These functions are depicted in Figure 6.1. The model problem is complemented with the corresponding Dirichlet boundary condition and suitable initial data.

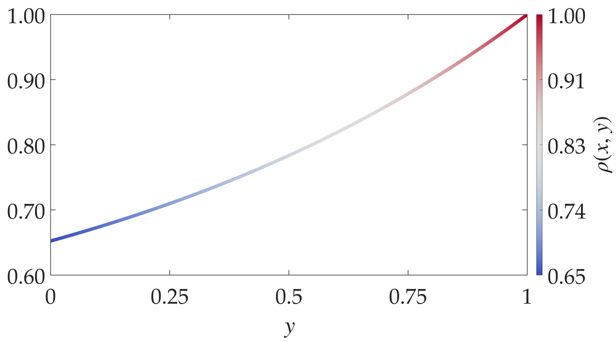

$$\rho(x,y) := 0.45 + 0.55\,\exp(-(1-y))\,,$$

$$\mathbf{u} = \exp(t)\,\rho(x,y)^{-1}\begin{pmatrix} \sin(\pi x)\,\cos(\pi y) \\ -\cos(\pi x)\,\sin(\pi y) \end{pmatrix},$$

$$p = \exp(t)\,\cos(\pi x)\,\exp(y)\,.$$

Figure 6.1: [Example 1] Graph of the porosity function (left) and analytical expressions of the porosity and manufactured solutions (right).

Tables 6.1 and 6.2 report the convergence history for a sequence of quasi-uniform mesh refinements using both PEERS_k and AFW_k elements, for $k \in \{0,1\}$. The results confirm that the optimal spatial convergence rates $\mathcal{O}(h^{k+1})$ predicted by Theorem 5.4 and Lemma 5.5 are achieved. Table 6.3 shows that, although the data is not piecewise constant, the error associated with the conservation of momentum (5.15) is close to zero. In Figure 6.2, we display some solutions at the final time obtained with the AFW_1 discretization with meshsize $h = 0.014$ and 20,000 triangle elements, representing 481,201 `DOF`.

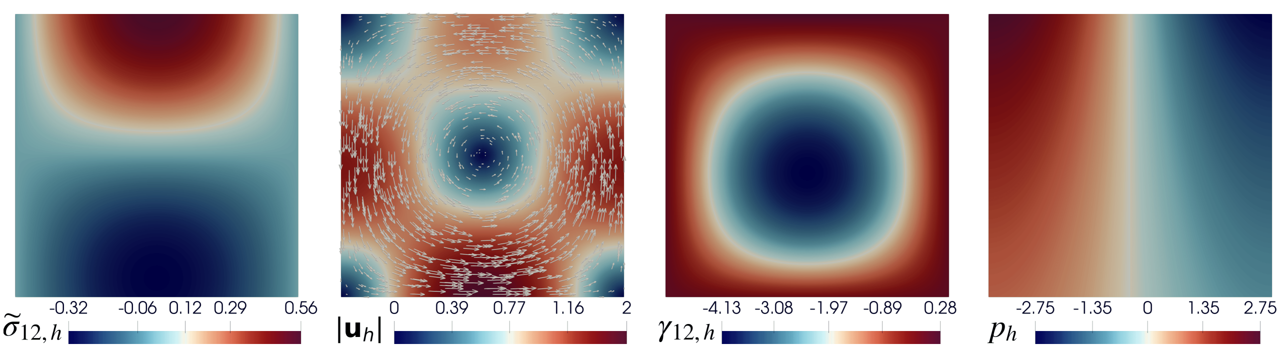

Figure 6.2: [Example 1] Computed stress component, magnitude of the velocity, vorticity component, and pressure field.

PEERS$_0$ discretization											
		$\|\mathbf{e}_{\widetilde{\boldsymbol{\sigma}}}\|_{\ell^2(0,T;\mathbb{X})}$		$\|\mathbf{e}_{\mathbf{u}}\|_{\ell^2(0,T;\mathbf{L}^s(\Omega))}$		$\|\mathbf{e}_{\mathbf{u}}\|_{\ell^\infty(0,T;\mathbf{L}^2(\Omega))}$		$\|\mathbf{e}_{\boldsymbol{\gamma}}\|_{\ell^2(0,T;\mathbb{L}^2(\Omega))}$		$\|\mathbf{e}_p\|_{\ell^2(0,T;\mathrm{L}^2(\Omega))}$	
DOF	h	error	rate	error	rate	error	rate	error	rate	error	rate
266	0.354	6.02E-01	–	3.33E-02	–	2.68E-01	–	3.04E-02	–	8.94E-02	–
1010	0.177	2.92E-01	1.047	1.70E-02	0.968	1.36E-01	0.980	7.64E-03	1.995	4.44E-02	1.009
3938	0.088	1.36E-01	1.101	8.57E-03	0.992	6.80E-02	0.996	2.50E-03	1.610	1.93E-02	1.200
15554	0.044	6.45E-02	1.076	4.29E-03	0.998	3.40E-02	0.999	9.58E-04	1.386	8.56E-03	1.175
54362	0.024	3.37E-02	1.032	2.29E-03	0.999	1.82E-02	1.000	3.85E-04	1.449	4.34E-03	1.081
150602	0.014	2.01E-02	1.012	1.37E-03	1.000	1.09E-02	1.000	1.80E-04	1.488	2.56E-03	1.031

AFW$_0$ discretization											
		$\|\mathbf{e}_{\widetilde{\boldsymbol{\sigma}}}\|_{\ell^2(0,T;\mathbb{X})}$		$\|\mathbf{e}_{\mathbf{u}}\|_{\ell^2(0,T;\mathbf{L}^s(\Omega))}$		$\|\mathbf{e}_{\mathbf{u}}\|_{\ell^\infty(0,T;\mathbf{L}^2(\Omega))}$		$\|\mathbf{e}_{\boldsymbol{\gamma}}\|_{\ell^2(0,T;\mathbb{L}^2(\Omega))}$		$\|\mathbf{e}_p\|_{\ell^2(0,T;\mathrm{L}^2(\Omega))}$	
DOF	h	error	rate	error	rate	error	rate	error	rate	error	rate
321	0.354	5.39E-01	–	3.33E-02	–	2.68E-01	–	8.60E-02	–	2.89E-02	–
1217	0.177	2.36E-01	1.189	1.70E-02	0.966	1.36E-01	0.981	4.33E-02	0.991	1.31E-02	1.143
4737	0.088	1.13E-01	1.072	8.57E-03	0.991	6.80E-02	0.995	2.16E-02	0.999	6.27E-03	1.060
18689	0.044	5.54E-02	1.022	4.29E-03	0.998	3.40E-02	0.999	1.08E-02	1.000	3.10E-03	1.017
65281	0.024	2.94E-02	1.007	2.29E-03	0.999	1.82E-02	1.000	5.77E-03	1.000	1.65E-03	1.005
180801	0.014	1.76E-02	1.002	1.37E-03	1.000	1.09E-02	1.000	3.46E-03	1.000	9.88E-04	1.002

Table 6.1: [Example 1, $k = 0$] Number of degrees of freedom, meshsizes, errors, and rates of convergence.

PEERS$_1$ discretization											
		$\|\mathbf{e}_{\widetilde{\boldsymbol{\sigma}}}\|_{\ell^2(0,T;\mathbb{X})}$		$\|\mathbf{e}_{\mathbf{u}}\|_{\ell^2(0,T;\mathbf{L}^s(\Omega))}$		$\|\mathbf{e}_{\mathbf{u}}\|_{\ell^\infty(0,T;\mathbf{L}^2(\Omega))}$		$\|\mathbf{e}_{\boldsymbol{\gamma}}\|_{\ell^2(0,T;\mathbb{L}^2(\Omega))}$		$\|\mathbf{e}_p\|_{\ell^2(0,T;\mathrm{L}^2(\Omega))}$	
DOF	h	error	rate	error	rate	error	rate	error	rate	error	rate
818	0.354	7.84E-02	–	5.43E-03	–	3.62E-02	–	8.99E-03	–	6.79E-03	–
3170	0.177	1.87E-02	2.067	1.39E-03	1.968	9.18E-03	1.977	2.62E-03	1.779	2.00E-03	1.762
12482	0.088	4.59E-03	2.029	3.49E-04	1.992	2.31E-03	1.994	7.54E-04	1.797	5.50E-04	1.863
49538	0.044	1.14E-03	2.011	8.75E-05	1.997	5.77E-04	1.999	2.02E-04	1.900	1.44E-04	1.937
173522	0.024	3.23E-04	2.005	2.49E-05	1.998	1.64E-04	2.000	5.87E-05	1.965	4.16E-05	1.973
481202	0.014	1.16E-04	1.995	9.00E-06	1.995	5.91E-05	1.999	2.13E-05	1.986	1.51E-05	1.987

AFW$_1$ discretization											
		$\|\mathbf{e}_{\widetilde{\boldsymbol{\sigma}}}\|_{\ell^2(0,T;\mathbb{X})}$		$\|\mathbf{e}_{\mathbf{u}}\|_{\ell^2(0,T;\mathbf{L}^s(\Omega))}$		$\|\mathbf{e}_{\mathbf{u}}\|_{\ell^\infty(0,T;\mathbf{L}^2(\Omega))}$		$\|\mathbf{e}_{\boldsymbol{\gamma}}\|_{\ell^2(0,T;\mathbb{L}^2(\Omega))}$		$\|\mathbf{e}_p\|_{\ell^2(0,T;\mathrm{L}^2(\Omega))}$	
DOF	h	error	rate	error	rate	error	rate	error	rate	error	rate
817	0.354	7.86E-02	–	5.40E-03	–	3.62E-02	–	1.16E-02	–	3.20E-03	–
3169	0.177	1.73E-02	2.181	1.39E-03	1.960	9.19E-03	1.978	2.97E-03	1.967	7.38E-04	2.115
12481	0.088	4.05E-03	2.098	3.49E-04	1.990	2.31E-03	1.994	7.50E-04	1.986	1.88E-04	1.976
49537	0.044	9.86E-04	2.037	8.75E-05	1.997	5.77E-04	1.999	1.88E-04	1.994	4.78E-05	1.973
173521	0.024	2.78E-04	2.014	2.49E-05	1.998	1.64E-04	2.000	5.37E-05	1.997	1.37E-05	1.984
481201	0.014	1.00E-04	1.997	9.00E-06	1.995	5.91E-05	1.999	1.93E-05	1.997	4.99E-06	1.983

Table 6.2: [Example 1, $k = 1$] Number of degrees of freedom, meshsizes, errors, and rates of convergence.

Example 2: Convergence against smooth exact solutions in a 3D domain

In the second numerical test, we study the convergence with respect to the spatial discretization using a manufactured solution in the unit cube $\Omega := (0,1)^3$. We set $s = 3$, which yields $\ell = 3/2$ (cf. (2.13)).

PEERS$_k$ discretization						
h	0.354	0.177	0.088	0.044	0.024	0.014
$\|\mathbf{e}_{\mathtt{m},0}\|_{\ell^\infty(0,T;\ell^\infty(\Omega))}$	1.25E-12	1.71E-12	3.66E-12	1.34E-11	3.21E-11	9.89E-11
$\|\mathbf{e}_{\mathtt{m},1}\|_{\ell^\infty(0,T;\ell^\infty(\Omega))}$	4.97E-12	2.32E-10	4.74E-09	1.58E-09	2.72E-09	3.38E-09

AFW$_k$ discretization						
h	0.354	0.177	0.088	0.044	0.024	0.014
$\|\mathbf{e}_{\mathtt{m},0}\|_{\ell^\infty(0,T;\ell^\infty(\Omega))}$	2.75E-12	3.64E-12	7.18E-12	1.98E-11	5.81E-11	2.04E-10
$\|\mathbf{e}_{\mathtt{m},1}\|_{\ell^\infty(0,T;\ell^\infty(\Omega))}$	2.94E-12	5.57E-12	1.34E-11	5.08E-11	1.66E-10	4.89E-10

Table 6.3: [Example 1, $k = 0, 1$] Conservation of momentum for the fully discrete scheme.

Similarly to the first example, the viscosity is $\mu = 1$, the permeability tensor is given by $\mathbf{K} := 10^{-2}\,\mathbb{I}$, and the porosity function along with the manufactured solutions are given in Figure 6.3. The datum $\mathbf{f}$ is computed according to this (cf. (2.1)).

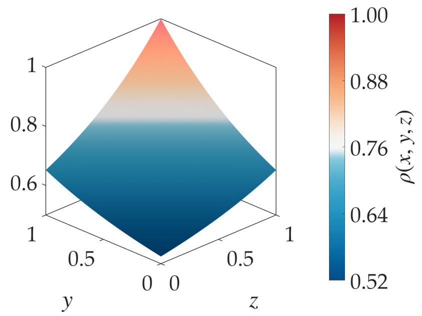

$$\rho(x, y, z) := 0.45 + 0.55\,\exp(-(2 - y - z))\,,$$

$$\mathbf{u} = \exp(t)\,\rho(x, y, z)^{-1}\begin{pmatrix} \sin(\pi x)\,\cos(\pi y)\,\cos(\pi z) \\ -2\cos(\pi x)\,\sin(\pi y)\,\cos(\pi z) \\ \cos(\pi x)\,\cos(\pi y)\,\sin(\pi z) \end{pmatrix},$$

$$p = \exp(t)\,\cos(\pi x)\,\exp(y + z)\,.$$

Figure 6.3: [Example 2] Graph of the porosity function (left) and analytical expressions of the porosity and manufactured solutions (right).

Table 6.4 shows the convergence history for a sequence of quasi-uniform mesh refinements using both PEERS$_0$ and AFW$_0$ elements. Once again, the optimal spatial convergence rates $\mathcal{O}(h^{k+1})$ predicted by Theorem 5.4 and Lemma 5.5 are confirmed. Regarding the conservation of momentum, Table 6.5 shows a behavior similar to that observed in the first example. Figure 6.4 displays the approximated solutions at the final time obtained with the PEERS$_0$ discretization on a mesh with size $h = 0.0962$ and 34,992 tetrahedral elements, corresponding to 656,266 degrees of freedom.

Example 3: Free fluid flow around a porous obstacle

Our final test aims to evaluate the performance of the proposed method in a more complex physical configuration, where a fluid interacts with a porous obstacle acting as a filter. This setting allows us to examine how the formulation captures the coupling between the free flow and the porous medium, as well as the influence of anisotropy and permeability contrasts on the global behavior of the flow. This benchmark problem was first introduced in [33] and later examined in [6,37]. We consider a channel Ω with dimensions $0.75\,[\mathrm{m}] \times 0.25\,[\mathrm{m}]$, through which a fluid of viscosity $\mu = 1.5 \cdot 10^{-5}\,[\mathrm{m}^2/\mathrm{s}]$ flows due to a left-to-right pressure drop of $1 \cdot 10^{-6}\,[\mathrm{m}^2/\mathrm{s}^2]$. The channel consists of two regions. The first one, Ω_{free}, is a free-fluid domain, whereas the second region represents a heterogeneous porous filter composed of an outer isotropic subregion Ω_{iso} and an inner anisotropic subregion Ω_{an}. More precisely,

PEERS$_0$ discretization											
		$\|\mathbf{e}_{\widetilde{\boldsymbol\sigma}}\|_{\ell^2(0,T;\mathbb{X})}$		$\|\mathbf{e}_{\mathbf{u}}\|_{\ell^2(0,T;\mathbf{L}^s(\Omega))}$		$\|\mathbf{e}_{\mathbf{u}}\|_{\ell^\infty(0,T;\mathbf{L}^2(\Omega))}$		$\|\mathbf{e}_{\boldsymbol\gamma}\|_{\ell^2(0,T;\mathbb{L}^2(\Omega))}$		$\|\mathbf{e}_{p}\|_{\ell^2(0,T;\mathrm{L}^2(\Omega))}$	
DOF	h	error	rate	error	rate	error	rate	error	rate	error	rate
7576	0.433	1.08E+00	–	4.19E-02	–	3.65E-01	–	5.04E-02	–	1.30E-01	–
25006	0.289	7.16E-01	1.001	2.84E-02	0.957	2.47E-01	0.968	2.19E-02	2.054	8.78E-02	0.960
58636	0.216	5.29E-01	1.058	2.14E-02	0.979	1.86E-01	0.985	1.30E-02	1.805	6.37E-02	1.114
195808	0.144	3.40E-01	1.087	1.43E-02	0.989	1.24E-01	0.993	6.85E-03	1.588	3.89E-02	1.219
656266	0.096	2.19E-01	1.089	9.58E-03	0.995	8.29E-02	0.997	3.78E-03	1.462	2.33E-02	1.268

AFW$_0$ discretization											
		$\|\mathbf{e}_{\widetilde{\boldsymbol\sigma}}\|_{\ell^2(0,T;\mathbb{X})}$		$\|\mathbf{e}_{\mathbf{u}}\|_{\ell^2(0,T;\mathbf{L}^s(\Omega))}$		$\|\mathbf{e}_{\mathbf{u}}\|_{\ell^\infty(0,T;\mathbf{L}^2(\Omega))}$		$\|\mathbf{e}_{\boldsymbol\gamma}\|_{\ell^2(0,T;\mathbb{L}^2(\Omega))}$		$\|\mathbf{e}_{p}\|_{\ell^2(0,T;\mathrm{L}^2(\Omega))}$	
DOF	h	error	rate	error	rate	error	rate	error	rate	error	rate
10081	0.433	9.49E-01	–	4.18E-02	–	3.65E-01	–	1.03E-01	–	5.88E-02	–
33049	0.289	6.01E-01	1.127	2.84E-02	0.957	2.47E-01	0.969	6.95E-02	0.964	3.41E-02	1.345
77185	0.216	4.38E-01	1.097	2.14E-02	0.978	1.86E-01	0.985	5.23E-02	0.984	2.37E-02	1.261
256609	0.144	2.85E-01	1.062	1.43E-02	0.989	1.24E-01	0.992	3.50E-02	0.993	1.48E-02	1.165
857305	0.096	1.87E-01	1.032	9.58E-03	0.995	8.29E-02	0.997	2.34E-02	0.997	9.52E-03	1.085

Table 6.4: [Example 2, $k=0$] Number of degrees of freedom, meshsizes, errors, and rates of convergence.

PEERS$_0$ discretization					
h	0.433	0.289	0.216	0.144	0.096
$\|\mathbf{e}_{\mathtt{m},0}\|_{\ell^\infty(0,T;\ell^\infty(\Omega))}$	7.96E-12	7.28E-12	7.30E-12	8.41E-12	9.32E-12

AFW$_0$ discretization					
h	0.433	0.289	0.216	0.144	0.096
$\|\mathbf{e}_{\mathtt{m},0}\|_{\ell^\infty(0,T;\ell^\infty(\Omega))}$	2.96E-12	3.87E-12	3.87E-12	4.56E-12	4.55E-12

Table 6.5: [Example 2, $k=0$] Conservation of momentum for the fully discrete scheme.

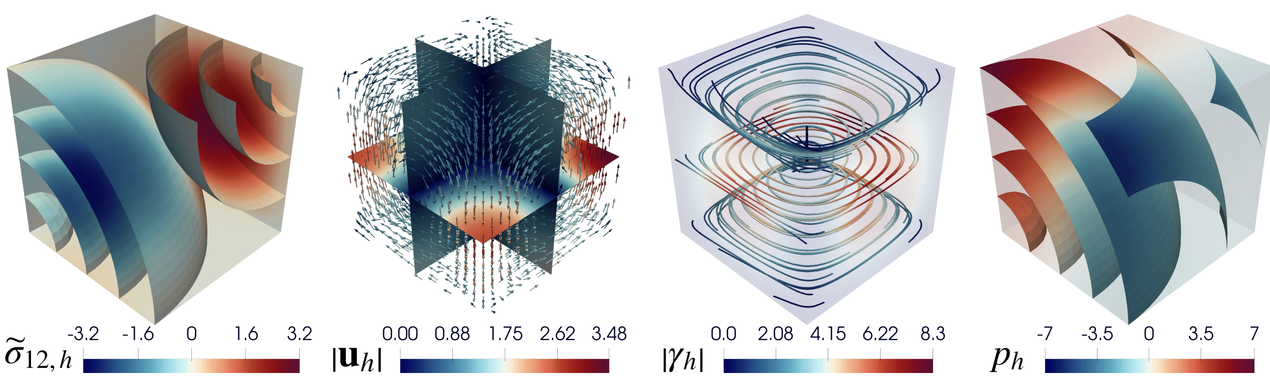

Figure 6.4: [Example 2] Computed stress component, magnitude of the velocity, vorticity streamlines, and pressure field.

the domain under consideration is given by $\Omega = \Omega_{\rm free} \cup \Omega_{\rm iso} \cup \Omega_{\rm an}$, where

$$\Omega_{\rm an} := (0.32, 0.385) \times (0.05, 0.12)\,, \quad \Omega_{\rm iso} := (0.25, 0.5) \times (0.2) \setminus \Omega_{\rm an}\,,$$

$$\text{and} \quad \Omega_{\rm free} := (0, 0.75) \times (0, 0.25) \setminus (\Omega_{\rm an} \cup \Omega_{\rm iso})\,.$$

We denote by $\Gamma = \Gamma_{\text{top}} \cup \Gamma_{\text{bottom}} \cup \Gamma_{\text{right}} \cup \Gamma_{\text{left}}$ the boundary of Ω, naturally partitioned into its corresponding sides. We illustrate the geometrical setting in Figure 6.5. There is no transition region between the free fluid and porous regions.

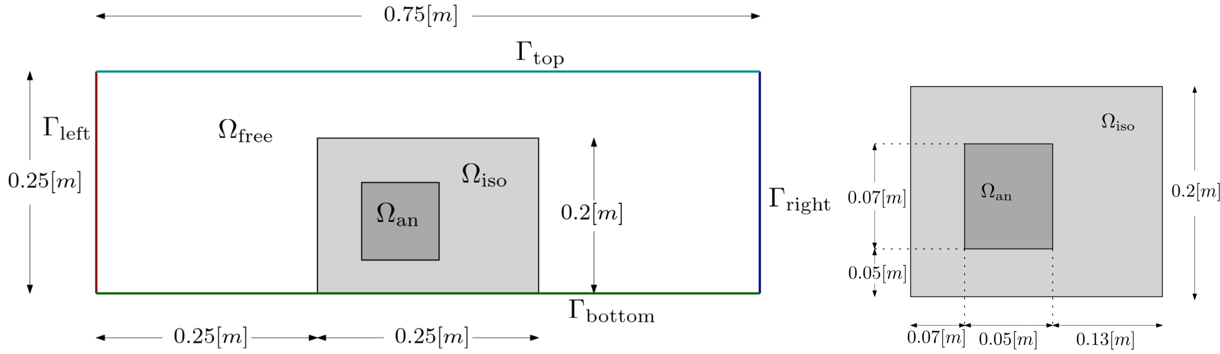

Figure 6.5: [Example 3] Geometrical configuration of the numerical experiment. The left panel shows the channel Ω, while the right panel depicts a detailed view of the porous filter consisting of isotropic and anisotropic regions.

In the porous filter, the permeability tensor $\mathbf{K}_*$, with $* \in \{\text{iso}, \text{an}\}$, is given by

$$\mathbf{K}_* := \mathbf{M}_* \, \mathbf{C}_* \, \mathbf{M}_*^{-1}, \quad \mathbf{M}_* := \begin{pmatrix} \cos(\alpha_*) & -\sin(\alpha_*) \\ \sin(\alpha_*) & \cos(\alpha_*) \end{pmatrix}, \quad \text{and} \quad \mathbf{C}_* := \begin{pmatrix} k_*/\beta_* & 0 \\ 0 & k_* \end{pmatrix}, \tag{6.1}$$

where k_* and β_* are positive parameters and α_* is the anisotropy angle. Clearly, $\alpha_{\text{iso}} = 0$ owing to the isotropy. We consider the parameters of the model as

$$\mathbf{K} := \begin{cases} +\infty & \text{in} \quad \Omega_{\text{free}}\,, \\ \mathbf{K}_{\text{iso}} & \text{in} \quad \Omega_{\text{iso}}\,, \\ \mathbf{K}_{\text{an}} & \text{in} \quad \Omega_{\text{an}}\,, \end{cases} \quad \text{and} \quad \rho := \begin{cases} 1 & \text{in} \quad \Omega_{\text{free}}\,, \\ \rho_{\text{iso}} & \text{in} \quad \Omega_{\text{iso}}\,, \\ \rho_{\text{an}} & \text{in} \quad \Omega_{\text{an}}\,. \end{cases}$$

In the forthcoming presentation, we shall consider different porosity functions and parameters for the permeability tensor in the porous region. We notice also that the fact that the permeability tensor is identically $+\infty$ in the free-fluid region means that $\mathbf{K}^{-1} \equiv \mathbf{0}$ in Ω_{free}.

No-slip boundary conditions are prescribed for the fluid velocity along the top and bottom walls of the channel, whereas the pressure drop is induced by a traction difference between the left and right boundaries. Namely,

$$\begin{gathered} \mathbf{u} = \mathbf{0} \quad \text{on} \quad \Gamma_{\text{top}} \cup \Gamma_{\text{bottom}} \times (0,T]\,, \quad \widetilde{\boldsymbol{\sigma}}\mathbf{n} = -p_{\text{in}}\,\mathbf{n} \quad \text{on} \quad \Gamma_{\text{left}} \times (0,T]\,, \\ \text{and} \quad \widetilde{\boldsymbol{\sigma}}\mathbf{n} = -p_{\text{out}}\,\mathbf{n} \quad \text{on} \quad \Gamma_{\text{right}} \times (0,T]\,, \end{gathered} \tag{6.2}$$

where $p_{\text{in}} = p_{\text{ref}} + 1 \cdot 10^{-6}$ [m^2/s^2], $p_{\text{out}} = p_{\text{ref}}$ and $p_{\text{ref}} := 1 \cdot 10^{-6}$ [m^2/s^2]. These conditions translate the Dirichlet boundary condition in (2.1) of our model into a mixed-type boundary condition. The analysis developed in the previous sections can readily be adapted to handle this case. In particular, one may employ a lifting of the normal trace in (6.2) and introduce a change of variable for the stress tensor, so that the formulation derived in Section 2.2 is now posed on $\mathbb{H}_N(\mathbf{div}_\ell;\Omega)$ instead of $\mathbb{H}_0(\mathbf{div}_\ell;\Omega)$, where $\mathbb{H}_N(\mathbf{div}_\ell;\Omega)$ stands for tensors in $\mathbb{H}(\mathbf{div}_\ell;\Omega)$ with vanishing normal trace on $\Gamma_{\text{left}} \cup \Gamma_{\text{right}}$. Then, the analysis proceeds in a similar manner, provided that suitable geometric conditions on the domain hold, for instance assumptions on the maximal interior angle. In our case, the domain is rectangular and therefore convex, so no technical issues arise. We omit further details and refer the reader to [18, eqs. (3.25)–(3.30)] for a more complete discussion. Finally, we set as initial condition and source term $\mathbf{u}_0 = \mathbf{0}$ and $\mathbf{f} = \mathbf{0}$, respectively.

In all the following experiments, we consider a total simulation time of $T = 80\,[\mathrm{s}]$ and the time step size is set as $\Delta t = 4\,[\mathrm{s}]$. The mesh consists of 63,221 triangles and the element sizes goes from $4 \cdot 10^{-3}$ in the bulk fluid to $1 \cdot 10^{-4}$ close to the interfaces (see Figure 6.9). For the spatial discretization, we employ the AFW_0 finite element triple (cf. (4.2)), which results in a total of 569,995 degrees of freedom in the implementation.

In our first experiment, we consider a simple case when the porosity function is constant in each region, given by $\rho_{\mathrm{iso}} \equiv 0.5$ and $\rho_{\mathrm{an}} \equiv 0.25$. Regarding the permeability tensor, we take $\alpha_{\mathrm{iso}} = 0$, $\beta_{\mathrm{iso}} = 1$, $k_{\mathrm{iso}} = 1 \cdot 10^{-4}$, $\alpha_{\mathrm{an}} = -\pi/4$, $\beta_{\mathrm{an}} = 100$, and $k_{\mathrm{an}} = 1 \cdot 10^{-6}$. In the free-fluid region, the flow circulates freely and tends to avoid the porous region, concentrating on the upper area of the filter due to the porous and permeability effects. The isotropic region, with higher permeability and porosity, allows the fluid to flow more freely, while the anisotropic region acts as a barrier that restricts flow in certain directions due to both its lower permeability and the directional dependence encoded by the rotation angle α_{an}. In turn, if we repeat the experiment with $k_{\mathrm{an}} = 1 \cdot 10^{-4}$, the contrast between the isotropic and anisotropic regions decreases significantly. In this case, the anisotropic layer becomes more permeable, allowing the fluid to penetrate and traverse it with less resistance. Consequently, the flow field tends to distribute more uniformly across the porous domain, rather than being diverted around the anisotropic region as in the previous configuration. In both scenarios, we observe that the conservation of momentum error is close to zero. Indeed, bearing in mind that the porosity is constant and $\mathbf{f} \equiv \mathbf{0}$, in order to verify that (5.15) holds, we compute $\|\rho\, d_t(\mathbf{u}_h) + \mu\, \boldsymbol{\mathcal{P}}_h^k(\mathbf{K}^{-1}\,\mathbf{u}_h) - \mathbf{div}(\boldsymbol{\sigma}_h)\|_{\ell^\infty(0,T;\ell^\infty(\Omega))}$, obtaining $9.54 \cdot 10^{-7}$ in both cases. In Figure 6.6, we display these results at the final time T. We only show the velocity profile for the sake of brevity.

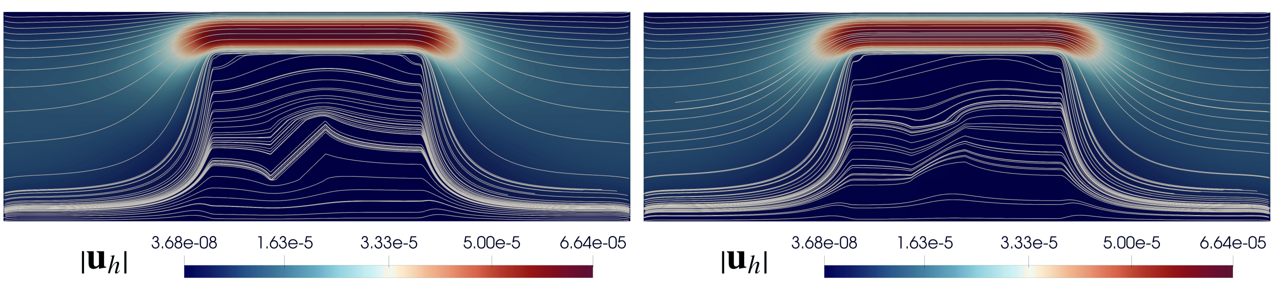

Figure 6.6: [Example 3] Computed streamlines of the velocity with piecewise constant porosity and $k_{\mathrm{an}} = 1 \cdot 10^{-6}$ (left) and $k_{\mathrm{an}} = 1 \cdot 10^{-4}$ (right).

As a second experiment, we consider the non-piecewise constant porosity functions given in Figure 6.7. In the isotropic region, we prescribe a linear variation of the porosity, representing a gradual compaction or deposition of the porous material. Physically, this choice models a medium whose microstructure becomes progressively denser along the horizontal axis, such as might occur due to sedimentation or pressure-induced compaction in filtration processes. On the other hand, in the anisotropic region, we consider an exponential porosity profile, decreasing from the outer boundary toward the interior of the inclusion. This choice mimics a boundary-layer-type behavior, where the porous structure becomes gradually denser as one moves inward, reflecting processes such as clogging, compression, or material deposition within the anisotropic medium. Such a profile provides a smooth yet strongly contrasting variation that highlights how the anisotropic permeability interacts with spatially varying microstructural properties. Notice that this choice is similar to those considered in Examples 1 and 2.

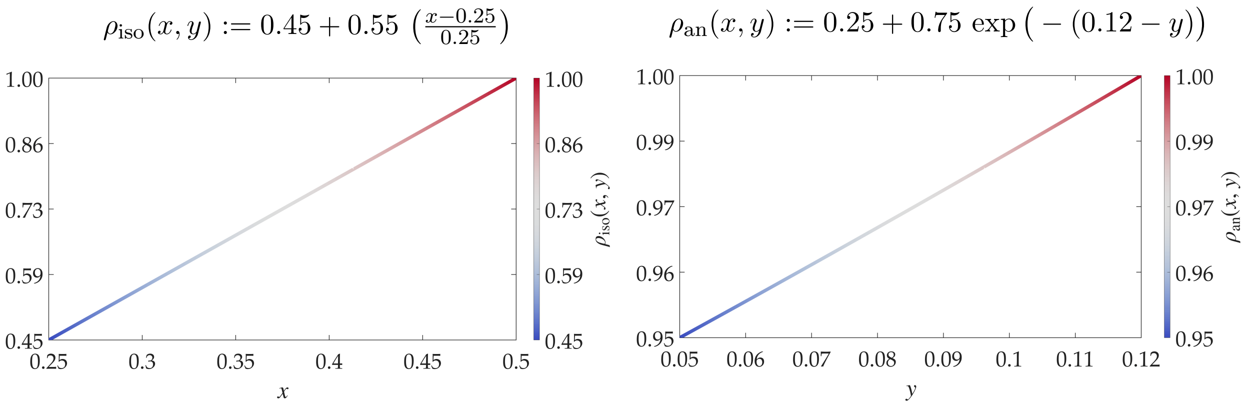

Figure 6.7: [Example 3] Porosity functions in the isotropic (left) and anisotropic (right) regions.

The permeability tensor is computed with parameters $\alpha_{\rm iso} = 0$, $\beta_{\rm iso} = 1$, $k_{\rm iso} = 1 \cdot 10^{-6}$, $\alpha_{\rm an} = \pi/4$, $\beta_{\rm an} = 100$, and $k_{\rm an} = 1 \cdot 10^{-6}$. The anisotropy angle $\alpha_{\rm an}$, unlike in the first test, takes a positive value, meaning that the principal permeability directions are rotated so that the fluid enters the anisotropic region from the upper side and exits through the lower one. Figure 6.8 shows the numerical results obtained with these parameters, which confirm the physical intuition regarding the direction of the flow induced by the anisotropy orientation. As in Figure 6.6, the fluid tends to move upward and bypass the porous filter, avoiding direct penetration through it. Similarly, inside the porous medium, the fluid still tends to circumvent the anisotropic region, although this effect is less pronounced because the permeability contrast is lower than in the previous test. In Figure 6.9, a zoomed view of the domain interfaces is presented, focusing on the upper-left corner of $\Omega_{\rm iso}$ and the entire interaction between $\Omega_{\rm an}$ and its surrounding region. We can observe that the fluid tends to concentrate near the corners, a behavior mainly driven by the anisotropy angle, which redirects the preferential flow paths along the principal directions of permeability. This effect highlights how the orientation of the anisotropic axes influences the local acceleration and deflection of the flow at the interface between both materials. Finally, we compute the error associated with the conservation of momentum (cf. (5.15)), now considering the non-piecewise constant porosity defined above and the datum $\mathbf{f} \equiv 0$ in Ω, thus obtaining

$$\|\boldsymbol{\mathcal{P}}_h^k(\rho\, d_t \mathbf{u}_h) + \mu \boldsymbol{\mathcal{P}}_h^k(\mathbf{K}^{-1}\, \mathbf{u}_h) - \mathbf{div}(\boldsymbol{\sigma}_h)\|_{\ell^\infty(0,T;\ell^\infty(\Omega))} = 9.76 \cdot 10^{-7}\,,$$

which confirms that momentum is conserved.

7 Conclusions

In this paper, we have introduced a new stress-velocity-vorticity formulation for the time-dependent Brinkman problem with spatially varying porosity, together with its mixed finite element approximation. This system models flow through porous media and acts as an intermediate regime between the Darcy and Stokes models. The proposed formulation offers several advantages. It naturally incorporates the porosity gradients and recovers the classical constant-porosity formulation as a particular case, for which all assumptions involving $\|\nabla\rho/\rho\|_{\mathbf{L}^\infty(\Omega)}$ are no longer required. Moreover, it enables the direct computation of physically meaningful quantities such as the Cauchy stress and vorticity tensors, while the pressure, eliminated from the formulation, as well as the velocity gradient, can be

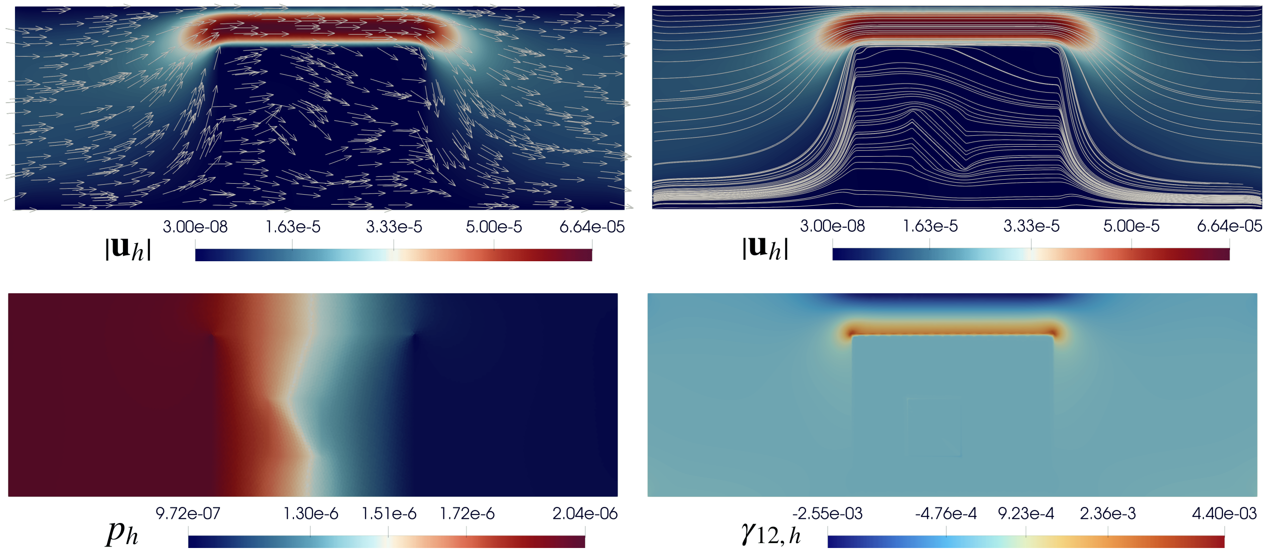

Figure 6.8: [Example 3] Computed velocity and its streamlines (top), and the pressure and component of the vorticity (bottom), with porosity function varying in space.

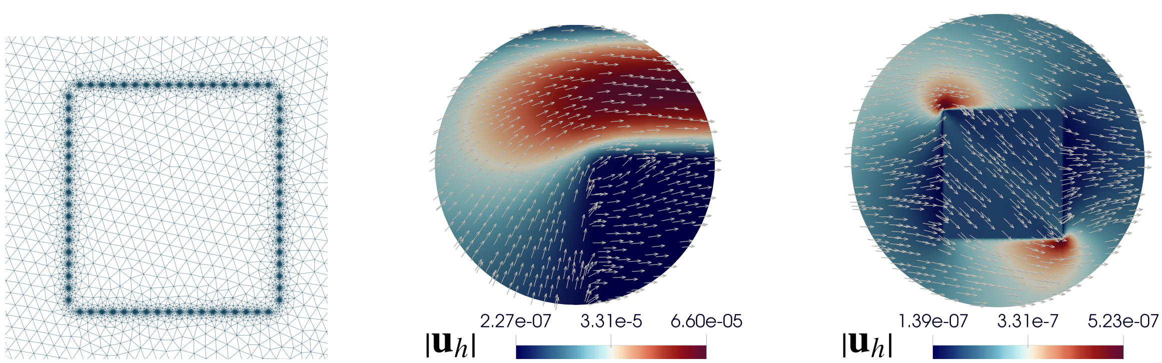

Figure 6.9: [Example 3] Zoom view of the computational mesh near the interface between Ω_{iso} and Ω_{an} (left). Zoom view of the computed velocity at the interfaces: free-fluid versus porous filter (center), and isotropic versus anisotropic regions (right).

easily reconstructed through a simple post-processing step. The theoretical analysis relies heavily on monotone operator techniques and is made possible by introducing a fixed-point strategy formulated in a suitable Bochner space. This approach appears to be extendable to other related equations, paving the way for the development of similar methods for more complex multiphysics problems, such as the coupling of the Brinkman model with heat or transport equations. At the discrete level, we have rigorously established the well-posedness of both the semi-discrete continuous-in-time and the fully discrete schemes, and we have developed the corresponding error analysis. Moreover, the proposed method inherits from the continuous problem the important property of being momentum conservative. From the numerical perspective, we have illustrated the robustness and accuracy of the method, even in scenarios involving challenging physical parameters. In particular, the last numerical example highlights the importance of mesh refinement near material interfaces, as illustrated in Figure 6.9. This observation motivates future work on developing an *a posteriori* error analysis for the proposed method, which could then be employed to guide adaptive mesh refinement and achieve more accurate approximations in this class of problems.

References

[1] M. S. Alnaes, J. Blechta, J. Hake, A. Johansson, B. Kehlet, A. Logg, C. Richardson, J. Ring, M. E. Rognes and G. N. Wells, *The FEniCS project version 1.5.* Arch. Numer. Softw. 3, 9–23 (2015).

[2] M. Álvarez, G. N. Gatica and R. Ruiz-Baier, *Analysis of a vorticity-based fully-mixed formulation for the 3D Brinkman-Darcy problem.* Comput. Methods Appl. Mech. Engrg. 307, 68–95 (2016).

[3] M. Amara and J. M. Thomas, *Equilibrium finite elements for the linear elastic problem.* Numer. Math. 33, 367–383 (1979).

[4] V. Anaya, R. Caraballo, S. Caucao, L. F. Gatica, R. Ruiz-Baier and I. Yotov, *A vorticity-based mixed formulation for the unsteady Brinkman–Forchheimer equations.* Comput. Methods Appl. Mech. Eng. 404 (2023).

[5] V. Anaya, G. N. Gatica, D. Mora and R. Ruiz-Baier, *An augmented velocity-vorticity-pressure formulation for the Brinkman equations.* Int. J. Numer. Methods Fluids 79, 109–137 (2015).

[6] C. Aricò, R. Helmig, D. Puleo and M. Schneider, *A new numerical mesoscopic scale one-domain approach solver for free fluid/porous medium interaction.* Comput. Methods Appl. Mech. Eng. 419 (2024).

[7] D. N. Arnold, F. Brezzi and J. Douglas, *PEERS: A new mixed finite element for plane elasticity.* Japan J. Appl. Math. 1, 347–367 (1984).

[8] D. N. Arnold, R. Falk and R. Winther, *Mixed finite element methods for linear elasticity with weakly imposed symmetry.* Math. Comp. 76, 1699–1723 (2007).

[9] D. Boffi, F. Brezzi and M. Fortin, *Mixed finite element methods and applications.* Springer Ser. Comput. Math. 44, Springer, Heidelberg (2013).

[10] H. C. Brinkman, *A calculation of the viscous force exerted by a flowing fluid on a dense swarm of particles.* Appl. Sci. Res. 1, 27–34 (1949).

[11] E. Burman and P. Hansbo, *Stabilized Crouzeix–Raviart element for the Darcy–Stokes problem.* Numer. Methods Partial Differential Eq. 21, 986–997 (2005).

[12] A. J. Bustos, S. Caucao and G. N. Gatica, *Mixed-primal and fully-mixed formulations for the convection-diffusion-reaction system based upon Brinkman–Forchheimer equations.* Preprint, Universidad de Concepción (2025). Available at https://ci2ma.udec.cl/pdf/prepublicaciones2/2025/pp25-13.pdf.

[13] A. J. Bustos, S. Caucao, G. N. Gatica and B. N. Venegas, *New fully mixed finite element methods for the coupled convective Brinkman–Forchheimer and nonlinear transport equations.* J. Sci. Comput. 104, Paper No. 64, 45 pp. (2025).

[14] M. Bukač, I. Yotov and P. Zunino, *An operator splitting approach for the interaction between a fluid and a multilayered poroelastic structure.* Numer. Methods Partial Differential Equations 31, 1054–1100 (2014).

[15] J. Camaño, C. García and R. Oyarzúa, *Analysis of a momentum conservative mixed-FEM for the stationary Navier–Stokes problem.* Numer. Methods Partial Differential Equations 37, no. 5, 2895–2923 (2021).

[16] G. Campaña, P. Muñoz and E. Otárola, *Finite element approximation for a convective Brinkman–Forchheimer problem coupled with a heat equation.* J. Sci. Comput. 104, Paper No. 21, 33 pp. (2025).

[17] S. Carrasco, S. Caucao and G. N. Gatica, *New mixed finite element methods for the coupled convective Brinkman–Forchheimer and double-diffusion equations.* J. Sci. Comput. 97, Paper No. 61, 49 pp (2023).

[18] S. Caucao, G. N. Gatica, S. R. Medrado and Y. D. Sobral, *Nonlinear twofold saddle point-based mixed finite element methods for a regularized $\mu(I)$-rheology model of granular materials.* J. Comput. Phys. 520 (2025).

[19] S. Caucao, G. N. Gatica and J. P. Ortega, *A three-field mixed finite element method for the convective Brinkman–Forchheimer problem with varying porosity.* J. Comput. Appl. Math. 451, Paper No. 116090, 21 pp (2024).

[20] S. Caucao, T. Li and I. Yotov, *A multipoint stress-flux mixed finite element method for the Stokes–Biot model.* Numer. Math. 152, no. 2, 411–473 (2022).

[21] S. Caucao, D. Mora and R. Oyarzúa, *A priori and a posteriori error analysis of a pseudostress-based mixed formulation of the Stokes problem with varying density.* IMA J. Numer. Anal. 36, no. 2, 947–983 (2016).

[22] S. Caucao, R. Oyarzúa, S. Villa-Fuentes and I. Yotov, *A three-field Banach spaces-based mixed formulation for the unsteady Brinkman–Forchheimer equations.* Comput. Methods Appl. Mech. Engrg. 394 (2022).

[23] S. Caucao and I. Yotov, *A Banach space mixed formulation for the unsteady Brinkman–Forchheimer equations.* IMA J. Numer. Anal. 41, no. 4, 2708–2743 (2021).

[24] B. Cockburn, J. Gopalakrishnan and J. Guzmán, *A new elasticity element made for enforcing weak stress symmetry.* Math. Comp. 79 (271), 1331–1349 (2010).

[25] C. I. Correa and G. N. Gatica, *On the continuous and discrete well-posedness of perturbed saddle-point formulations in Banach spaces.* Comput. Math. Appl. 117, 14–23 (2022).

[26] A. Ern and J.-L. Guermond, *Finite elements II—Galerkin approximation, elliptic and mixed PDEs.* Texts Appl. Math., 73, Springer, Cham (2021).

[27] G. N. Gatica, *A Simple Introduction to the Mixed Finite Element Method. Theory and Applications.* SpringerBriefs in Mathematics. Springer, Cham (2014).

[28] G. N. Gatica, L. F. Gatica and A. Márquez, *Analysis of a pseudostress-based mixed finite element method for the Brinkman model of porous media flow.* Numer. Math., 126, 635–677 (2014).

[29] G. N. Gatica, N. Núñez and R. Ruiz-Baier, *New non-augmented mixed finite element methods for the Navier–Stokes–Brinkman equations using Banach spaces*. J. Numer. Math. 31(4), 343–373 (2023).

[30] G. N. Gatica, R. Oyarzúa, R. Ruiz-Baier and Y. D. Sobral, *Banach spaces-based analysis of a fully-mixed finite element method for the steady-state model of fluidized beds*. Comput. Math. Appl. 84, 244–276 (2021).

[31] J. Guzmán and M. Neilan, *A family of nonconforming elements for the Brinkman problem*. IMA Journal of Numerical Analysis 32, 1484–1508 (2012).

[32] J. S. Howell, M. Neilan and N. J. Walkington, *A dual-mixed finite element method for the Brinkman problem*. SMAI J. Comput. Math. 2, 1–17 (2016).

[33] O. Iliev and V. Laptev, *On numerical simulation of flow through oil filters*. Comput Visual Sci 6, 139–146 (2004).

[34] S. Lee and L. Mu, *A Uniform and Pressure-Robust Enriched Galerkin Method for the Brinkman Equations*. J Sci Comput 99, 39 (2024).

[35] M. Lonsing and R. Verfürth, *On the stability of BDMS and PEERS elements*. Numer. Math. 99, 131–140 (2004).

[36] A. Quarteroni and A. Valli, *Numerical Approximation of Partial Differential Equations*. Springer Series in Computational Mathematics, 23. Springer-Verlag, Berlin (1994).

[37] M. Schneider, D. Gläser, K. Werishaupt, E. Coltman, B. Flemisch and R. Helmig, *Coupling staggered-grid and vertex-centered finite-volume methods for coupled porous-medium free-flow problems*. J. Comput. Phys. 482 (2023).

[38] R. E. Showalter, *Monotone Operators in Banach Space and Nonlinear Partial Differential Equations*. Mathematical Surveys and Monographs, 49. American Mathematical Society, Providence, RI (1997).

[39] R. E. Showalter, *Nonlinear degenerate evolution equations in mixed formulations*. SIAM J. Math. Anal. 42(5), 2114–2131 (2010).

[40] R. Stenberg, *A family of mixed finite elements for the elasticity problem*. Numer. Math. 53(5), 513–538 (1988).

Centro de Investigación en Ingeniería Matemática (CI²MA)

PRE-PUBLICACIONES 2025

2025-15 Sergio Caucao, Ricardo Oyarzúa, Segundo Villa-Fuentes: *A priori and a posteriori error analyses of a fully-mixed finite element method for the coupled Navier Stokes / Darcy problem*

2025-16 Juan Barajas-Calonge, Raimund Bürger, Pep Mulet, Luis M. Villada: *A second-order invariant-region-preserving scheme for a transport-flow model of polydisperse sedimentation*

2025-17 Raimund Bürger, Stefan Diehl, María Carmen Martí, Yolanda Vásquez: *A numerical scheme for a model of a flotation column including the transport of liquid components*

2025-18 Raimund Bürger, Enrique D. Fernández Nieto, José Garres-Díaz, Jorge Moya: *Well-balanced physics-based finite volume schemes for Saint-Venant-Exner-type models of sediment transport*

2025-19 Harold D. Contreras, Paola Goatin, Luis M. Villada: *Well-posedness of a nonlocal upstream-downstream traffic model*

2025-20 Thierry Coulbois, Anahi Gajardo, Pierre Guillon, Victor H. Lutfalla: *Aperiodic monotiles: from geometry to groups*

2025-21 Esteban Henriquez, Tonatiuh Sanchez-Vizuet, Manuel Solano: *An unfitted HDG discretization for a model problem in shape optimization*

2025-22 Fernando Artaza-Covarrubias, Tonatiuh Sanchez-Vizuet, Manuel Solano: *A coupled HDG discretization for the interaction between acoustic and elastic waves*

2025-23 Eider Aldana, Ricardo Oyarzúa, Jesús Vellojín: *Numerical analysis of a three-field formulation for a reverse osmosis model*

2025-24 Julio Aracena, Florian Bridoux, Maximilien Gadouleau, Pierre Guillon, Kevin Perrot, Adrien Richard, Guillaume Theyssier: *On the Dynamics of Bounded-Degree Automata Networks*

2025-25 Daniel Cajas Guijarro, John Cajas Guijarro: *Resonant and non-resonant double Hopf bifurcation in a 4D Goodwin model with wage inequality*

2025-26 Alonso J. Bustos, Sergio Caucao: *A Banach space mixed formulation for the unsteady Brinkman problem with spatially varying porosity*

Para obtener copias de las Pre-Publicaciones, escribir o llamar a: Director, Centro de Investigación en Ingeniería Matemática, Universidad de Concepción, Casilla 160-C, Concepción, Chile, Tel.: 41-2661324, o bien, visitar la página web del centro: `http://www.ci2ma.udec.cl`




Centro de Investigación en
Ingeniería Matemática (CI²MA)
Universidad de Concepción

Casilla 160-C, Concepción, Chile
Tel.: 56-41-2661324/2661554/2661316
http://www.ci2ma.udec.cl